博士学位论文基本信息

<table>
<tr><td>学位论文题目</td><td colspan="5">视觉-前庭觉感觉传入一致性影响老年人站姿稳定性的脑肌耦合控制机制</td></tr>
<tr><td>作者</td><td>杨毅</td><td>主学科</td><td>体育学</td><td>交叉学科</td><td>生物医学工程</td></tr>
<tr><td>授予学位时间</td><td>2024.6.30</td><td colspan="2">答辩前评阅成绩</td><td colspan="2">3优2良</td></tr>
<tr><td colspan="6">论文的交叉性和主要创新点概述（限300字）</td></tr>
<tr><td colspan="6">本论文针对老年人站姿稳定性衰退的神经生理学机制，融合多自由度运动平台控制、视觉虚拟现实显示、多模态站姿稳定性检测、EEG功能脑网络成像及脑-肌耦合控制检测等技术，开展了视觉-前庭觉多感觉冲突对老年人站姿稳定性影响及其脑-肌耦合控制机制的实验研究。主要创新成果如下：（1）构建了国内首个集视觉-前庭觉多向冲突干预、站姿稳定性检测和sEMG-EEG信号同步采集的技术平台，建立了脑-肌耦合控制算法模型，为多感觉冲突下老年人站姿稳定性变化规律及神经机制研究提供了方法学基础。（2）研究发现，老年人在视觉-前庭觉反向冲突下的站姿稳定性显著低于年轻人，且更易受视觉神经传入信息影响。（3）揭示了老年人站姿稳定性在多感觉冲突下变化较大的原因，可能与上行本体感觉信息传入较弱和下行运动控制输出失匹配有关，导致脑-肌耦合控制系统鲁棒性下降。研究成果对揭示老年人站姿稳定性衰退的神经生理机制具有重要理论意义，并为康复训练提供了应用指导。论文获评“2024年浙江大学优秀博士学位论文”。</td></tr>
<tr><td colspan="6">主要代表性交叉创新性成果情况限（填3项）
（期刊名称，级别，5年平均影响因子，他引次数，及本人排序/总人数/导师排序）</td></tr>
<tr><td colspan="6">（1）体育科学，人文社科权威期刊，6.4，34，1/6/6
（2）生理学报，浙大一级期刊，1.5，4，1/7/7
（3）Neuroscience Bulletin，SCI二区，5.4，3，2/5/5</td></tr>
</table>

www.cisszgty.com
bjb@ciss.cn

中国体育科学学会主办

ISSN 1000-677X
CN 11-1295/G8

体育科学 第12期 二〇二〇年（第四十卷）

体育科学

CHINA SPORT SCIENCE

国家社科基金资助期刊
中国科协科技期刊精品建设项目
中文体育类核心期刊
中国人文社会科学权威期刊
CSSCI来源期刊

2020年12月(第40卷)

12

CHINA SPORT SCIENCE
VOL.40,No.12,DECEMBER,2020
CN11-1295/G8 * 1981 * m * 16 * 96 * zh * P * ¥25. 00 * 4500 * 08 * 2020-12

CONTENTS

体育科学

（月 刊）

TIYU KEXUE

国家体育总局　主管

中国体育科学学会　主办

2020 年（第 40 卷）第 12 期

（2020 年 12 月 15 日出版）

目　次

研究报告

综述与进展

争鸣与探索

期刊基本参数：CN11-1295/G8 * 1981 * m * 16 * 96 * zh * P * ¥25.00 * 4500 * 08 * 2020-12

体 育 科 学
CHINA SPORT SCIENCE
2020年(第40卷)第12期
Vol. 40,No.12,63-72,2020
文章编号:1000-677X(2020)12-0063-10
DOI:10.16469/j.css.202012006

复杂人体运动冗余控制的肌肉协同理论研究进展与展望

杨 毅[1],彭玉鑫[1],郝增明[1],刘 宇[2],王 新[3],王 健[4,5*]

(1. 浙江大学 教育学院,浙江 杭州 310028;2. 上海体育学院,上海 200438;
3. 沈阳体育学院,辽宁 沈阳 110102;4. 浙江大学 运动科学与健康工程研究所,浙江 杭州 310028;
5. 浙江大学 心理科学研究中心,浙江 杭州 310028)

摘 要:神经肌肉系统是一个开放复杂巨系统,中枢神经系统如何协调不同肌肉活动一直是运动神经科学研究中长期存在的核心科学理论问题。不论是对整体运动描述,还是对肢体局部运动描述,在人体运动控制领域中都会涉及冗余控制的问题。肌肉协同理论认为,神经系统通过同时募集若干个肌肉协同,以模块化控制的方式减轻冗余运动控制的计算负担。研究回顾了肌肉协同理论的起源和基本观点,总结了肌肉协同数学模型类型和肌肉协同分析的基本过程,重点探讨与分析了其在体育科学、临床医学和机器人控制方面的应用。虽然目前有关肌肉协同理论生理证据的结论有不同观点,但已有研究证实,肌肉协同存在于脊椎动物和人体的冗余控制系统,可以很好地解释中枢神经系统对肌肉活动的控制机制。通过设计多样化任务实验范式,利用理论建模工作来严格检验肌肉协同的模块化假设、探讨潜在的神经机制,仍是未来需要重点关注和研究的方向。

关键词:人体运动;运动控制;冗余控制;肌肉协同
中图分类号:G804.5 **文献标识码:**A

人类的运动行为(如站立、走、跑、跳等)有赖于自身运动控制。控制运动的神经结构从低级到高级依次分为脊髓、脑干下行系统和大脑皮层运动区3个层级,各层级功能分工不同。神经科学方面的研究表明,运动控制是中枢神经系统(central nervous system,CNS)以层级和并行方式协同处理实现的。运动控制的中心问题是CNS如何产生实现各种行为目标所需的肌肉活动模式。人类个体是开放的复杂巨系统(钱学森 等,1990),运动时大脑必须处理一个由大约10^7个神经纤维、600块肌肉和200个关节等组成的神经肌肉骨骼系统,这导致在神经、肌肉和关节空间可形成的自由度(degree of freedom, DOF)数量n远超过运动所在空间的维数m($m<n$)。因此,无论是人体的单一肢体运动,还是整体运动,其运动控制都极具冗余控制的特征(林辉杰 等,2012;王爱文 等,2017;Hirashima et al.,2016;Latash,2012;Latash et al.,2002)。这种人体运动的冗余控制(redundancy control)问题,也称"Bernstein问题"、多自由度问题。

针对复杂人体运动的冗余控制问题,Winter(2009)提出神经肌肉骨骼系统的四层整合理论(Neuro-musculo-skeletal integration):第1层整合是对α运动神经元的所有兴奋/抑制输入的神经求和;第2层整合是指对肌肉内所有募集的运动单元求和,形成肌腱张力;第3层整合是各个关节轴上所有主动肌和拮抗肌的肌肉力矩进行求和;第4层被认为是协同层,通过整合2个或多个关节处各肌肉力矩,共同协调实现动作任务。这种整合、协调过程称为"协同"(synergy)。该理论认为肌肉力矩是CNS控制实现特定任务的最终特征,如支撑力矩(the support moment)可用于量化行走过程中下肢所募集肌肉的激活模式(Winter, 1980)。另外,在人体运动的神经肌肉控制机制方面,Bernstein(1967)首次提出一种模块化控制理论,认为层级控制的运动系统包含一组离散的低层级元素结构——运动协同(movement synergies)。大脑明确地将真正的协同作用储存在特定的神经回路中,这些神经回路的联合作用产生对肌肉有任务效率的运动输入,由此可以减少因冗余控制问题引起的计算成本。这种在运动时协

收稿日期: 2020-06-11; **修订日期:** 2020-12-02
基金项目: 国家重点研发计划"科技冬奥"重点专项(2018YFF0300501)。
第一作者简介: 杨毅(1984-),男,在读博士研究生,主要研究方向为人体姿势控制,E-mail:yangyi1023@zju.edu.cn。
***通信作者简介:** 王健(1961-),男,教授,博士,主要研究方向为人因工效学,E-mail:pclabeeg@zju.edu.cn。

同作用的低层级元素结构，在肌肉活动这一层次被称为肌肉协同（muscle synergies）。

个体感知周围环境，结合自身认知解析任务需求，最终选择和执行一系列动作以完成目标任务。具体的运动行为是个体、任务和环境3因素相互作用产生的，为了使运动按预期进行，CNS不仅需要指定大量的输出变量，还必须考虑对运动执行施加的各种生物力学要求或约束（华安珂 等，2019；刘宇，2010；王楚婕 等，2013；王健等，2017；王开元 等，2018）。而肌肉协同是在CNS中编码还是由于任务约束而被激活，目前对于这种肌肉协同的起源是否是神经性起源问题还存有争议。虽然有针对动物，如青蛙（Bizzi et al.，2008；D'Avella et al.，2005）、老鼠（Tresch et al.，1999）和猫（Desrochers et al.，2019；Ting et al.，2007）等和人类（Chvatal et al.，2013）的研究都为肌肉协同理论神经起源提供了直接的生理学证据，但有部分与肌肉协同神经性起源观点相矛盾的实验对这一理论提出了挑战（Kutch et al.，2008；Valero-Cuevas et al.，2009）。Kutch等（2008）利用运动系统信号相关噪声特性来估计产生微小指尖力期间的肌肉激活，然后通过检查不同作用力方向的可变性的形状估算潜在的肌肉募集程度。其研究结果表明，完成该任务是独立募集单个肌肉，而不是通过肌肉协同同时募集多个肌肉来实现。对这类支持肌肉协同假说的实验进行批评的主要观点在于肌肉协同反映任务约束，而不是反映了神经控制策略。随着表面肌电图（surface electromyography，sEMG）和功能性磁共振成像（functional magnetic resonance imaging，fMRI）数据分析的发展，当前结论倾向于将肌肉协同认为是存在于大脑和脊髓中的时空成分，从而支持其神经性起源观点。每个个体都可能使用不同的肌肉激活模式来达到相同的任务目标。基于肌肉协同理论的研究表明不同个体的运动存在一种共同的模块化神经控制机制——肌肉协同。肌肉协同理论可以很好地解释CNS对肌肉的控制机制，从而揭示神经系统的内在功能模式。近年来，国内外学者对肌肉协同理论及其应用的研究越来越多（Cheng et al.，2019；Israely et al.，2018；Singh et al.，2018），本研究就国内外肌肉协同理论的研究进展及其在体育科学、临床医学和机器人控制方面的应用进行综述，以期深刻认识和理解肌肉协同理论，并展望其未来研究和应用的发展趋势。

1 肌肉协同理论

复杂人体运动的冗余控制问题或者多自由度问题，目前主要提出了3个主要理论。

1）消除理论（elimination theory）。该理论认为CNS通过将DOF数量减少到执行任务所需的数量来解决问题（Latash et al.，2007）。这种对DOF的"冻结"源自Bernstein提出的假设，在当代人类运动行为的研究中经常被引用。消除DOF的概念主要是在运动学层面上提出的，而未考虑力量、肌肉、运动单元或多关节任务中的冗余。

2）最优化理论（optimization theory）。其基本思想来源于数学和工程学。最优化是一种通过考虑成本函数中包含的附加条件，在无限种可能性中选择最优解的方法。最优化理论通常被认为是指大脑不断地为它所面临的每一个运动任务计算全局最优（Berret et al.，2019）。研究者们通常依靠计算机进行数学运算来构造最佳的运动指令。这类研究的限制性在于他们只关注优化计算的最终结果，而没有解决大脑如何实现优化的问题。最优化理论有助于理解"为什么"某些动作会比其他动作最终被执行，但它并不能说明大脑实际上是如何触发该最优策略的。因此，大脑是如何选择一个使运动消耗成本最小化的解决方案，对该问题的理解尚不明确。

3）肌肉协同理论（muscle synergies theory）。该理论是一种模块化控制理论，通常认为层级控制的运动系统包含一组离散的低层级元素结构，可以减少由冗余控制问题引起的计算成本。这种低层级元素结构可被称为运动模块（motor modules）、运动原语（motor primitives），或在研究肌肉活动特征时，被称为肌肉协同。大脑明确地将真正的协同作用储存在特定的神经回路中，这些神经回路的联合作用产生对肌肉有任务效率的运动输入。该理论从生物力学分析角度来看，肌肉协同作用过程中，肌肉收缩产生人体多环节链运动时的肌肉力矩。然后，CNS通过整合互动力矩（interactive torque）、重力矩和接触力矩等，精妙准确地进行关节间动力学耦合控制（dynamic coupling）（Zajac et al.，1989），从而优美地完成既定运动目标（孙宇亮，2014）。例如，在上肢的运动协同控制方面，针对绘画任务中关节力矩和肌肉活动的研究表明，肩关节运动由该处的肌肉力矩驱动，而肘关节运动由肩关节处产生的互动力矩驱动，肌肉力矩仅负责调控互动力矩，由位于该关节的肌肉主动收缩来完成（Dounskaia et al.，2002）。另外，在下肢的运动协同控制方面，研究者们通过构建短跑时下肢的基于环节角的环节互动动力学模型，分析了小腿角加速度在髋、膝和足关节处的互动力矩（Hunter et al.，2004）。国内研究者在此基础上的研究表明，支撑期和摆动期时，强壮的股后肌群在这些关节处产生的肌肉力矩在整合、控制外力矩和互动力矩时十分重要（魏书涛 等，2010；Huang et al.，2013；Liu et al.，2017）。为完成目标活动任务，进行关节间动力学耦合控制，要求各相关肌肉群进行协同控制。因此，肌肉协同理论可较好揭示这一复杂运动过程的CNS冗余控制机制。

在人体的运动控制领域，对人体进行的从整体运动到某肢体运动的各种层面上的描述，都会涉及冗余控制的问题。Bernstein在1967年提出以肌肉群的概念解释CNS

在维持身体姿势中的冗余控制问题。在过去的几十年里，对人类和动物运动的研究积累了大量证据来支持神经肌肉骨骼系统模块化控制概念（Alessandro et al.，2013；Bizzi et al.，2008；Flash et al.，2005）。CNS通过结合相对较少的特定空间和/或时间的肌肉活动模式（即肌肉协同）生成必要的肌肉收缩模式来实现目标任务行为（Chiovetto et al.，2013；D'Avella et al.，2003）。

不同学者对肌肉协同给出了不同定义。Safavynia等（2011）认为，肌肉协同代表一个子运动任务库，神经系统可灵活结合其中的子运动任务来产生复杂而自然的运动。某个运动子任务（即肌肉协同）定义了身体各部分执行该任务所需的各肌肉共同激活的固定比例。D'Avella等（2003）认为，肌肉协同是能被下行神经控制信号调制的骨骼肌组合。具体来说，CNS通过某种线性组合的方式激活若干个具有不同功能性的模块化协同结构来完成复杂运动行为，这些协同结构的绝对激活水平由下行神经信号调控（Ting et al.，2007）。肌肉协同被认为是由CNS募集，通过灵活调控各肌肉收缩以完成各种日常行为动作的最小单位。综上，肌肉协同是可被下行神经信号调制，具有时间-空间固有激活特征的一组肌肉组合，是人体层级运动控制的基本控制单元。

1.1 肌肉协同降维特征

肌肉协同是CNS控制下可实现灵活控制以完成日常运动行为的由若干个肌肉组合。这种模块化的控制方式是解决Bernstein问题的有效途径，在人和动物的实验研究以及计算机模拟研究中得到证实。Berniker等（2009）建立了低维控制器模型，证明了降维控制策略可以在不影响结果表现的情况下简化控制过程。

1.2 肌肉协同的功能特征

肌肉协同的功能特征表现在：1）对同一任务，不同肌肉协同会被募集，且各肌肉协同有不同功能。例如，健康成年人手膝爬行时，可在各肢体中分别提取支撑相协同和摆动相协同，前者主要在爬行的支撑相激活，后者主要在摆动相激活（Chen et al.，2017）；2）对于不同运动任务，存在功能相似的肌肉协同。D'Avella等（2005）对青蛙在行走、跳跃、游泳运动研究发现，所提取的各个肌肉协同均被调用。肌肉协同自身决定了其功能，并可在不同的运动行为中被调用。Torres-Oviedo等（2006，2007）通过实验发现了其中某个协同对维持静态站姿下的四足间的相对平衡有重要作用。Chvatal等（2013）在研究静态站立受外部干扰时和步行时的肌肉活动时，提取出相似的肌肉协同。Barroso等（2014）从步行试验中提取的肌肉协同作用与骑自行车过程中提取的协同作用相似。完成不同任务时可能会募集相同的肌肉协同，而任务目标的特异性在个别具有特征性的肌肉协同中得到体现（Ting et al.，2007），对于肌肉协同功能特征的理解，有助于更好地理解运动的神经控制机制。

1.3 肌肉协同的增龄效应

在成人运动过程中，躯干和腿部肌肉的肌电活动是由一些与运动模式、方向、速度和身体支撑无关的肌肉协同来解释的（Clark et al.，2010；Ivanenko et al.，2004；Sheynikhovich et al.，2009）。关于肌肉协同的发展也有其他假设：1）成人所固化的肌肉协同模式是从最初大量的运动模式中选择出来的；2）原始模式被抛弃，取而代之的是全新的模式；3）原始模式被保留和调整，而新的模式在成长过程中被添加。很明显，这些假设反映了对神经网络发展过程中的不同约束。为了区分这些可能性，Dominici等（2011）比较了新生儿和学步儿童、学龄前儿童和成人的肌肉协同特征。研究发现，有2个肌肉协同模式在新生儿迈步阶段被保留，而另外2个肌肉协同模式在此阶段之后发展。而对于年轻人与老年人，老年人的肌肉协同特征减少并有所改变（Vernooij et al.，2016）。这也能反映出人类衰老不仅与个别肌肉的变化有关，还与它们之间的协调有关。

1.4 肌肉协同模型分类

肌肉协同通过选择一小部分肌肉来构建可在不同条件下执行任务目标的动作模块。肌肉协同之所以是动作模块，是因为它们反映一组在不同情况下可重复的激活肌肉激活模式。如公式（1）所示，用于将执行各种运动任务时收集的多通道sEMG信号矩阵$M_{X\times T}$，经矩阵分解提取肌肉协同后，包括反映空间特征的协同结构矩阵$W_{X\times S}$和反映时序特征的肌肉激活系数矩阵$C_{S\times T}$（其中X为肌电采集通道数，T为计算样本数量，S为肌肉协同数量，E为残差）。从空间上看，在不同肌肉间，一个$W_{X\times S}$能反映一组肌肉间激活强度关系。从时间上看，一个$C_{S\times T}$能反映一个肌肉协同结构中不同肌肉间的关系是时不变或时变的。根据不同的数学模型与理论假设，公式（1）表示的肌肉协同模型可分为时间型、同步型、时变型和统一型4种。

$$M_{X\times T}=W_{X\times S}\times C_{S\times T}+E \tag{1}$$

时间型肌肉协同（temporal muscle synergies，TEMMS）的数学模型如公式（2）所示，TEMMS属于时不变协同（time-invariant synergies）（Chiovetto et al.，2010，2012；Dominici et al.，2011；Ivanenko et al.，2004）。这里的"时不变"是指肌肉激活系数矩阵c_i不随时间变化而变化。c_i可通过简单地缩放和叠加在一起来重建每一块肌肉实际活动$m(t)$。P为时间肌肉协同数量。TEMMS可利用因子分析（factor analysis，FA）方法提取（Ivanenko et al.，2004）。

$$m(t)=\sum_{i=1}^{P}w_i(t)c_i+e \tag{2}$$

同步型肌肉协同（synchronous muscle synergies，SYNMS）的是一种时不变、空间固定的肌肉协同。数学模型与TEMMS较为相似，如公式（3）所示，其中N为空间肌肉协同数量，$m(t)$为在t时刻所采集的sEMG信号，$c_j(t)$为在t时刻第j个协同结构w_j中各肌肉的激活系数，e为残差。

在协同结构w_j中，所有包括的肌肉被同时激活，且相对激活水平不变。各个协同结构中肌肉的激活水平由与之唯一对应的一条肌肉激活曲线$c_j(t)$同步调控（Ting et al.，2012，2015）。

$$m(t)=\sum_{j=1}^{N}c_j(t)w_j+e \tag{3}$$

时变型肌肉协同（time-varying muscle synergies，TVAMS）是肌肉激活的内在时间-空间模式，肌肉激活模式由随时间变化的肌肉协同组合产生，也就是说，一组肌肉的协调激活与每一块肌肉的特定时间过程相结合（Bizzi et al.，2008；D'Avella et al.，2005；Dominici et al.，2011；Overduin et al.，2012；Scano et al.，2019）。肌电信号输出由各协同募集时的振幅和时间延迟决定。TVAMS模型如公式（4）所示，其中R为肌肉协同数量，e为残差，w_k为第k个协同结构。c_k和t_k分别为该协同对应的非负缩放系数和时间延迟，其中t_k负责调节w_k协同结构的激活时序，h_k负责控制w_k协同结构的激活水平。w_k中肌肉间的相对激活水平随时间变化，$w_k(t-t_k)$反映第k个协同在其激活起始时刻后$(t-t_k)$处的肌肉激活水平。TVAMS由D'Avella（2003）等首次提出，可利用类似于NMF的方法来提取。

$$m(t)=\sum_{k=1}^{R}c_k w_k(t-t_k)+e \tag{4}$$

统一型肌肉协同。统一型肌肉协同（unifying muscle synergies，UNFMS），也可称为时间×空间肌肉协同（space by time synergies）模型（Delis et al.，2014；Hinnekens et al.，2020）。时不变和时变UNFMS数学模型如公式（5）、公式（6）所示，单个肌肉模式都可以表示为时间模块$w_i(t)$和空间模块w_j的双重线性组合。P和N分别为时间模块和空间模块的数量。c_{ij}和t_{ij}分别为i时间模块、j空间模块的标量激活系数和时间延迟。神经生理学研究表明，肌肉激活模式可由空间模块或时间模块的肌肉协同模块进行组合产生，这是构成具备统一性UNFMS模型的证据。空间模块对应于所谓的同步、时不变或空间固定协同效应；时间模块对应于所谓的肌肉激活模式、前运动驱动、运动原语或时间固定协同效应。

$$m(t)=\sum_{i=1}^{P}\sum_{j=1}^{N}w_i(t)c_{ij}w_j+e \tag{5}$$

$$m(t)=\sum_{i=1}^{P}\sum_{j=1}^{N}w_i\left(t-t_{ij}\right)c_{ij}w_j+e \tag{6}$$

2 肌肉协同分析

肌电信号是深层肌肉活动的生理变化（电信号）直接测量得到的信号活动，能间接反映CNS的运动控制指令。因此，肌肉协同一般从肌肉活动数据中提取。sEMG因其采集时的无创性，使用较为广泛。sEMG肌肉协同分析（图1）通过对完成目标运动任务时肌肉产生的sEMG信号进行矩阵分解来进行，主要过程包括：1）sEMG预处理，目标是利用数字信号处理算法对原始sEMG信号进行预处理，得到归一化包络矩阵；2）肌肉协同提取，目的是将已进行预处理的sEMG信号进行矩阵分解，得到肌肉协同结构矩阵W和协同激活系数矩阵C；3）肌肉协同评价，对在不同变量条件下所提取的肌肉协同模式（协同结构、激活系数）进行相关性分析。

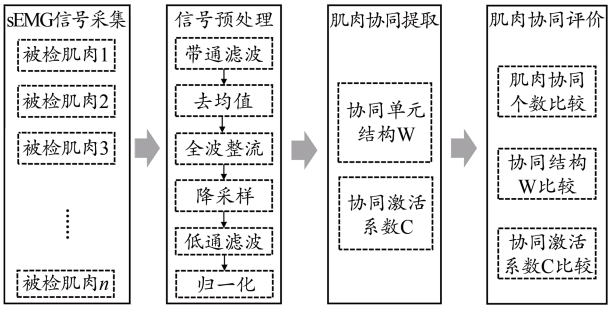

图1 肌肉协同分析流程

Figure 1. Procedure of Muscle Synergies Analysis

2.1 sEMG信号预处理

sEMG信号预处理通过在肌肉协同提取前依次经过带通滤波、去均值、全波整流、降采样、低通滤波和归一化等处理得到sEMG包络矩阵。带通滤波和陷波处理可消除漂移、混叠效应和工频干扰。低通滤波和高通滤波可分别消除高频噪声和运动伪影。全波整流用来计算sEMG包络线（Myers et al.，2003）。对经全波整流后的包络线低通滤波，可确保没有高频信号成分改变包络形状，且截止频率越低包络线越平滑。为保证不同对象或肌肉的sEMG同等重要性和处理结果不倾向幅值较大的信号，归一化常利用完成目标任务时的最大自主收缩（maximum voluntary vontraction，MVC）（Ting et al.，2005）、被检肌肉电信号的峰值或单位方差（Cheung et al.，2012）来计算，最终实现无偏协同提取。降采样利于降低计算成本，加快肌肉协同提取时的迭代收敛过程。Kieliba等（2018）比较了因选择不同归一化方法和带通滤波截止频率参数进行预处理而对肌肉协同提取与被试间相似性（inter-subject similarity，ISS）的影响，结果表明，无论是采用何种归一化（最大自主收缩MVC或信号自身最大振幅），还是带通滤波器（20～500 Hz或50～500 Hz）都没有显著改变协同权重。然而，归一化可改变一组协同的方差值。通过比较不同的低通滤波器（0.5 Hz、4 Hz、10 Hz、20 Hz）发现，增加低通滤波器的截止频率可以降低由一些肌肉协同的信息重构率（variability accounted for，VAF），并影响个体肌肉的贡献。低通滤波截止频率0.5 Hz时可使包络线极其平滑，并能增强活动肌肉和非活动肌肉的对比。

2.2 矩阵分解方法

肌肉协同提取通过对经预处理后的多通道sEMG信号包络线进行矩阵分解来实现。多通道sEMG信号的肌

肉协同结构（空间分布）及其激活系数（时间分布）的估计是一个盲源分离问题，可通过矩阵分解技术来估计基向量集（协同结构）。根据不同数学模型和对协同模块的不同约束假设（如正交性、独立性或非负性），可使用不同的矩阵分解算法来提取肌肉协同模块（Delis et al.，2014）。典型算法有主成分分析（principal component analysis，PCA）（Gorkovenko et al.，2019；Ranganathan et al.，2012）、FA（Ivanenko et al.，2004）、独立成分分析（independent component analysis，ICA）（Hyvärinen et al.，2000）、非负矩阵分解（non-negative matrix factorization，NMF）等（Lee et al.，1999；Tresch et al.，2006）。

矩阵分解算法的选择由肌肉协同数学模型和其约束条件来决定。例如，NMF假设待分解原始数据M、协同结构W和激活系数C是非负的。PCA是特征去均值化，使协同作用之间具有正交性。FA假设激活系数不相关。ICA假设激活系数统计独立。然而，多数算法识别非常相似的协同效应。另外，Tresch等（2006）比较了多种不同矩阵分解算法在模拟和实验数据集上的性能，结果表明，PCA在识别肌肉协同上较FA、ICA、NMF效果差得多。ICA对于有恒方差高斯噪声的数据处理效果良好，而当数据有信号相关噪声和协同激活因数相关时受损。NMF相比PCA、FA算法，在数据分析上鲁棒性较好。研究者也通过尝试其他矩阵分解算法来提取肌肉协同。Ebied等（2019）利用张量表征肌肉活动，首次提出一种基于高阶张量分解的肌肉协同提取方法——consTD。Ebied等（2018）提出，二阶盲源识别方法（second-order blind identification，SOBI）用于评估在腕关节运动分类，并比较PCA、ICA和NMF算法用于对模拟和sEMG实验数据进行肌肉协同提取的性能。结果表明：在没有降维情况下，SOBI比其他3种方法结果更好；在肌电电极数量有限时，SOBI方法更适用，但性能仍显不足。但当采集的肌电信号通道足够多时，NMF表现最佳。总体来说，NMF在生理学上与肌电信号更相关，因为非负值信号能很好地反映肌肉收缩行为（肌肉不能被“负”激活），从而具有更好的解释性，因此被广泛采用。

2.3 肌肉协同评价

2.3.1 肌肉协同数量

在分析不同姿势任务时肌肉协同的差异时，最常用的是比较所提取的肌肉协同数量。确定肌肉协同数量的最主要方法是基于VAF曲线的方法（Allen et al.，2019）。VAF的计算公式如公式（7）所示，其中X、T分别为被检肌肉数量和采样点数量。M为待分解的sEMG包络矩阵，M_{con}为所构造矩阵，根据肌肉协同模型不同而不同。VAF参数的取值范围为[0，1]。从矩阵分解角度来讲，肌肉协同数量越多，VAF值越大，表示重构精度越高，即M_{con}和M越接近。

基于VAF曲线确定肌肉协同数量的方法，大概可分为4种：1）VAF阈值法（Torres-Oviedo et al.，2006）。当VAF参数值大于设定阈值时，可认为所分解出肌肉协同矩阵W和C可充分重构原始sEMG信号。用于确定肌肉协同数量时，VAF阈值常设在0.80～0.95 SYNMS（Gizzi et al.，2011；Rodriguez et al.，2013）、0.65～0.80 TVAMS（D’Avella et al.，2005；Overduin et al.，2008）、0.9左右TEMMS等。2）VAF曲线趋直法（Cheung，2005）。当协同数目从1开始增加时，VAF斜率变化是一个由初期变化急剧、后期变化缓慢的过程，最后斜率值逐渐趋近于0，这意味着当前所取的肌肉协同数量n对于提升重构原始sEMG的效果不明显。因此，根据VAF曲线近似于直线时判定应提取的协同数目（Cheung et al.，2009；Santuz et al.，2020；Tresch et al.，2006）。3）VAF曲线斜率最大法（Tresch et al.，2006）。选取VAF斜率变换最大时对应的协同数量。4）VAF增量阈值法（Cheung et al.，2009）。选取当协同的提取数量进一步增加时，VAF的增加小于75%时对应的数量。

$$\mathrm{VAF}=1-\frac{\sum_{i=1}^{X}\sum_{j=1}^{T}\left(M-M_{\mathrm{con}}\right)^{2}}{\sum_{i=1}^{X}\sum_{j=1}^{T}\left(M-\overline{M}\right)^{2}} \tag{7}$$

基于VAF曲线方法因受人体执行目标任务时生物力学条件约束，导致确定协同的准确数量时并没有“金标准”。而且，肌肉协同的提取与数量选择，易受信号噪声的影响，换言之，基于VAF曲线方法，会将噪声引起的肌肉协同被提取出来。因此，有学者利用不同分类算法，如二次判别分析（quadratic siscriminant analysis，QDA）、线性判别分析法（Linear Discriminant Analysis，LDA）、朴素贝叶斯法（naive bayes，NB）和K最近邻（K-Nearest Neighbor，KNN）等和统计检验方法提出自动任务解码算法（Delis et al.，2013），以此选择最佳的肌肉协同数量。

2.3.2 肌肉协同的相似性

为了比较不同任务条件下的肌肉协同差异，通常使用皮尔森相关系数（Pearson’s correlation coefficient）、圆形互相关系数（circular cross-correlation coefficient）来度量不同肌肉协同结构矩阵或激活系数矩阵向量间的相似性（Frère et al.，2012）。皮尔森相关系数计算公式如公式（8）所示，当$r>0.9$时，即认为具有较强相似性。

$$r=\frac{n\sum_{i}^{n}x_i y_i-\sum_{i}^{n}x_i\sum_{i}^{n}x_i}{\sqrt{n\sum_{i}^{n}x_i^2-\left(\sum_{i}^{n}x_i\right)^2}\sqrt{\mathrm{n}\sum_{i}^{n}y_i^2-\left(\sum_{i}^{n}y_i\right)^2}} \tag{8}$$

3 肌肉协同理论应用

3.1 在体育科学中的应用

基于肌肉协同分析已经在各项体育活动研究中得以

应用（Vaz et al.，2016）。了解协同结构中各肌肉的相对激活水平有助于理解运动项目的规律，从而指导训练并降低受伤概率，最终提高运动表现。Matsunaga等（2017）分析了跑步10 min前后的肌肉协同：与之前的研究相似，肌肉协同数量一致；前3个肌肉协同相似，但第4个肌肉协同激活骨盆区域周围肌肉的活动从躯干区域开始，这可能是在脚部撞击时，更容易受伤的原因，因为肌肉协同因长时间跑步而改变，其姿势控制会从躯干转移到下肢。

对于体操项目，Frère等（2012）对9名国家级水平的体操运动员在完成向后大回环动作时的肌肉协同进行了研究，发现前2种肌肉协同在被试之间一致，但第3种协同表现出可变性。第3种协同作用的可变性可能与较低水平的神经控制有关，而与生物力学约束无关。躯干、手臂和肩膀肌肉的协同作用进一步限制了肩关节的伸展，从而降低了受伤的概率。

对于骑行项目，Hug等（2010）研究受过训练的骑行者的下肢肌肉活动，发现9名被试能提出相似的3个肌肉协同。Turpin等（2016，2017）研究了在高强度骑行中使用站立姿势相对于坐姿的优势，结果表明，在下肢肌肉方面，采用2种骑行姿势时的肌肉协同作用结构相似，但功率输出达到600 W时伸肌激活时间存在差异。因此，研究建议只有当功率输出大于600 W时，才能利用站立姿势。至于上肢肌肉，站立时更活跃，所以，即使上肢没有产生能量输出，教练员和运动员也应该训练肢体间的协调性，以提高运动员的成绩。因为协同作用激活系数和肌肉协同向量都能被技能学习所调节，所以，未经过训练的骑行者可以训练自己获得类似的肌肉，以提高运动表现。

对于赛艇项目，Shaharudin等（2014，2016）分析了未受训练的被试分别在滑动型和固定型的划船机上进行划船运动的差异，结果与以往的研究结果一致（Torres-Oviedo et al.，2010），肌肉协同的激活曲线被调节，但其协同结构保持不变。中枢神经系统对肌肉的激活权重分配有所不同，神经系统不断做出调整，以优化肌肉协同完成划船运动，使在滑动型划船机（腿部肌肉）和固定型划船机（背部肌肉）上划桨时减少损伤。研究建议在训练阶段进行肌肉协调性的优化，以提高训练的经济性。

对于冰上曲棍球项目，Kim等（2018）研究了韩国冰球国家队运动员和没有冰上运动或其他专业运动训练经验的健康成年人在平衡受到干扰时肌肉活动的差异。研究发现，在干扰起始阶段，优秀运动员中出现了与头部的控制有关特定肌肉协同。该协同可以反映头部位置突然改变时（如在轻快的加速和减速滑冰中）控制平衡的特殊能力。因此，冰球运动员通过平衡训练，避免了外部干扰而产生受伤的潜在风险。肌肉协同分析为这种训练策略提供了一种量化评价工具。

对于举重项目，Kristiansen等（2016）研究了不同力量训练是否会影响举重运动员和未接受训练对象在卧推时的肌肉协同变异性。经过5周的卧推力量训练后，肌肉协同有一个对象内变异，而那些未接受训练的对象则没有这种变异。根据所获得的结果，肌肉协同的内部组成可以作为评价运动员卧推成绩的一个指标。因此，教练员可以考虑在训练和康复计划中监测肌肉协同的变化，从而合理完善和评估训练内容。

这类研究主要关注肌肉协同分析在运动训练中的应用，此外，肌肉协同理论在人体多关节运动控制仿真中也得到了应用（Ezati et al.，2019）。Meyer等（2016）提出一种基于肌肉协同的神经肌肉骨骼仿真框架来预测中风患者的步行运动。通过建立3种不同模型——肌肉激活控制模型（每条腿35块）、关节扭矩控制模型和肌肉协同控制模型（每条腿5个），对比分析和评估了3种模型在2种速度（0.5 m/s和0.8 m/s）下被试的步行运动学和动力学的能力。研究发现，在0.5 m/s的模型校准速度下，这3种控制方法都能很好地预测受试者的行走运动学和动力学参数；而速度为0.8 m/s时，只有肌肉激活控制模型和肌肉协同控制模型才能很好地预测，且肌肉协同控制模型可以最准确地预测新的步态周期。当预测被试如何以1.1 m/s的速度行走时，肌肉协同控制模型可预测步态周期，并且接近根据步速和步幅之间的线性关系所估算的步态周期。Shourijeh等（2020）为解决步行生物力学仿真中静态优化时，最小化拮抗肌的共激活以及可能的关节僵硬等问题，提出一种协同优化算法（synergy optimization，SynO）。该算法优化估算肌肉激活上的协同结构如何影响步行过程中计算出的下半身关节刚度。随着协同个数从2增加到6时，髋部和膝盖屈曲的最大和平均关节刚度降低，而静态优化算法产生最低的关节刚度值，结果表明，SynO可通过增加肌肉的共同激活作用来增加关节的僵硬度，而且以较少数量的肌肉协同作用行走会导致关节僵硬度增加，甚至可能增加稳定性。

3.2 在临床上的应用

中风、脑瘫、脊髓损伤和帕金森病等患者常伴有运动功能障碍，其主要病因是神经功能障碍。临床上，因为运动过程中的神经活动难以直接测量，所以大多数运动能力评估测试都集中在行为和运动学水平上进行（瓮长水等，2004；尹傲冉 等，2014；Safavynia et al.，2011）。但行为或运动学结果的改变可能是由多种不同的神经功能异常导致。肌肉活动反映了运动神经元活动，因此，对运动功能障碍人群进行肌肉协同分析，有利于识别执行各种任务时的大脑活动变化。Cheung等（2012）研究了不同严重程度中风患者患侧和健侧的手臂肌肉协同特征，揭示了皮质损伤后肌肉协同的3种不同作用模式——保留（preservation）、合并（merging）和分级（fractionation）。在同一患者中可能同时存在2个或所有的肌肉协同作用模

式。另外，这些模式与运动功能受损程度和中风后的持续时间有关。对于轻、中度患者，健侧和患侧的肌肉协同属保留模式，尽管激活系数有差异，但协同结构相似；对重度患者，患侧的肌肉协同数量减少，属合并模式。其他学者对中风后亚急性患者步态期间肌肉协同的研究表明，肌肉协同的合并模式是亚急性脑卒中患者的重要标志，运动功能改变并不依赖于肌肉协同的数量，其合并程度与肌肉力量的增加和踝关节角度范围的增加负相关（Hashiguchi et al.，2016）。肌肉协同的分级机制仅在中风多年后的慢性中风患者中发现，患侧的肌肉协同数量较健侧有所增加，而且是健侧肌肉协同的分级。肌肉协同的这种分级机制可增加四肢和肌肉控制的灵活性，弥补中风导致的远端关节运动受损。Steele 等（2015）在研究脑瘫患者步态过程时发现，与健康的受试者相比，脑瘫患者肌肉协同数量减少。Fox 等（2013）研究了不完全脊髓损伤儿童在完成不同任务活动时的肌肉协同表现，结果发现与健康儿童相比，他们的肌肉协同数量减少。

国内学者也利用肌肉协同分析，在脑瘫、中风患者的临床康复与评价应用上进行了研究（汤璐，2017；Ji et al.，2018）。肌肉协同分析为临床医生提供洞察潜在的神经运动策略和肌肉活动的功能结果。

3.3 在机器人控制方面的应用

受人体姿势控制理论的启发，肌肉协同分析技术在基于 sEMG 的实时假肢，如手（Catalano et al.，2014）、上肢（Rasool et al.，2016）、下肢（Afzal et al.，2017）等控制中应用较多（Alessandro et al.，2013），其主要思路是利用肌肉协同分解提取运动意图特征，从而识别目标任务特征。例如，Choi 等（2011）使用非负性肌肉协同矩阵，将前臂肌肉活动映射到 4 个预定义的腕关节运动意图（屈/伸和桡/尺侧活动）。类似地，Jiang 等（2014）使用 NMF 算法提取肌肉协同，随后使用该算法实时获取控制信号控制手腕屈/伸和旋前/旋后。Berniker 等（2009）利用肌肉协同和低维模型构建了一个性能接近全维控制器的简化控制器。Rasool 等（2016）提出一种基于肌肉协同的任务识别算法（muscle synergy based task discrimination，MSD）控制下臂假肢，通过概率独立成分分析（probabilistic independent component analysis，pICA）来获得特定任务的肌肉协同。然后根据状态空间的过程动力学模型，并结合一个有约束的卡尔曼滤波器来实时估计控制信号。基于肌肉协同理论的在机器人假肢控制，可实现更灵活的动作控制。

4 总结与展望

肌肉协同理论认为复杂人体运动的冗余控制是以肌肉协同为基本单元来进行的，它假定 CNS 使用少量肌肉协同的灵活组合来激活肌肉。肌肉协同理论的研究已取得较大进展，研究者常通过 2 种不同方法产生肌肉活动验证肌肉协同假设：1）直接刺激运动系统；2）使人类或动物执行具体目标行为。前者是人为地刺激神经系统中的多个位置，可产生相对较少的肌肉激活模式。一部分对脊椎动物直接刺激其运动系统的研究为肌肉协同理论提供了生理学证据，且另一部分研究通过对行为过程中 sEMG 的统计分析提取出肌肉协同也可检验这个假设，但这些研究一些证据仍是间接的，难以证伪。有部分与之相矛盾的实验对这一假设提出了挑战，这类研究的主要观点在于肌肉协同反映任务约束，而不能反映 CNS 的运动控制策略。因此，需要有更能批判性地评估这一假设的实验。

为了验证肌肉协同理论，获得直接证据，未来关于肌肉协同的研究方向有：1）通过设计多样化任务实验范式，营造多自由度的冗余控制环境来验证肌肉协同。实验设计的关键是在足够丰富的行为条件下检查记录的 sEMG。肌肉协同可以解释的行为条件的范围越广，这种解释的支持就越多；2）通过理论建模工作来严格检验肌肉协同的模块化假设并评估其潜在的神经起源。肌肉协同理论是一种不同于最优化理论的方法，但并不互相排斥。在肌肉活动中发现的维数减少可能是最优化控制的一种结果，不能归因于严格意义上的神经硬连线协同效应，特别是当肌肉协同是通过对任务执行过程中的 sEMG 信号进行矩阵分解提取出来时。

参考文献：

林辉杰，严波涛，刘占锋，等，2012. 运动协调的定量方法以及在专项技术分析领域的研究进展[J]. 体育科学，32(3)：81-91.

刘宇，2010. 生物力学在运动控制与协调研究中的应用[J]. 体育科学，30(11)：62-73.

钱学森，于景元，戴汝为，1990. 一个科学新领域：开放的复杂巨系统及其方法论[J]. 自然杂志，13(1)：3-10.

孙宇亮，2014. 走、跑过程中人体下肢多关节运动控制策略的研究[D]. 上海：上海体育学院.

汤璐，2017. 小儿脑瘫运动功能障碍评估研究[D]. 合肥：中国科学技术大学.

王爱文，罗冬梅，2017. 人体运动控制理论及计算模型的研究进展[J]. 体育科学，37(8)：58-68.

王楚婕，王健，2013. 姿势控制增龄化研究进展[J]. 中国康复医学杂志，28(5)：483-486.

王健，袁立伟，张芷，等，2017. 视觉预期和注意指向对姿势和动作肌肉预期和补偿姿势调节的影响[J]. 心理学报，49(7)：920-927.

王开元，刘宇，2018. “神经启动”技术增强运动表现[J]. 体育科学，38(1)：96-97.

魏书涛，刘宇，傅维杰，等，2010. 短跑运动控制的生物力学分析[J]. 体育科学，30(9)：37-43.

瓮长水，赵承军，毕胜，等，2004. 脑卒中偏瘫患者静态和动态平衡评定的研究[J]. 中国康复理论与实践，10(1)：50-52.

尹傲冉，倪朝民，2014. 脑卒中患者不对称步态与平衡控制的研究进展[J]. 中国康复医学杂志，29(9)：897-900.

AFZAL T，IQBAL K，WHITE G，et al.，2017. A method for locomotion mode identification using muscle synergies[J]. IEEE T Neur

Sys Reh，25(6)：608-617.

ALESSANDRO C，DELIS I，NORI F，et al.，2013. Muscle synergies in neuroscience and robotics：from input-space to task-space perspectives[J]. Front Comput Neurosc，doi：10.3389/fncom.2013.00043.

ALLEN J L，KESAR T M，TING L H，2019. Motor module generalization across balance and walking is impaired after stroke[J]. J Neurophysiol，122(1)：277-289.

BARROSO F O，TORRICELLI D，MORENO J C，et al.，2014. Shared muscle synergies in human walking and cycling[J]. J Neurophysiol，112(8)：1984-1998.

BERNIKER M，JARC A，BIZZI E，et al.，2009. Simplified and effective motor control based on muscle synergies to exploit musculoskeletal dynamics[J]. P Natl Acad Sci USA，106(18)：7601-7606.

BERNSTEIN N，1967. The Coordination and Regulation of Movements[M]. New York：Pergamon Press.

BERRET B，DELIS I，GAVEAU J，et al.，2019. Optimality and Modularity in Human Movement：From Optimal Control to Muscle Synergies[M]// VENTURE G. Biomechanics of Anthropomorphic Systems. Cham，Switzerland：Springer，Cham：105-133.

BIZZI E，CHEUNG V C K，D'AVELLA A，et al.，2008. Combining modules for movement[J]. Brain Res Rev，57(1)：125-133.

CATALANO M G，GRIOLI G，FARNIOLI E，et al.，2014. Adaptive synergies for the design and control of the Pisa/IIT SoftHand[J]. Int J Robot Res，33(5)：768-782.

CHEN X，NIU X，WU D，et al.，2017. Investigation of the intra-and inter-limb muscle coordination of hands-and-knees crawling in human adults by means of muscle synergy analysis[J]. Entropy-Switz，doi：10.3390/e19050229.

CHENG R，SUI Y，SAYENKO D，et al.，2019. Motor control after human SCI through activation of muscle synergies under spinal cord stimulation[J]. IEEE T Neur Sys Reh，27(6)：1331-1340.

CHEUNG V C K，2005. Central and sensory contributions to the activation and organization of muscle synergies during natural motor behaviors[J]. J Neurosci，25(27)：6419-6434.

CHEUNG V C K，PIRON L，AGOSTINI M，et al.，2009. Stability of muscle synergies for voluntary actions after cortical stroke in humans[J]. P Natl Acad Sci USA，106(46)：19563-19568.

CHEUNG V C K，TUROLLA A，AGOSTINI M，et al.，2012. Muscle synergy patterns as physiological markers of motor cortical damage[J]. P Natl Acad Sci USA，109(36)：14652-14656.

CHIOVETTO E，BERRET B，DELIS I E A，2013. Investigating reduction of dimensionality during single-joint elbow movements：A case study on muscle synergies[J]. Front Comput Neurosc，doi：10.3389/fncom.2013.00011.

CHIOVETTO E，BERRET B，POZZO T，2010. Tri-dimensional and triphasic muscle organization of whole-body pointing movements[J]. Neuroscience，170(4)：1223-1238.

CHIOVETTO E，PATANÈ L，POZZO T，2012. Variant and invariant features characterizing natural and reverse whole-body pointing movements[J]. Exp Brain Res，218(3)：419-431.

CHOI C，KIM J，2011. Synergy matrices to estimate fluid wrist movements by surface electromyography[J]. Med Eng Phys，33(8)：916-923.

CHVATAL S A，TING L H，2013. Common muscle synergies for balance and walking[J]. Front Comput Neurosc，doi：10.3389/fncom.2013.00048.

CLARK D J，TING L H，ZAJAC F E，et al.，2010. Merging of healthy motor modules predicts reduced locomotor performance and muscle coordination complexity post-stroke[J]. J Neurophysiol，103(2)：844-857.

D'AVELLA A，BIZZI E，2005. Shared and specific muscle synergies in natural motor behaviors[J]. P Natl Acad Sci USA，102(8)：3076-3081.

D'AVELLA A，SALTIEL P，BIZZI E，2003. Combinations of muscle synergies in the construction of a natural motor behavior[J]. Nat Neurosci，6(3)：300-308.

DELIS I，BERRET B，POZZO T，et al.，2013. Quantitative evaluation of muscle synergy models：A single-trial task decoding approach[J]. Front Comput Neurosci，doi：10.3389/fncom.2013.00008.

DELIS I，PANZERI S，POZZO T，et al.，2014. A unifying model of concurrent spatial and temporal modularity in muscle activity[J]. J Neurophysiol，111(3)：675-693.

DESROCHERS E，HARNIE J，DOELMAN A，et al.，2019. Spinal control of muscle synergies for adult mammalian locomotion[J]. J Physiol，597(1)：333-350.

DOMINICI N，IVANENKO Y P，CAPPELLINI G，et al.，2011. Locomotor primitives in newborn babies and their development[J]. Science，334(6058)：997-999.

EBIED A，KINNEY-LANG E，SPYROU L，et al.，2019. Muscle activity analysis using higher-order tensor models：Application to muscle synergy identification[J]. IEEE Access，7：27257-27271.

EBIED A，KINNEY-LANG E，SPYROU L，et al.，2018. Evaluation of matrix factorisation approaches for muscle synergy extraction[J]. Med Eng Phys，57：51-60.

EZATI M，GHANNADI B，MCPHEE J，2019. A review of simulation methods for human movement dynamics with emphasis on gait[J]. Multibody Syst Dyn. 47(3)：265-292.

FLASH T，HOCHNER B，2005. Motor primitives in vertebrates and invertebrates[J]. Curr Opin Neurobiol，15(6)：660-666.

FOX E J，TESTER N J，KAUTZ S A，et al.，2013. Modular control of varied locomotor tasks in children with incomplete spinal cord injuries[J]. J Neurophysiol，110(6)：1415-1425.

FRÈRE J，HUG F，2012. Between-subject variability of muscle synergies during a complex motor skill[J]. Front Comput Neurosc，doi：10.3389/fncom.2012.00099.

GIZZI L，NIELSEN J F，FELICI F，et al.，2011. Impulses of activation but not motor modules are preserved in the locomotion of subacute stroke patients[J]. J Neurophysiol，106(1)：202-210.

GORKOVENKO A V，LEHEDZA O V，ABRAMOVYCH T I，et al.，2019. Evaluation of the complexity of control of simple linear hand movements using principal component analysis[J]. Neurophysiology，51(2)：132-140.

HASHIGUCHI Y，OHATA K，KITATANI R，et al.，2016. Merging and fractionation of muscle synergy indicate the recovery process in patients with hemiplegia：The first study of patients after subacute stroke[J]. Neural Plast，doi：10.1155/2016/5282957.

HINNEKENS E，BERRET B，DO M，et al.，2020. Modularity underlying the performance of unusual locomotor tasks inspired by developmental milestones[J]. J Neurophysiol，123(2)：496-510.

HIRASHIMA M，OYA T，2016. How does the brain solve muscle redundancy? Filling the gap between optimization and muscle synergy hypotheses[J]. Neurosci Res，104：80-87.

HUANG L，LIU Y，WEI S，et al.，2013. Segment-interaction and its relevance to the control of movement during sprinting[J]. J Biomech，46(12)：2018-2023.

HUG F，TURPIN N A，GUÉVEL A，et al.，2010. Is interindividual

variability of EMG patterns in trained cyclists related to different muscle synergies?[J]. J Appl Physiol，108(6)：1727-1736.

HUNTER J P，MARSHALL R N，MCNAIR P J，2004. Segment-interaction analysis of the stance limb in sprint running[J]. J Biomech，37(9)：1439-1446.

HYVÄRINEN A，OJA E，2000. Independent component analysis：Algorithms and applications[J]. Neural Networks，13(4-5)：411-430.

ISRAELY S，LEISMAN G，CARMELI E，2018. Neuromuscular synergies in motor control in normal and poststroke individuals[J]. Rev Neurosci，29(6)：593-612.

IVANENKO Y P，POPPELE R E，LACQUANITI F，2004. Five basic muscle activation patterns account for muscle activity during human locomotion[J]. J Physiol，556(1)：267-282.

JI Q，WANG F，ZHOU R，et al.，2018. Assessment of ankle muscle activation by muscle synergies in healthy and post-stroke gait[J]. Physiol Meas，doi：10.1088/1361-6579/aab2ed.

JIANG N，REHBAUM H，VUJAKLIJA I，et al.，2014. Intuitive，online，simultaneous，and proportional myoelectric control over two degrees-of-freedom in upper limb amputees[J]. IEEE T Neur Sys Reh，22(3)：501-510.

KIELIBA P，TROPEA P，PIRONDINI E，et al.，2018. How are muscle synergies affected by electromyography pre-processing?[J]. IEEE T Neur Sys Reh，26(4)：882-893.

KIM M，KIM Y，KIM H，et al.，2018. Specific muscle synergies in national elite female ice hockey players in response to unexpected external perturbation[J]. J Sport Sci，36(3)：319-325.

KRISTIANSEN M，SAMANI A，MADELEINE P，et al.，2016. Effects of 5 weeks of bench press training on muscle synergies：A randomized controlled study[J]. J Strength Cond Res，30(7)：1948-1959.

KUTCH J J，KUO A D，BLOCH A M，et al.，2008. Endpoint force fluctuations reveal flexible rather than synergistic patterns of muscle cooperation[J]. J Neurophysiol，100(5)：2455-2471.

LATASH M L，2012. The bliss（not the problem）of motor abundance（not redundancy）[J]. Exp Brain Res，217(1)：1-5.

LATASH M L，SCHOLZ J P，SCHOENER G，2007. Toward a new theory of motor synergies[J]. Motor Control，11(3)：276-308.

LATASH M L，SCHOLZ J P，SCHÖNER G，2002. Motor control strategies revealed in the structure of motor variability[J]. Exerc Sport Sci Rev，30(1)：26-31.

LEE D D，SEUNG H S，1999. Learning the parts of objects by non-negative matrix factorization[J]. Nature，401(6755)：788-791.

LIU Y，SUN Y，ZHU W，et al.，2017. The late swing and early stance of sprinting are most hazardous for hamstring injuries[J]. J Sport Health Sci，6(2)：133-136.

MATSUNAGA N，IMAI A，KANEOKA K，2017. Comparison of muscle synergies before and after 10 minutes of running[J]. J Phys Ther Sci，29(7)：1242-1246.

MEYER A J，ESKINAZI I，JACKSON J N，et al.，2016. Muscle synergies facilitate computational prediction of Subject-Specific walking motions[J]. Front Bioeng Biotechnol，doi：10.3389/fbioe.2016.00077.

MYERS L J，LOWERY M，O'MALLEY M，et al.，2003. Rectification and non-linear pre-processing of EMG signals for cortico-muscular analysis[J]. J Neurosci Meth，124(2)：157-165.

OVERDUIN S A，D AVELLA A，CARMENA J M，et al.，2012. Microstimulation activates a handful of muscle synergies[J]. Neuron，76(6)：1071-1077.

OVERDUIN S A，D'AVELLA A，ROH J，et al.，2008. Modulation of muscle synergy recruitment in primate grasping[J]. J Neurosci，28(4)：880-892.

RANGANATHAN R，KRISHNAN C，2012. Extracting synergies in gait：Using EMG variability to evaluate control strategies[J]. J Neurophysiol，108(5)：1537-1544.

RASOOL G，IQBAL K，BOUAYNAYA N，et al.，2016. Real-time task discrimination for myoelectric control employing task-specific muscle synergies[J]. IEEE T Neur Sys Reh，24(1)：98-108.

RODRIGUEZ K L，ROEMMICH R T，CAM B，et al.，2013. Persons with Parkinson's disease exhibit decreased neuromuscular complexity during gait[J]. Clin Neurophysiol，124(7)：1390-1397.

SAFAVYNIA S A，TORRES-OVIEDO G，TING L H，2011. Muscle synergies：Implications for clinical evaluation and rehabilitation of movement[J]. Top Spinal Cord Inj Rehabil，17(1)：16-24.

SANTUZ A，BRÜLL L，EKIZOS A，et al.，2020. Neuromotor dynamics of human locomotion in challenging settings[J]. iScience，doi：10.1016/j.isci.2019.100796.

SCANO A，DARDARI L，MOLTENI F，et al.，2019. A comprehensive spatial mapping of muscle mynergies in mighly variable upper-limb movements of healthy subjects[J]. Front Physiol，doi：10.3389/fphys.2019.01231.

SHAHARUDIN S，AGRAWAL S，2016. Muscle synergies during incremental rowing VO_{2max} test of collegiate rowers and untrained subjects[J]. J Sport Med Phys Fit，56(9)：980-989.

SHAHARUDIN S，ZANOTTO D，AGRAWAL S，2014. Muscle synergies of untrained subjects during 6 min maximal rowing on slides and fixed ergometer[J]. J Sport Sci Med，13(4)：793-800.

SHEYNIKHOVICH D，CHAVARRIAGA R，STRÖSSLIN T，et al.，2009. Is there a geometric module for spatial orientation? Insights from a rodent navigation model[J]. Psychol Rev，116(3)：540-566.

SHOURIJEH M S，FREGLY B J.，2020. Muscle synergies modify optimization estimates of joint stiffness during walking[J]. J Biomec Eng，doi：10.1115/1.4044310.

SINGH R E，IQBAL K，WHITE G，et al.，2018. A systematic review on muscle synergies：From building blocks of motor behavior to a neurorehabilitation tool[J]. Appl Bionics Biomech，(2)：1-15.

STEELE K M，ROZUMALSKI A，SCHWARTZ M H，2015. Muscle synergies and complexity of neuromuscular control during gait in cerebral palsy[J]. Dev Med Child Neurol，57(12)：1176-1182.

TING L H，CHIEL H J，TRUMBOWER R D，et al.，2015. Neuromechanical principles underlying movement modularity and their implications for rehabilitation[J]. Neuron，86(1)：38-54.

TING L H，CHVATAL S A，SAFAVYNIA S A，et al.，2012. Review and perspective：Neuromechanical considerations for predicting muscle activation patterns for movement[J]. Int J Numer Meth Bio，28(10)：1003-1014.

TING L H，MACPHERSON J M，2005. A limited set of muscle synergies for force control during a postural task[J]. J Neurophysiol，93(1)：609-613.

TING L H，MCKAY J L，2007. Neuromechanics of muscle synergies for posture and movement[J]. Curr Opin Neurobiol，17(6)：622-628.

TORRES-OVIEDO G，MACPHERSON J M，TING L H，2006. Muscle synergy organization is robust across a variety of postural perturbations[J]. J Neurophysiol，96(3)：1530-1546.

TORRES-OVIEDO G，TING L H，2007. Muscle synergies characterizing human postural responses[J]. J Neurophysiol，98(4)：2144-2156.

TORRES-OVIEDO G，TING L H，2010. Subject-specific muscle syn-

ergies in human balance control are consistent across different biomechanical contexts[J]. J Neurophysiol, 103(6): 3084-3098.

TRESCH M C, CHEUNG V C K, D'AVELLA A, 2006. Matrix factorization algorithms for the identification of muscle synergies: Evaluation on simulated and experimental data sets[J]. J Neurophysiol, 95(4): 2199-2212.

TRESCH M C, SALTIEL P, BIZZI E, 1999. The construction of movement by the spinal cord[J]. Nat Neurosci, 2(2): 162-167.

TURPIN N A, COSTES A, MORETTO P, et al., 2016. Upper limb and trunk muscle activity patterns during seated and standing cycling[J]. J Sport Sci, 35(6): 557-564.

TURPIN N A, COSTES A, MORETTO P, et al., 2017. Can muscle coordination explain the advantage of using the standing position during intense cycling?[J]. J Sci Med Sport, 20(6): 611-616.

VALERO-CUEVAS F J, VENKADESAN M, TODOROV E, 2009. Structured variability of muscle activations supports the minimal intervention principle of motor control[J]. J Neurophysiol, 102(1): 59-68.

VAZ J R, OLSTAD B H, CABRI J, et al., 2016. Muscle coordination during breaststroke swimming: comparison between elite swimmers and beginners[J]. J Sport Sci, 34(20): 1941-1948.

VERNOOIJ C A, RAO G, BERTON E, et al., 2016. The effect of aging on muscular dynamics underlying movement patterns changes[J]. Front Aging Neurosci, doi: 10.3389/fnagi.2016.00309.

WINTER D A, 1980. Overall principle of lower limb support during stance phase of gait[J]. J Biomech, 13(11): 923-927.

WINTER D A, 2009. Biomechanics and motor control of human movement[M]. Fourth ed. New Jersey, USA: John Wiley & Sons.

ZAJAC F E, GORDON M E, 1989. Determining muscle's force and action in multi-articular movement[J]. Exerc Sport Sci Rev, 17(1): 187-230.

Research Progress and Prospect of Muscle Synergies Theory for Redundancy Control of Complex Human Movement

YANG Yi[1], PENG Yuxin[1], HAO Zengming[1], LIU Yu[2], WANG Xin[3], WANG Jian[4, 5*]

1. College of Education, Zhejiang University, Hangzhou 310028, China; 2. Shanghai University of Sport, Shanghai 200438, China; 3. Shenyang Sport University, Shenyang 110102, China; 4. Institute of Kinesiology and Sports Engineering, Zhejiang University, Hangzhou 310028; 5. Center for Psychological Sciences, Zhejiang University, Hangzhou 310028, China

Abstract: The neuromuscular system is an open complex giant system. The coordination between the central nervous system and activities of different muscles is a long-standing core scientific theoretical problem in sports neuroscience research. In the field of human motor control, redundancy control not only exits in the description of whole-body movement but also the description of local limb movement. Muscle synergies theory suggests that the nervous system can reduce the computational burden of redundancy control through modular control by recruiting several muscles simultaneously. This study retrospected the origin and basic viewpoints of muscle synergies theory, and summarized the mathematical models and basic process of muscle synergies analysis. In addition, this study focused on the application of muscle synergies theory in sports science, clinic and robot control. Although there are different views on the physiological evidence of muscle synergies theory, studies have confirmed that muscle synergies exist in vertebrate and human redundancy control systems, which can well explain the central nervous system's control mechanism of muscle activity. Future research should still focus on the exploration of modular hypothesis and mechanisms of muscle synergies by designing experimental paradigms for diverse tasks and theoretical modeling work.

Keywords: *human movement; motor control; redundancy control; muscle synergies*

体育科学（月刊）

2020年(第40卷)第12期

1981年创刊

主　　管：国家体育总局

主　　办：中国体育科学学会

编辑出版：国家体育总局体育科学研究所

《体育科学》编辑部

印　　刷：廊坊市百花印刷有限公司

国内发行：北京市报刊发行局

国内订阅：全国各邮政局

国外发行：中国国际图书贸易集团有限公司

国外发行代号：BM708

地　　址：北京体育馆路11号

邮政编码：100061

电　　话：010-87182590　87182589

网　　址：www.cisszgty.com

邮　　箱：bjb@ciss.cn

CHINA SPORT SCIENCE

Vol. 40, No.12, December, 2020

Founded in 1981

Administrated by General Administration of Sport of China

Sponsored by China Sport Science Society

Edited by the Editorial Department of CHINA SPORT SCIENCE of the China Institute of Sport Science

Domestic Distribution: Beijing Bureau for Distribution of Newspapers and Journals

Oversea Distribution: China International Book Trading Corporation, Beijing 100044, China, BM708

Address: 11 Tiyuguan Road, Beijing, P.R.China

ZIP Code: 100061

Tel: 8610-87182590　87182589

http://www.cisszgty.com

E-mail: bjb@ciss.cn

ISSN 1000-677X

CN 11-1295/G8

邮发代号：2-436

期刊出版许可证 京期出证字第0165号

国内定价：每册25元 全年300元　每月15日出版

ISSN 1000-677X

12>

9 771000 677202

ISSN 0371-0874
CN 31-1352/Q

生理学报

Acta Physiologica Sinica

Volume 75, Number 6, December 25, 2023

健康衰老专辑

专辑主编：张 星，陈厚早，冯智辉，肖意传，高 峰

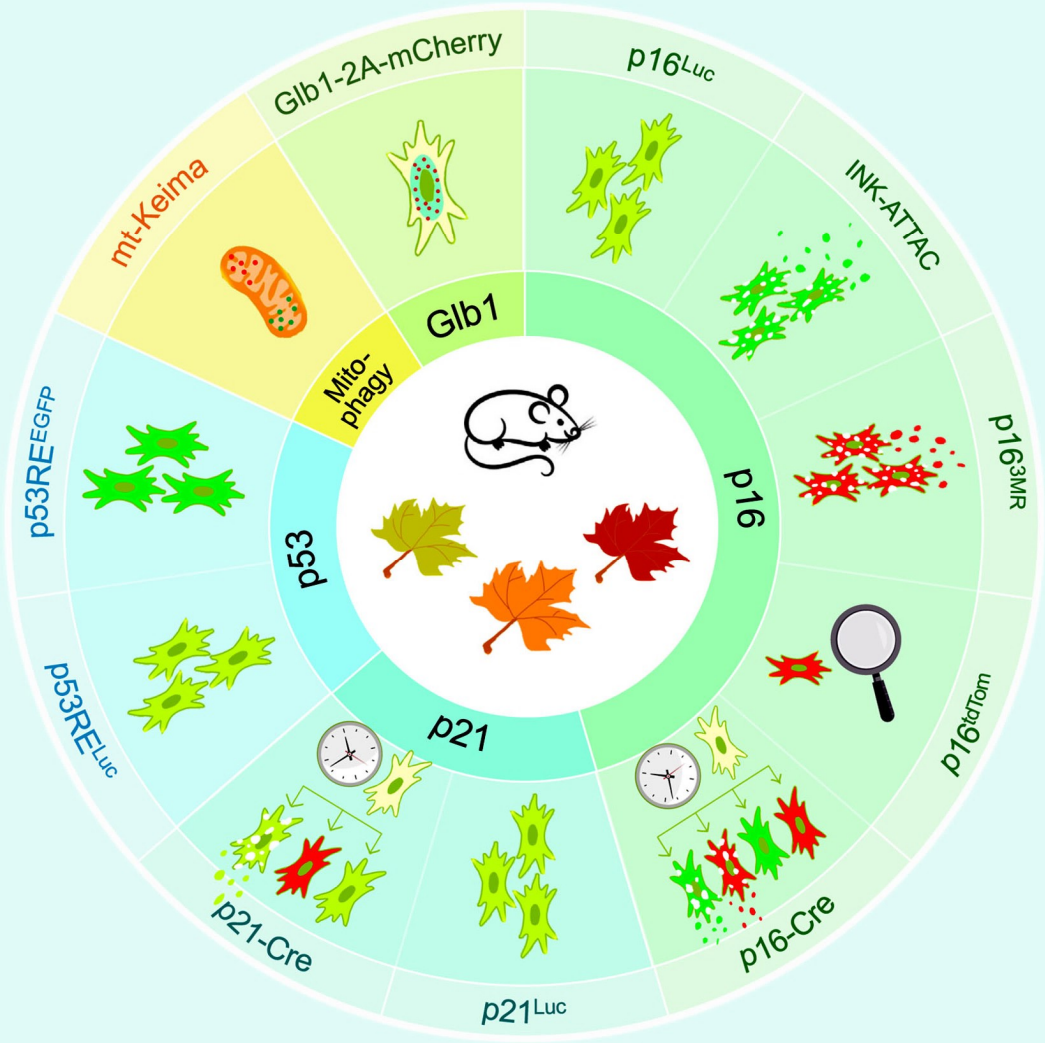

Live-imaging aging reporter mice (see pages 836–846)

中 国 科 学 院 主管
中国科学院上海营养与健康研究所
中 国 生 理 学 会 主办
《 生 理 学 报 》 编 辑 部 出版

生理学报 SHENGLI XUEBAO

2023年12月25日　　第75卷 第6期

(继续《中国生理学杂志》 1927年创刊)

目　次

健康衰老专辑

编者按

综述

研究论文

ACTA PHYSIOLOGICA SINICA

Vol. 75, No. 6, December 25, 2023

(Continuing *The Chinese Journal of Physiology* Started in 1927)

CONTENTS

Special Issue on Healthy Aging

EDITORIAL

REVIEWS

ORIGINAL ARTICLES

生理学报 *Acta Physiologica Sinica*, December 25, 2023, 75(6): 918–926
DOI: 10.13294/j.aps.2023.0089 http://www.actaps.com.cn; https://actaps.sinh.ac.cn

研究论文

视觉-前庭觉输入一致性影响老年人站姿稳定性及其脑电图脑网络特征

杨 毅[1]，王国正[2]，华安珂[1]，郝增明[3]，黄 聪[1]，刘 军[2]，王 健[1,*]

浙江大学[1]运动科学与健康工程研究所；[2]生物医学工程学院，杭州 310028；[3]中山大学附属第一医院，广州 510062

摘 要：衰老是影响站姿稳定性控制和导致跌倒频发的重要因素，但其作用机制尚不完全清楚。本研究旨在通过对比老年人和青年人在视觉-前庭觉输入一致和冲突条件下站姿稳定性及站姿脑电图(electroencephalogram, EEG)脑网络节点连接强度的差异，探讨衰老弱化站姿稳定性控制的EEG脑网络节点连接强度效应。无神经肌肉系统疾病的老年人(n = 18)和青年人(n = 18)志愿者参与本研究。用虚拟现实技术(virtual reality, VR)操作视觉旋转刺激(顺时针和逆时针)，用水平旋转平台操作前庭觉旋转刺激(顺时针)，根据感觉输入在水平面的方向差异性将视觉和前庭觉输入一致性分为视觉-前庭觉输入一致和视觉-前庭觉输入冲突。依据站姿足底压力中心(center of pressure, COP)移动轨迹检测站姿稳定性，用EEG信号采集和有向网络分析技术观察EEG脑网络连接节点连接强度。结果显示，老年人在视觉-前庭觉输入冲突条件下COP前后方向摆动速度、总轨迹长以及前后和左右方向样本熵等站姿稳定性表现方面明显不及青年人，视皮质节点连接强度明显大于青年人，颞上皮质节点连接强度明显低于青年人。以上结果提示，老年人在站姿平衡控制中对视觉依赖性高；老年人无法很好应对视觉-前庭觉输入不一致引起的感觉冲突，导致站姿稳定性差。本研究结果对今后老年人平衡功能评估和跌倒预防训练具有重要的实践意义。

关键词：视觉-前庭觉输入冲突；站姿稳定性；脑电图脑网络；节点连接强度

The effect of visual-vestibular sensory input consistency on standing stability and electroencephalogram brain network characteristics in the elderly

YANG Yi[1], WANG Guo-Zheng[2], HUA An-Ke[1], HAO Zeng-Ming[3], HUANG Cong[1], LIU Jun[2], WANG Jian[1,*]

[1]*Kenisiology and Health Engineering Institute;* [2]*School of Biomedical Engineering, Zhejiang University, Hangzhou 310028, China;* [3]*The First Affiliated Hospital, Sun Yat-sen University, Guangzhou 510062, China*

Abstract: Aging is a crucial factor influencing postural stability control and contributing to frequent falls, yet its underlying mechanisms remain incompletely understood. This study aims to explore the effects of aging on postural stability control by comparing differences in postural stability and node strength of electroencephalogram (EEG) brain network between elderly and young people under the conditions of congruent and incongruent visual-vestibular sensory inputs. Eighteen elderly volunteers without neuromuscular disorders and eighteen young individuals participated in the present study. Virtual reality (VR) technology was employed to manipulate visual rotation stimuli (clockwise and counterclockwise), and a horizontal rotating platform was used for vestibular rotation stimuli (clockwise). Based on the directional disparity of sensory input in the horizontal plane, visual-vestibular input consistency was categorized as congruent and incongruent. Postural stability was assessed by the center of pressure (COP) trajectory, and EEG signals were collected and analyzed using directed network analysis to observe EEG brain network node connectivity strength. The results revealed that, under conditions of incongruent visual-vestibular sensory inputs, the elderly exhibited significantly inferior postural stability performance in terms of COP anterior-posterior (Y-axial) sway speed, total path length, anterior-posterior and medial-lateral sample entropy, compared to the

This work was supported by the Science and Technology Commission of the Military Commission 173 Plan Technical Field Fund (No. B27005).

*Corresponding author. Tel: +86-571-888845877; E-mail: pclabeeg@zju.edu.cn

young adults. Moreover, the node connectivity strength of visual cortex in the elderly was notably higher, while node connectivity strength of superior temporal cortex was significantly lower than that in the young adults. These findings suggest that the elderly have a heightened reliance on visual information in postural control and an impaired ability to cope with sensory conflicts arising from incongruent visual-vestibular sensory inputs, leading to compromised postural stability. The outcomes of this study hold significant implications for future assessments of balance function in the elder and fall prevention trainings.

Key words: visual-vestibular input conflict; postural stability; EEG brain network; node connection strength

随着衰老的发生和发展，维系站姿稳定性的姿势控制系统 (postural control system) 功能逐渐弱化，从而导致老年人站姿平衡能力受损，跌倒现象频发 [1]。研究表明，摔倒是老年人最常见和最严重的生活事件和重大公共卫生问题，可导致骨折、损伤、残疾、引发心理恐惧、增加反复跌倒风险、降低日常生活能力和生存质量以及增加社会医疗成本等 [2]。跌倒已经成为老年人意外死亡和非致命意外伤害的主要原因，占意外死亡的 55.8% [3]。流行病学研究显示，65 岁以上老年人群跌倒发生率在美国为 30%，日本为 13.7%，印度为 53%，中国为 26.4%[4]。在老年跌倒事件中，5% 导致骨折，5%~10% 导致其它损伤 [5]。在入院原因中，跌倒是其它伤害的 5~6 倍 [2]。老年女性跌倒发生率高于男性 [6]。

老年跌倒是由多种原因造成的，包括肌肉力量衰退 [7, 8]、视觉、前庭觉和本体觉功能减退、平衡控制功能弱化和认知障碍等个体因素以及药物作用、饮酒和突发外部姿势干扰等外部环境因素 [9]，各种原因导致的老年跌倒均在生理学本质上与大脑姿势控制系统功能有着复杂的因果关系 [10]。姿势控制特指姿势控制系统为实现动静态身体重心稳定和肢体空间定位而完成的一系列大脑多感觉姿势信息整合与姿势肌肉运动控制活动，是姿势控制系统、姿势控制任务和环境因素相互作用的结果。其中，姿势信息整合，又称多感觉信息整合 (multisensory integration)，特指姿势控制系统通过赋权 (weighting) 和变权 (reweighting) 机制将来自视觉、前庭觉、本体觉和皮肤触觉等相同或者不同姿势感觉通道的冗余信息整合与构建为统一的、有效的和稳定的内部姿势表征的姿势信息加工处理过程 [11]。视觉系统通过视网膜将光线转化为神经信号，在姿势平衡控制中提供关于外部环境和身体空间信息，如身体与地面之间的角度和距离、水平和垂直方向、物体运动和速度变化等 [12]。前庭觉系统是内耳中耳石和半规管提供相对于重力和惯性力的位置和加速度信息 [11]。姿势肌肉控制特指姿势控制系统通过前馈控制、反馈控制和随意控制原理实现的姿势肌肉预期姿势调节、补偿姿势调节和随意姿势调节活动。

目前研究站姿平衡时，常采用足底压力中心 (center of pressure, COP) 数据进行定量评估，分析时较多采用线性指标，如左右方向 (X 轴方向) 和前后方向 (Y 轴方向) 摆动速度、摆动幅度，以及总轨迹长和摆动面积等。但是，因为人体姿势控制和衰老过程均具有复杂非线性动力学特征 [13]，所以 COP 信号是一种非线性、非平稳的时间序列，这导致传统线性指标在评价站姿平衡控制上存在一定局限性，例如 Zhou 等人 [14] 研究发现身体晃动的传统分析指标无法预测老年人未来跌倒的概率。样本熵 (sample entropy) 及多尺度样本熵 (multi-scale sample entropy) 是一类基于信息熵的分析信号复杂度的方法 [15]，当系统的复杂度越高，其值越大，因此可用于评价 COP 时间序列的复杂度，可以作为站姿平衡控制评估的非线性指标。脑电图 (electroencephalogram, EEG) 因高采样率、低成本、便携和无创的优势，在神经科学研究中得到了广泛应用。目前脑网络分析能揭示大脑结构和功能，特别是图论作为描述和量化复杂网络的方法得到了发展。一般而言，功能连接可衡量不同电极或脑区间的相互关系，常见的基于 EEG 构建脑功能网络的方法是将电极测量或经过溯源分析后的脑区作为网络节点，通过计算相干性 (coherence) 值来衡量节点之间的功能连接强弱，以这种方式构成的脑网络是无向的。因此，在分析姿势干扰下姿势反应内部机制时，需进行因果连接 (有向连接) 分析，常见的指标是基于格兰杰因果关系的指标，例如偏定向相干性 (partial directed coherence, PDC)[16]、定向传递函数 (directed transfer function)[17] 等。

老年人在应对各种突发姿势干扰和感觉冲突刺激过程中表现出明显不同于青年人和成年人的多种姿势控制反应模式 [18]，如动静态站姿稳定性差、预期姿势调节启动慢、补偿姿势调节响应时间长以及随意姿势控制效率低等，但其内在神经控制机制尚

不完全清楚。本研究通过同步操作视觉和前庭觉刺激变化方向，对比老年人和青年人在视觉 - 前庭觉输入一致和冲突条件下身体站姿稳定性和站姿大脑 EEG 脑网络节点连接强度的差异性，以期明确衰老弱化站姿稳定性控制的脑机制。

1 材料和方法

1.1 被试 随机招募 60~69 岁社区健康老年人 24 名和在校大学生 22 名。因在实验中出现迈步或身体剧烈晃动排除 6 名老年人和 4 名青年人，最后确定 18 名老年人和 18 名青年人为本研究实验对象 (表 1)。对老年被试采用 Berg 平衡量表 (Berg balance scale, BBS) 和蒙特利尔认知评估量表 (Montreal cognitive assessment, MoCA) 进行跌倒风险和认知能力进行筛查。老年被试纳入标准：(1) 年龄 ≥ 60 岁；(2) 无认知功能障碍，MoCA 得分 > 26，若教育水平 ≤ 12 年，则标准为 MoCA 得分 > 25；(3) 无跌倒史和跌倒风险，BBS 得分 > 56。排除标准：(1) 被诊断有神经损伤和其他慢性疾病；(2) 有跌倒史。对老年人和青年人被试，基本纳入标准有：(1) 右利腿；(2) 裸眼视力或矫正视力正常；(3) 被试在参加本实验前的 6 个月内，无下肢损伤，无神经、精神类疾病或服用精神类、镇静剂等药物；(4) 实验前 2 天未摄入酒精、咖啡等刺激性物质；(5) 实验前 24 h 内未从事剧烈运动，无任何肌肉疲劳现象。所有被试之前均没有参加过类似的实验，知晓本研究的目的，了解实验流程和注意事项，自愿参加本研究并签署知情同意书，被试在实验结束后获得一定酬劳。本研究的所有实验内容都符合《赫尔辛基宣言》，而且通过浙江大学心理科学研究中心伦理委员会的审核 (编号 2020-003)。

1.2 实验仪器和材料 本研究使用的实验仪器包括 Nintendo Wii Fit 平衡板 (日本)、VIVE 虚拟现实 (virtual reality, VR) 头盔 (VIVE PRO EYE 2，HTC Corporation，台北)、旋转平台 (全控科技，南京) 和 32 导联脑电记录仪 (EE-225，ANT Neuro，Hengelo，荷兰)。通过自编 Unity3D 程序同步控制旋转平台及 VIVE VR 头盔中视觉场景 (实验室模拟场景) 的活动，实现视觉 - 前庭觉输入一致性的不同组合。

1.3 实验设计和流程 本研究采用 2 (年龄分组：老年组、青年组) × 2 (视觉 - 前庭觉输入一致性：一致、冲突) 的混合设计。自变量为年龄分组和视觉 - 前庭觉输入一致性，其中被试群体为组间变量，多感觉干扰为组内变量。本研究通过旋转平台控制前庭觉刺激信息 (速度为顺时针 30°/s)，Unity3D 程序控制 VR 头盔视觉刺激信息 (速度为 0、−60°/s)。通过 2 种组合方式设置了“感觉一致”和“感觉冲突”两种平衡干扰条件。感觉一致时，VR 场景速度为 0，旨在模拟在日常生活场景中绝大部分自然运动情况；感觉冲突时，VR 场景速度为 −60°/s，旨在实现日常生活场景中个别视觉 - 前庭觉冲突的运动情况。在正式实验之前，首先安排被试熟悉各实验条件，并排除对 VR 场景眩晕不适的被试。练习结束后，被试充分休息，然后佩戴脑电帽并将 Wii 平衡板固定在选择平台上方，确保旋转平台的中心与 Wii 平衡板的中心保持一致。本实验要求被试佩戴 VR 头盔站立在 Wii 平衡板上，双脚裸足自然站立 (站立位置进行标记，使得不同条件测试时的站立位置相同)，双手交叉放于胸前，保持头部固定。另外，要求被试在整个测试过程中保持睁眼，双眼平视前方，努力维持站姿稳定，避免迈步 (如图 1 所示)。实验开始时，被试佩戴 VR 眼镜，保持睁眼且目视前方，安静站立 30 s。此时平台和 VR 场景均静止，要求被试保持身体平衡。此阶段所采集的数据作为

表1. 老年和青年受试者基本情况

Table 1. Demographics of elderly and young subjects

	Young (n = 18)	Elderly (n = 18)	P value*
Age (years)	23.80 ± 2.20	63.90 ± 3.12	< 0.001
Gender (male, female)	14, 8	13, 10	N/A
Weight (kg)	70.00 ± 20.96	68.80 ± 12.90	0.825
BMI	23.30 ± 5.16	24.90 ± 4.41	0.285
MoCA score	N/A	27.30 ± 1.45	N/A
BBS score	N/A	55.74 ± 0.54	N/A

Mean ± SD. BMI, body mass index; MoCA, Montreal cognitive assessment; BBS: Berg balance scale. *: independent-samples t-test was used to determine the differences in these characteristics between young and old subjects. N/A, not applicable.

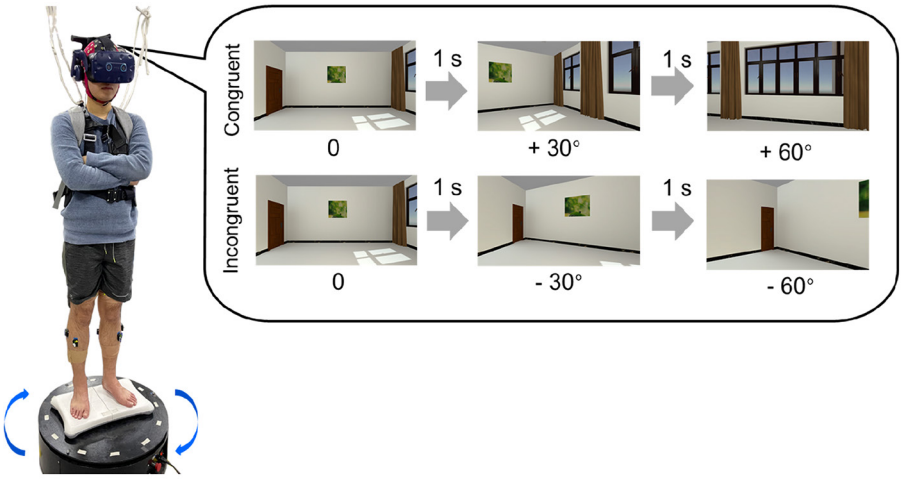

图 1. 实验测试图。采用视觉虚拟现实(VR)技术操作视觉旋转刺激(顺时针和逆时针)，采用水平旋转平台操作前庭觉旋转刺激(逆时针)，根据感觉输入在水平面的差异性将视觉和前庭觉输入一致性分为视觉-前庭觉输入方向一致和视觉-前庭觉输入方向冲突

Fig. 1. Schematic diagram of experiment. Virtual reality (VR) technology was used to operate visual rotation stimulation (clockwise and counterclockwise), and horizontal rotation platform was used to operate vestibular rotation stimulation (clockwise). According to the difference of sensory inputs in the horizontal plane, the consistency of visual and vestibular inputs was divided into two conditions: congruent and incongruent.

基线数据。然后，按照随机顺序向每位被试呈现“感觉一致”和“感觉冲突”实验刺激条件，每个条件均持续 36 s，且只完成一次 (避免学习和预期效应 [19])。期间安排 5 min 静坐休息，以避免不同条件间的相互影响。

1.4 数据采集 COP 数据采集设备为 Wii 平衡板，采样频率为 100 Hz。COP 数据采集前须校准。EEG 数据采集设备为 ANT Neuro 公司生产的脑电采集系统 (EE-225，ANT Neuro，荷兰)，采样频率设为 1 000 Hz。实验共采集被试的 32 通道数据 (顺序依次为：FP1、FP2、F7、F3、FZ、F4、F8、FC5、FC1、FC2、FC6、T7、C3、CZ、C4、T8、CP5、CP1、CP2、CP6、P7、P3、PZ、P4、P8、POZ、O1、OZ、O2、M1、M2 和 GND。其中 GND 是右耳后的乳突处，M1 和 M2 是参考电极)。电极放置标准采用国际 10-20 标准导联系统。EEG 数据采集前须清洗被试头部，吹干头部后佩戴脑电帽，并注入导电膏，使每个电极的阻抗值小于 5 kΩ。在线滤波设置为 0.5~100 Hz 带通滤波。采集过程中要求被试平视前方，保持头部与身体不动，尽可能维持站姿平衡。COP 和 EEG 数据同步进行采集，采样时间均为 66 s。

1.5 数据预处理 采用自编 MATLAB 2021b 程序和 EEGLAB 工具包进行数据分析。针对 COP 数据，进行 20 Hz 的 4 阶巴特沃斯低通滤波并去除均值。针对 EEG 数据的处理步骤包括：(1) 数据导入；(2) 降采样为 100 Hz；(3) 1~48 Hz 带通滤波；(4) 50 Hz 陷波去工频干扰；(5) 用伪影空间重构 (artifact subspace reconstruction, ASR) 方法去除被试的体动伪迹，阈值设为 ± 20 倍标准差；(6) 独立成分分析 (independent component analysis, ICA) 方法进一步移除眨眼、肌肉伪迹、心电图信号以及线性噪声等干扰信号；(7) 用波束成形 (beamforming) 方法进行溯源分析。该方法是一种空间滤波技术，它通过对各个电极的信号进行加权和合并，来估计特定大脑区域的活动。该方法已被证明在对低密度 EEG 数据进行源定位和功能连接性分析方面具有良好的性能 [20]，进行源重建时，由于皮层的神经元产生的同步活动是 EEG 的主要来源，为了降低反问题的复杂性和模糊性，将源限制在皮层范围内，并将重建的时序数据投影到布罗德曼图谱 (Brodmann atlas)；(8) 聚类到感兴趣脑区 (region of interest, ROI)。本研究目的和实验范式涉及到视觉和前庭觉输入、运动感知、大脑决策和运动意图等方面，所以随后聚类了 6 个 ROI 脑区：背外侧前额叶皮质 (dorsolateral prefrontal cortex, DLPFC)、前眼皮质 (frontal eye field, FEF)、感觉运动皮质 (sensorimotor cortex, SMC)、

后顶叶皮质 (posterior parietal cortex, PPC)、颞上皮质 (superior temporal cortex, STC) 以及视皮质 (visual cortex, VC)；(9) 以窗长 6 ，滑动窗步长 2 s 进行分段。平台旋转 6 s 时，场景累计旋转 180°，被试得以体验完所有视觉场景。以 2 s 作为步长，增加了重叠窗口，可增加实验结果稳定性 ；(10) 数据保存。

1.6 指标计算 针对 COP 数据，本研究计算了平均摆动速度、总轨迹长和样本熵 [15]。平均摆动速度计算方法见公式 (1)，其中 *Vel* 代表参与者的摆动速度，*N* 是 COP 的采样点数，*t* 是持续时间，*x* 是 X 轴 (身体左右方向) 坐标，*y* 是 Y 轴 (身体前后方向) 坐标。摆动总轨迹长计算方法见公式 (2)，其中 *PL* 表示总轨迹长。样本熵计算方法见公式 (3)，其中 *SampEn* 表示样本熵，*m* 表示嵌入维数，*r* 表示相似性容忍度 (通常选为原始数据标准差的一定比例)，*N* 是 COP 采样点数，*A*(*m, r*) 表示长度为 *m* 的子序列的匹配数。针对 EEG 数据，本研究采用基于格兰杰因果关系的 PDC 指标构建了因果连接。所构建的网络是一种加权有向网络。本研究计算了 ROI 脑区节点连接强度 (node strength)，其定义为与该节点相连的边的权重总和 [4]。节点 p_k 的连接强度可通过对所有流入该节点和流出该节点的权重值进行求和求得，见公式 (4)，其中 $w(p_k, p_i)$ 是节点 p_k 和节点 p_i 连边的权重值。组水平的网络通过平均每个被试的 EEG 网络来建立。节点连接强度越高，说明该节点在脑网络信息传递和整合过程中发挥的作用越大。

$$Vel=\sum_{i=1}^{N}\frac{\sqrt{\left(x(i+1)-x\right)^2+\left(y(i+1)-y\right)^2}}{t} \quad (1)$$

$$PL=\sum_{i=1}^{N}\sqrt{\left(x(i+1)-x\right)^2+\left(y(i+1)-y\right)^2} \quad (2)$$

$$SampEn(m,r,N)=-\ln\left(\frac{A(m,r)}{B(m,r)}\right) \quad (3)$$

$$NodeStrength\left(p_k\right)=\sum_{i=1}^{N}w\left(p_k,p_i\right) \quad (4)$$

1.7 统计学分析 结果数据用 mean ± SEM 来表示。数据统计检验采用 SPSS 25.0 软件进行。采用双因素方差分析 (two-way ANOVA) 考察被试年龄分组和视觉 - 前庭觉输入一致性对 COP 在 X 和 Y 轴方向的摆动速度、COP 总轨迹长、COP 在 X 和 Y 轴方向的样本熵以及 6 个 ROI 脑区皮质节点连接强度的影响，显著性水平设为 $\alpha = 0.05$。

2 结果

2.1 年龄分组和视觉-前庭觉输入一致性对站姿平衡的影响

年龄分组和视觉 - 前庭觉输入一致性对站姿稳定性的影响见图 2。双因素方差分析表明，年龄分组和视觉 - 前庭觉输入一致性对站姿 COP 摆动速度 Y 轴 (年龄分组 $F = 9.249$，$P = 0.005$ ；视觉 - 前庭觉输入一致性 $F = 22.576$，$P < 0.001$)、COP 总轨迹长 (年龄分组 $F = 18.221$，$P < 0.001$ ；视觉 - 前庭觉输入一致性 $F = 4.478$，$P = 0.042$)、COP 在站姿支撑面 X 轴 (年龄分组 $F = 8.492$，$P = 0.006$ ；视觉 - 前庭觉输入一致性 $F = 22.518$，$P < 0.001$) 和 Y 轴 (年龄分组 $F = 15.037$，$P < 0.001$ ；视觉 - 前庭觉输入一致性 $F = 26.278$，$P < 0.001$) 的样本熵均具有明显主效应。其中，年龄分组和视觉 - 前庭觉输入一致性对站姿 COP X 轴样本熵存在交互作用 ($F = 6.480$，$P = 0.016$)。简单效应分析表明，老年人在视觉 - 前庭觉输入冲突条件下 COP X 轴样本熵明显小于一致条件 ($P < 0.001$)，而青年人在冲突条件下 COP X 轴样本熵与一致条件时的差异无显著性 ($P = 0.129$)。

2.2 年龄分组和视觉-前庭觉输入一致性对ROI脑区皮质节点连接强度的影响

年龄分组和视觉 - 前庭觉输入一致性对 ROI 脑区节点连接强度的影响见图 3。双因素方差分析结果显示，FEF ($F = 7.320$, $P = 0.011$)、SMC ($F = 7.886$, $P = 0.008$)、PPC ($F = 6.970$, $P = 0.012$)、STC ($F = 15.644$, $P < 0.001$) 和 VC ($F = 9.359$, $P = 0.004$) 的节点连接强度均具有明显的年龄主效应。事后比较显示，视觉 - 前庭觉输入冲突条件时，老年人 FEF ($P = 0.005$) 和 STC ($P < 0.001$) 的节点连接强度明显小于年轻人，而老年人 VC ($P = 0.004$) 的节点连接强度明显大于年轻人。SMC ($F = 4.858$, $P = 0.034$) 和 PPC ($F = 7.813$, $P = 0.008$) 具有明显的视觉 - 前庭觉输入一致性主效应。另外，年龄分组和视觉 - 前庭觉输入一致性对 FEF ($F = 4.525$, $P = 0.041$) 和 STC ($F = 27.584$, $P < 0.001$) 存在交互作用。简单效应分析结果显示，老年人对视觉 - 前庭觉冲突条件时的 FEF 节点连接强度明显小于青年人 ($P = 0.003$) ；老年人对视觉 - 前庭觉冲突条件时的 STC 节点连接强度明显小于视觉 - 前庭觉一致条件 ($P = 0.005$)。

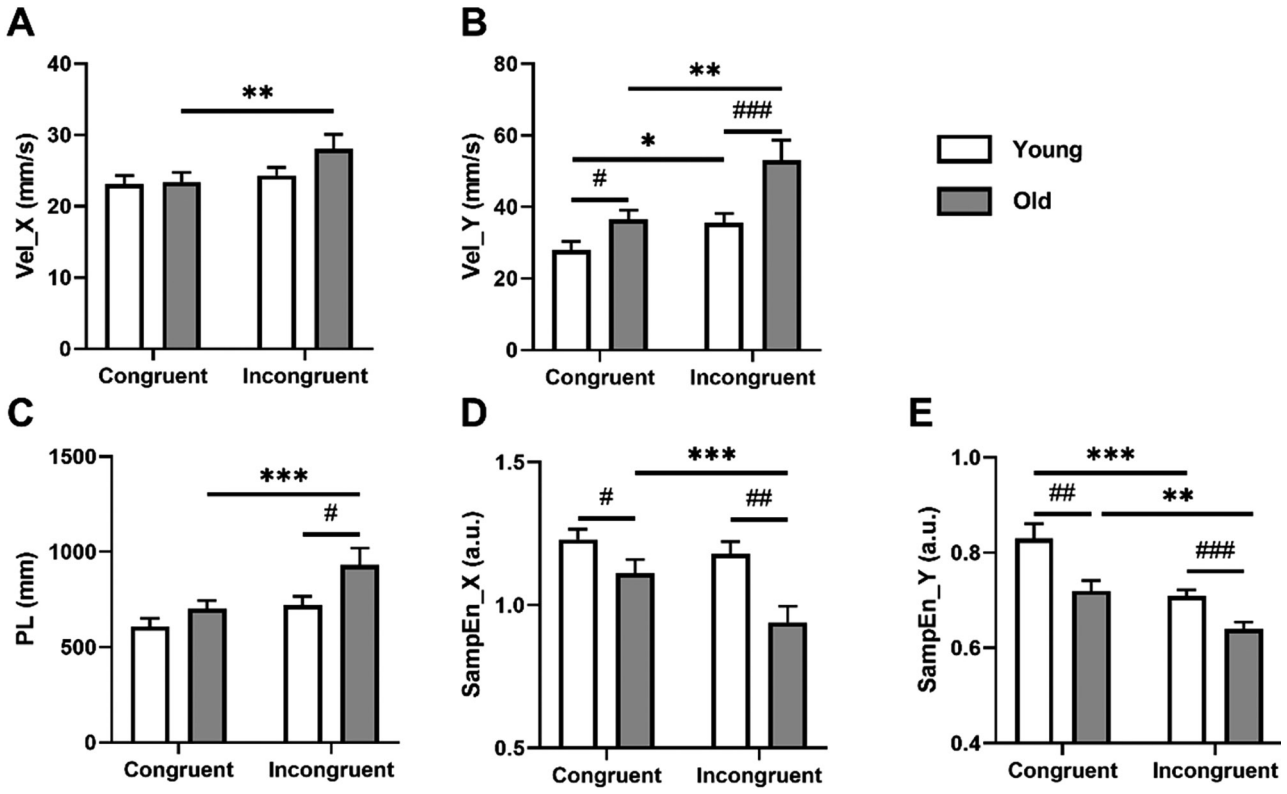

图 2. 年龄分组和视觉-前庭觉输入一致性对站姿稳定性的影响

Fig. 2. Effects of age and visual-vestibular input congruency on posture stability. *A:* X-axial (medial-lateral) sway velocity (Vel_X) of center of pressure (COP); *B:* Y-axial (anterior-posterior) sway velocity (Vel_Y) of COP; *C:* Path length (PL) of COP; *D:* X-axial sample entropy (SampEn_X) of COP; *E:* Y-axial sample entropy (SampEn_Y) of COP. * represents significant differences in interaction, main effects and intra-group comparisons. $^{*}P < 0.05$, $^{**}P < 0.01$, $^{***}P < 0.001$. # means that there are significant differences between different age groups under the same conditions. $^{\#}P < 0.05$, $^{\#\#}P < 0.01$, $^{\#\#\#}P < 0.001$. Mean ± SEM, $n = 18$. a.u., arbitrary unit.

3 讨论

本研究通过对比老年人和青年人在视觉 - 前庭觉输入一致和冲突条件下站姿稳定性和站姿 EEG 脑网络节点连接强度的差异性，探讨衰老弱化站姿稳定性控制的 EEG 脑网络节点连接强度效应。本研究结果显示，老年人在视觉 - 前庭觉输入冲突条件下 COP 前后方向摆动速度、总轨迹长以及前后、左右方向样本熵等站姿稳定性表现明显不及青年人，VC 节点连接强度明显大于青年人，STC 节点连接强度明显小于青年人。此外，视觉 - 前庭觉输入冲突条件下，老年人 COP 前后方向摆动速度、总轨迹长以及前后、左右方向样本熵等站姿稳定性表现明显不及视觉 - 前庭觉输入一致条件下表现。在冲突条件下老年人 STC 脑区节点强度明显小于青年人，而在一致条件下，老年人在该脑区的激活强度与青年人的差异无显著性。以上结果提示，老年人在站姿平衡控制中对视觉依赖性高。另外，STC 涉及感觉冲突信息处理，在视觉 - 前庭觉输入冲突条件下，老年人难以应对感觉冲突，导致老年人站姿稳定表现较青年人差。

在站姿稳定性方面，本研究结果显示，衰老和感觉冲突都能导致 COP 前后方向摆动速度增大，总轨迹长增加和样本熵减小，但年龄分组和视觉 - 前庭觉输入冲突有明显交互效应，视觉 - 前庭觉输入冲突对老年人站姿稳定的不利影响明显大于青年人。先前也有一些学者也报道了和上述结果类似的现象。Poulain 等研究显示，视觉在姿势控制中的作用随着年龄的增长而增加，这种倾向在 40 岁就开始，并且在 60 岁后加速变化 [9]。Palazzo 等人研究显示，在静态站立时老年人就比青年人更依赖于视觉信息来调节姿势 [21]。Peterka 等在感觉统合测试中也发现，年龄较大的被试更容易受到感觉冲突的影响，容易产生知觉错觉和视觉主导 [22]。

本研究还对 COP 数据的复杂性进行测量。姿

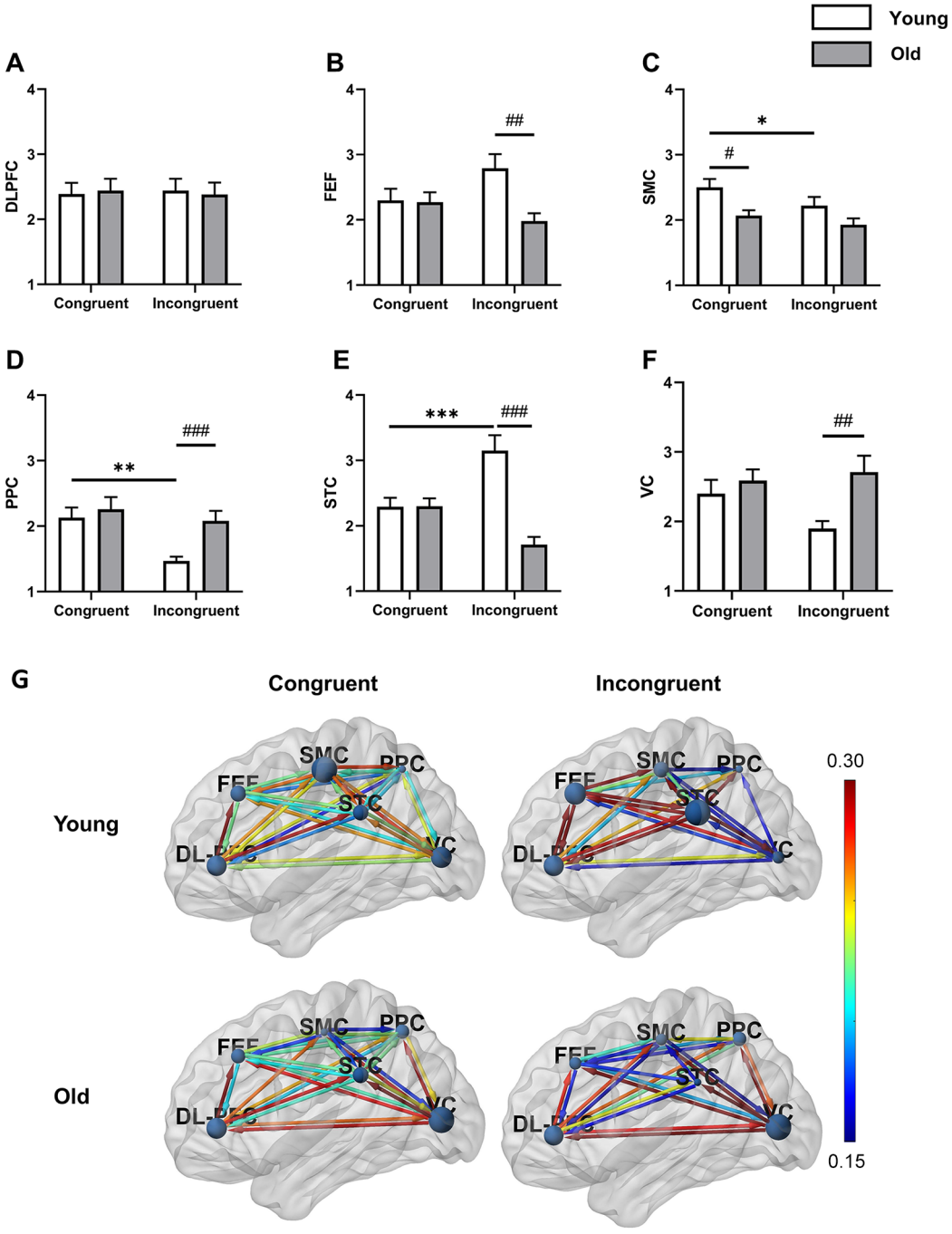

图 3.年龄分组和视觉-前庭觉输入一致性对6个目标脑区皮质节点连接强度的影响

Fig. 3. Effects of age and visual-vestibular input congruency on node strength of six cortical regions. *A*: Node strength of dorsolateral prefrontal cortex (DLPFC); *B*: Node strength of frontal eye field (FEF); *C*: Node strength of sensorimotor cortex (SMC); *D*: Node strength of posterior parietal cortex (PPC); *E*: Node strength of superior temporal cortex (STC); *F*: Node strength of visual cortex (VC). Two-way mixed-effects ANOVA was used. * represents significant differences in interaction, main effects and intra-group comparisons. $^{*}P < 0.05$, $^{**}P < 0.01$, $^{***}P < 0.001$. # means that there are significant differences among different age groups under the same conditions. $^{\#}P < 0.05$, $^{\#\#}P < 0.01$, $^{\#\#\#}P < 0.001$. Mean ± SEM, $n = 18$. *G*: Average directed functional connectivity strength between six cortical regions in the young and eldly groups under the congruent and incongruent conditions. Color bars code for partial directed coherence (PDC) value (min = 0.15, max = 0.30). The lines connecting six nodes represent the group average node strengths, with a redder color indicating stronger connections. The size of the nodes corresponds to their strength.

势控制是一个复杂的过程，涉及多个生理系统和控制机制之间的相互作用。一般认为，姿势控制的复杂性越高表明系统越灵活、适应性更强，能够有效应对环境扰动或感官挑战，而复杂度越低，说明其系统越僵化、越脆弱[23, 24]。本研究结果显示，年龄分组对 COP 在站姿支撑面 X 轴和 Y 轴的样本熵有明显效应，COP 的复杂性随着年龄增加而降低，这与前人的研究结果相一致[25]。Lipsitz 等人提出的“复杂性损失假说”认为生理系统产生复杂相互作用网络的能力下降会导致生理功能恶化[26]。本研究结果还显示，在冲突条件下 COP 样本熵值降低，提示感觉冲突也降低了身体摆动的复杂度。较低的样本熵值表明，COP 信号更具规则性和可预测性。当从不同感觉中组合信息时，姿势控制系统需要灵活地整合共同来源的感觉信息。不一致(冲突)条件给“大脑找麻烦”，导致被试在感官冲突的识别、自我空间认知上出现困难，进而降低多感觉整合的灵活性，表现为样本熵降低。另外，感觉冲突和年龄存在交互效应，表明老年人的姿势控制复杂度受到感觉冲突的影响明显大于青年人，表现在老年人僵化、脆弱的姿势控制系统难以针对感觉冲突调整姿势控制策略。

虽然以往研究表明老年人对冲突难以适应，并形成视觉依赖，但其背后神经机制目前尚不完全清楚。有学者认为这是因为老年人普遍存在前庭觉的严重退化，所以更依赖相对完好的视觉信息。如 Higgen 等的研究显示，老年人的体感阈值增加程度远大于视觉阈值[27]。本研究结果显示，老年人在感觉冲突时的 VC 节点强度显著大于青年人，这也为老年人感觉冲突下的视觉依赖提供了神经科学层面证据。也有学者认为老年人对冲突的不适应和视觉依赖主要的原因可能是多感觉交互的因果推断能力下降，导致他们无法快速准确地判断感觉信息的来源，难以将不可靠的视觉信息分离[28]，这可能也是老年人多感觉变权能力下降的本质原因。但这种解释是从知觉和平衡表现得出的结论，一直缺少神经生理学的直接证据。本研究结果显示，青年人可以在视觉 - 前庭觉输入冲突时降低 PPC 的节点强度，而老年人不能。PPC 一直被认为是视觉信息和感觉运动信息整合的区域，本研究组前期研究也证明了这点[29]。此外，本研究结果显示，在视觉 - 前庭觉输入一致时，老年人和青年人的皮质网络连接模式比较相似；但在感觉冲突时，青年人可以降低 VC、PPC、SMC 之间的连接，抑制了冲突的视觉信息和感觉运动的整合；而老年人在感觉输入冲突时仍然保持和感觉输入一致时相近的网络连接。这些皮质网络层面的研究结果为老年人的因果推断能力下降供了强烈的证据。

综上所述，本研究结果表明老年人对多感觉信息来源推断的能力显著下降，这导致老年人依赖视觉进行平衡控制，难以分离与不可靠或与自我运动冲突的视觉信息，表现出僵化、脆弱的站姿平衡控制方式。这些发现对制定改善老年人姿势控制和降低跌倒风险的干预措施具有重要意义。例如，可以设计有针对性的训练计划来促进老年人更有效的感觉运动策略。此外，本研究结果提示感觉冲突在评估和干预老年人姿势控制中具有重要性。传统的平衡评估可能无法完全反映老年人在现实生活中处理感官冲突时所面临的挑战。因此，将感觉冲突场景纳入姿势控制的评估中，可以对老年人的平衡能力进行更具功效的评估，并为有针对性的干预措施的设计提供信息。

参考文献

1 Salari N, Darvishi N, Ahmadipanah M, Shohaimi S, Mohammadi M. Global prevalence of falls in the older adults: a comprehensive systematic review and meta-analysis. J Orthop Surg Res 2022; 17(1): 334.

2 Ganz DA, Latham NK. Prevention of falls in community-dwelling older adults. New Engl J Med 2020; 382(8): 734–743.

3 Osoba MY, Rao AK, Agrawal SK, Lalwani AK. Balance and gait in the elderly: A contemporary review. Laryngoscope Investig Otolaryngol 2019; 4(1): 143–153.

4 Dsouza SA, Rajashekar B, Dsouza HS, Kumar KB. Falls in Indian older adults: a barrier to active ageing. Asian J Gerontol Geriatr 2014; 9(1): 1–8.

5 Kannus P, Parkkari J, Koskinen S, Niemi S, Palvanen M, Järvinen M, Vuori I. Fall-induced injuries and deaths among older adults. JAMA 1999; 281(20): 1895–1899.

6 Johansson J, Nordström A, Nordström P. Greater fall risk in elderly women than in men is associated with increased gait variability during multitasking. J Am Med Dir Assoc 2016; 17(6): 535–540.

7 Rubega M, Di Marco R, Zampini M, Formaggio E, Menegatti E, Bonato P, Masiero S, Del Felice A. Muscular and cortical activation during dynamic and static balance in the elderly: A scoping review. Aging Brain 2021; 1: 100013.

8 Zhou YZ (周永战), Chen PJ, Xiao WH. Mechanism of the

occurrence of sarcopenia in the elderly. Acta Physiol Sin (生理学报) 2018; 70(4): 445–454 (in Chinese).

9 Poulain I, Giraudet G. Age-related changes of visual contribution in posture control. Gait Posture 2008; 27(1): 1–7.

10 Andersson V, Vecchio F, Miraglia F, Rossini PM, Renvall H, Taubøll E, Maestú F, Haraldsen IH. Source-level EEG and graph theory reveal widespread functional network alterations in focal epilepsy. Clin Neurophysiol 2021; 132(7): 1663–1676.

11 Hua AK (华安珂), Feng JS, Meng J, Peng YX, Wang J. Research progress of human upright posture control and multisensory integration. Space Med Med Eng (航天医学与航天工程) 2019; 32(2): 183–188 (in Chinese).

12 Redfern MS, Yardley L, Bronstein AM. Visual influences on balance. J Anxiety Disord 2001; 15(1–2): 81–94.

13 Cohen AA, Ferrucci L, Fülöp T, Gravel D, Hao N, Kriete A, Levine ME, Lipsitz LA, Olde Rikkert MGM, Rutenberg A, Stroustrup N, Varadhan R. A complex systems approach to aging biology. Nat Aging 2022; 2(7): 580–591.

14 Zhou J, Habtemariam D, Iloputaife I, Lipsitz LA, Manor B. The complexity of standing postural sway associates with future falls in fommunity-dwelling older adults: The MOBILIZE Boston Study. Sci Rep 2017; 7(1): 2924.

15 Busa MA, van Emmerik REA. Multiscale entropy: A tool for understanding the complexity of postural control. J Sport Health Sci 2016; 5(1): 44–51.

16 Mierau A, Pester B, Hülsdünker T, Schiecke K, Strüder HK, Witte H. Cortical correlates of human balance control. Brain Topogr 2017; 30(4): 434–446.

17 Peterson SM, Ferris DP. Group-level cortical and muscular connectivity during perturbations to walking and standing balance. Neuroimage 2019; 198: 93–103.

18 Lee YJ, Chen B, Aruin AS. Older adults utilize less efficient postural control when performing pushing task. J Electromyogr Kinesiol 2015; 25(6): 966–972.

19 Xie L, Wang J. Anticipatory and compensatory postural adjustments in response to loading perturbation of unknown magnitude. Exp Brain Res 2019; 237(1): 173–180.

20 Nguyen-Danse DA, Singaravelu S, Chauvigné LAS, Mottaz A, Allaman L, Guggisberg AG. Feasibility of reconstructing source functional connectivity with low-density EEG. Brain Topogr 2021; 34(6): 709–719.

21 Palazzo F, Nardi A, Lamouchideli N, Caronti A, Alashram A, Padua E, Annino G. The effect of age, sex and a firm-textured surface on postural control. Exp Brain Res 2021; 239(7): 2181–2191.

22 Peterka RJ, Black FO. Age-related changes in human posture control: sensory organization tests. J Vestib Res 1990; 1(1): 73–85.

23 Lipsitz LA. Dynamics of stability: the physiologic basis of functional health and frailty. J Gerontol A Biol Sci Med Sci 2002; 57(3): B115–B125.

24 Zhou J, Manor B, Liu D, Hu K, Zhang J, Fang J. The complexity of standing postural control in older adults: a modified detrended fluctuation analysis based upon the empirical mode decomposition algorithm. PLoS One 2013; 8(5): e62585.

25 Pethick J, Winter SL, Burnley M. Physiological complexity: influence of ageing, disease and neuromuscular fatigue on muscle force and torque fluctuations. Exp Physiol 2021; 106(10): 2046–2059.

26 Lipsitz LA, Goldberger AL. Loss of ‘complexity’ and aging: Potential applications of fractals and chaos theory to senescence. JAMA 1992; 267(13): 1806–1809.

27 Higgen FL, Heine C, Krawinkel L, Göschl F, Engel AK, Hummel FC, Xue G, Gerloff C. Crossmodal congruency enhances performance of healthy older adults in visual-tactile pattern matching. Front Aging Neurosci 2020; 12: 74.

28 Jones SA, Noppeney U. Ageing and multisensory integration: A review of the evidence, and a computational perspective. Cortex 2021; 138: 1–23.

29 Wang G, Yang Y, Wang J, Hao Z, Luo X, Liu J. Dynamic changes of brain networks during standing balance control under visual conflict. Front Neurosci 2022; 16: 1003996.

Neurosci. Bull. January, 2024, 40(1):79–89
https://doi.org/10.1007/s12264-023-01143-5

www.neurosci.cn
www.springer.com/12264

ORIGINAL ARTICLE

Multisensory Conflict Impairs Cortico-Muscular Network Connectivity and Postural Stability: Insights from Partial Directed Coherence Analysis

Guozheng Wang[1,2,3] · Yi Yang[3] · Kangli Dong[1] · Anke Hua[3] · Jian Wang[3,4] · Jun Liu[1,2]

Received: 19 February 2023 / Accepted: 16 July 2023 / Published online: 22 November 2023

Abstract Sensory conflict impacts postural control, yet its effect on cortico-muscular interaction remains underexplored. We aimed to investigate sensory conflict's influence on the cortico-muscular network and postural stability. We used a rotating platform and virtual reality to present subjects with congruent and incongruent sensory input, recorded EEG (electroencephalogram) and EMG (electromyogram) data, and constructed a directed connectivity network. The results suggest that, compared to sensory congruence, during sensory conflict: (1) connectivity among the sensorimotor, visual, and posterior parietal cortex generally decreases, (2) cortical control over the muscles is weakened, (3) feedback from muscles to the cortex is strengthened, and (4) the range of body sway increases and its complexity decreases. These results underline the intricate effects of sensory conflict on cortico-muscular networks. During the sensory conflict, the brain adaptively decreases the integration of conflicting information. Without this integrated information, cortical control over muscles may be lessened, whereas the muscle feedback may be enhanced in compensation.

Keywords Cortico-muscular interaction · Postural control · Virtual reality · Electroencephalogram · Electromyography · Sensory integration

Introduction

Maintaining standing balance is a challenging task for the brain, as it requires a precise combination of multisensory information to control the muscles executing coordinated movements [1]. However, sensory information is not always congruent. Issues in postural balance control mainly arise from ambiguity in visual information. The visual system is particularly susceptible to "deception", where the movement of environmental objects and self-movement can generate comparable visual stimuli. For example, sitting in a stationary train carriage can produce an illusion of self-motion if the train on an adjoining track moves off. In VR (virtual reality) games or moving vehicles, individuals may incorrectly integrate conflicting visual and non-visual information, potentially resulting in vertigo and unstable posture [2, 3]. To overcome these challenges, the brain must process multisensory information flexibly, harmonizing congruent sensory inputs while minimizing interference from discordant information [4, 5].

Numerous studies have demonstrated the brain's ability to discern the source of sensory cues [6–8], segregating sensory information from different sources and combining that from the same sources in proportion to their reliability [9, 10]. By analyzing the dynamic changes in brain networks,

Supplementary Information The online version contains supplementary material available at https://doi.org/10.1007/s12264-023-01143-5.

✉ Jian Wang
pclabeeg@zju.edu.cn

✉ Jun Liu
liujun@zju.edu.cn

1 Key Laboratory for Biomedical Engineering of Ministry of Education, College of Biomedical Engineering & Instrument Science, Zhejiang University, Hangzhou 310058, China

2 Taizhou Key Laboratory of Medical Devices and Advanced Materials, Research Institute of Zhejiang University-Taizhou, Taizhou 318000, China

3 Department of Sports Science, College of Education, Zhejiang University, Hangzhou 310058, China

4 Center for Psychological Science, Zhejiang University, Hangzhou 310058, China

recent research has also found evidence supporting the idea that the brain can flexibly process multi-sensory information, establishing that the consistency of sensory information can influence the information interaction of the cortical network [11]. Nevertheless, as we all know, standing balance control entails not only the brain's integration of sensory signals but also the control of muscle activity. Thus, does the consistency of sensory information influence the interaction between cortical and muscle information? This question remains to be answered.

Cortico-muscular network analysis is widely used to investigate the neural mechanisms of the sensorimotor system [12, 13]. The first report about cortico-muscular coupling was published in 1995 [14]. Since then, numerous human and monkey studies have identified synchronous oscillations in the contralateral sensorimotor cortex and muscle during continuous muscle contraction [15, 16]. Initially, it was hypothesized that cortico-muscular coherence was driven by cortico-spinal efferents, which essentially reflect the cortical control over the muscular system [17, 18]. Some studies further demonstrated that population firing among corticospinal neurons encodes motor cortical oscillations and thereby transmits them to spinal motoneurons [19, 20]. However, recent studies have revealed that this is not the sole source of cortico-muscular coupling [21–23]. With the development of directed functional connectivity technology, it was revealed that there is significant directed coherence in both the ascending (EMG→EEG) and descending (EEG→EMG) directions, indicating that humans have bidirectional cortico-muscular coherence [23, 24]. The downstream pathway entails motor commands that provide voluntary control of muscle contraction. The upstream pathway involves somatosensory feedback, which sends sensory information from the muscles and other bodily regions back to the brain. Consequently, directionality is crucial in the examination of cortico-muscular interactions.

In recent years, cortico-muscular coupling during balance control has also been scrutinized. Ozdemir *et al*. reported that during postural perturbations, compared to the baseline, the increase in cortico-muscular coherence (CMC) for the rectus femoris muscle was more pronounced in the elderly, while the increase in CMC for the tibialis anterior muscle was more evident in the young group [25]. Liang *et al*. reported that the connectivity from the cortex to the muscle increases with task difficulty [26]. Both the standing balance task and age have an impact on cortico-muscular coupling. However, the question of whether the congruency of sensory information influences cortico-muscular coupling remains unresolved.

It is widely acknowledged that the brain evaluates the source of multi-modal sensory cues based on sensory input, integrating signals from common sources while separating independent signals. Previous research has found that the connectivity between major brain regions, including the posterior parietal, visual, somatosensory, and motor cortices, is generally weaker during sensory conflict compared to controls [11]. This suggests a decrease in multisensory integration within the brain under sensory conflict. In this study, we hypothesize that reduced connectivity within the sensory network results in decreased cortical control over muscles. This hypothesis stems from the fact that multisensory interaction is crucial for providing spatial location and other essential information required for successful motion planning and execution. Furthermore, according to the theory of reliability-weighted sensory integration, the brain assigns different weights to sensory inputs based on their reliability or accuracy. The more reliable or accurate a sensory input is, the greater the weight the brain assigns to it. We proposed that when the brain adaptively reduces its integration of unreliable visual information, such as that induced by virtual reality (VR) headsets, somatosensory feedback from the muscle to the cortex may be amplified as a compensatory mechanism.

To test our hypothesis, we used an integrated system combining a rotating platform and a VR headset to expose participants to both congruent and incongruent multisensory stimuli. We recorded EEG, EMG, and center of pressure (COP) data from the participants and analyzed the directional information interaction between the cortex and muscles using partial directed coherence analysis (PDC).

Materials and Methods

Participants

In this study, 25 college students recruited through online advertising volunteered to participate. Participants were required to have no neurological, skeletal, or muscular problems, and possess normal vision or corrected vision. The experiment was approved by the Ethics Committee of the Psychological Science Research Center at Zhejiang University (Ethics Approval Number: 2020-003), and written consent for the publication of any potentially identifiable images or data was obtained. All participants signed informed consent forms prior to participating. During the experiment, 4 participants were excluded from data analysis due to strides or stumbles. Subsequent statistical analyses included EEG and COP data from 21 participants (11 men and 10 women). In addition, due to falling off or the EMG electrodes becoming loose during the experiment, the statistical analysis only included EMG data from 19 participants (10 men and 9 women).

Experimental Design

During the experiment, the participants stood on a rotating platform (All Controller, Nanjing, China), hands on their chests, and wore a VR helmet (VIVE PRO 2, HTC Corp., New Taipei). They were instructed to keep their eyes open and look straight ahead, though blinking was permitted. Participants subsequently maintained their balance under either "congruent" or "incongruent" conditions, following a random sequence as depicted in Fig. 1 and Video S1. In the congruent condition, the goal was to present multisensory information that closely resembled natural conditions. The incongruent condition aimed to show participants who were rotating clockwise, the visual scene they would expect to see while rotating counterclockwise. Before the actual experiment, all participants were thoroughly informed of the procedures and given a trial run for familiarization. Considering the adaptation effect of standing balance, only one trial was completed per participant per condition.

In the study, the rotating platform rotated clockwise at a speed of 30°/s. We established two experimental conditions—congruent and incongruent—by presenting two motion visual scenes *via* the VR helmet. In the "congruent" condition, the goal was to present sensorimotor information that resembled natural conditions. In this case, the participant's body rotated clockwise in synchrony with the platform, relative to the ground. Meanwhile, the Inertial Measuring Unit of the VR helmet captured the participant's movement and adjusted the visual angle of the virtual scene accordingly. As a result, the participant's visual scene appeared stationary relative to the ground but moved counterclockwise at a speed of 30°/s relative to itself, mimicking what would occur in a static environment.

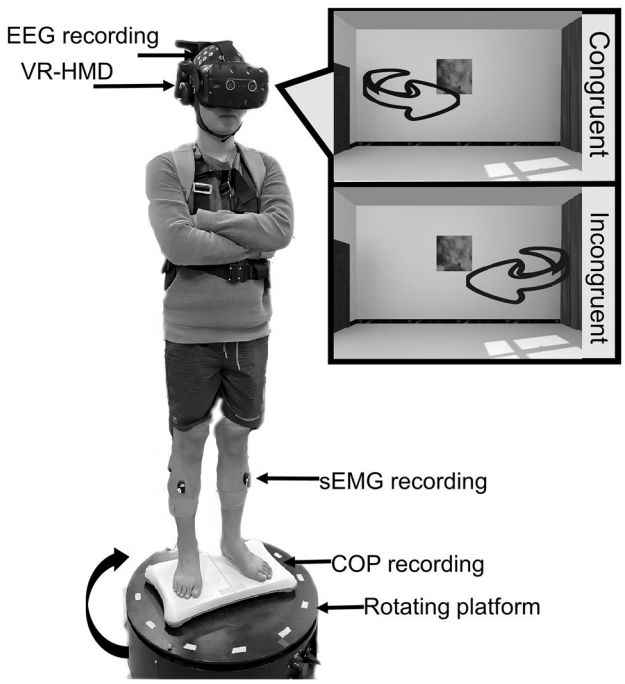

Fig. 1 Schematic of the experimental setup and installation. During the experiment, the participant stands on the rotating platform holding the chest with the hands and maintains balance under both "congruent" and "incongruent" conditions. The rotating platform always rotates clockwise relative to the ground at 30°/s. In contrast, the visual scene rotates counterclockwise relative to the participants at the same speed under congruent conditions and rotates clockwise relative to the participant at the same speed under incongruent conditions. VR-HMD, virtual reality-head-mounted display; sEMG, surface electromyography; COP, center of pressure.

Under incongruent conditions, we aimed to present visual motion information that conflicted with the actual body motion of the participant. Specifically, the participant's body rotated clockwise at a speed of 30°/s relative to the ground. Simultaneously, the visual scene displayed in the VR helmet rotated clockwise at 60°/s relative to the ground. This discrepancy generated an illusion in which the participants perceived themselves as rotating counterclockwise at a speed of 30°/s, despite their actual physical rotation being clockwise at 30°/s.

During the two tasks, participants were instructed to stand still for 30 s before the platform and visual scene began to rotate at a constant speed for 36 s. After the platform came to a stop, participants were instructed to continue standing still for an additional 30 s, followed by a 5-min rest period before beginning the next task. The acceleration phase initiated by the rotating platform was completed within 2 s. To minimize the impact of platform initiation and termination on data stability, we analyzed only data collected between 8 and 28 s after the platform rotation was initiated.

Data Collection and Preprocessing

Data from 32 EEG channels data were collected using ANT Neuro EEG caps (EE-225, ANT Neuro, Hengelo, The Netherlands), and 6-channel calf muscle data were collected by wireless EMG systems (Trigno, Delsys, MA, USA), and COP data were gathered by the Wii balance board (Nintendo, Kyoto, Japan). The impedance was maintained below 5 kΩ by using a sampling rate of 1000 Hz for both EEG and EMG data. The placement of the 32 EEG electrodes conformed to the 10–20 international standard. EMG data for the soleus (SOL), medial gastrocnemius (GM), and peroneus longus (PL) were recorded on each leg. The placement of the EMG electrodes was determined according to the SENIAM (surface EMG for a non-invasive assessment of muscles) guidelines (see https://www.seniam.org/ for details). The electrodes featured a bipolar Ag/AgCl surface with a fixed inter-electrode distance of 1 cm and a size of 10 mm × 1 mm. Double-sided tape was used to secure the electrodes. The skin was shaved,

abraded, and cleaned with alcohol before electrode placement. The Wii balance board, strategically placed in the center of the platform, was used to record COP data at a sampling rate of 100 Hz. Numerous studies have confirmed the accuracy and validity of the Wii balance board for COP measurements [27, 28]. To further investigate the impact of sensory conflict on cognition, a mid-experiment survey exploring participants' spatial orientation and conflict perception was administered to 18 participants. Specifically, after completing each task, participants were asked a question to determine their spatial orientation: "What is your direction of rotation? Please select clockwise (1) or counterclockwise (0)."

All data were preprocessed using our customized MatLab (2021b, MathWorks, MA, USA) script. COP data were filtered with a 20 Hz low-pass filter. Sway area, considered a measure of overall postural performance, quantifies 95% of the total area covered in the medial-lateral (ML) and anterior-posterior (AP) directions, using an ellipse to fit the COP data [29]. Furthermore, the complexity of COP was calculated using multi-scale sample entropy (MSE), which is a technique for measuring the complexity or regularity of time series data at multiple scales. It is an extension of the concept of sample entropy [30]. In this study, we calculated the MSE of the COP trajectory during platform rotation in both the AP and ML directions. We used an 8 times scale factor and set the parameters m to 2 and r to 0.15, as recommended in previous studies [31].

Figure 2 depicts the EEG and EMG data processing workflow. The EEG and EMG data were filtered through a 1–48 Hz band-pass filter, and the 50 Hz line noise was eliminated using the EEGLAB Cleanline plug-in [32]. For EMG data, full-wave rectification was additionally required. Furthermore, for EEG data, we used artifact subspace reconstruction (ASR) to eliminate data segments contaminated by substantial artifacts, such as body movements [33]. We set the threshold at 20 SDs, ensuring the retention of at least 65% of the data (to maintain data synchronization, corresponding segments were removed from the EMG data). ASR is an automated, online-compatible, component-based method that effectively removes transient or large-amplitude artifacts from EEG data. According to the study by Chang *et al.*, the optimal ASR parameter is between 20 and 30, which achieves a balance between the elimination of non-brain signals and the preservation of brain activity [34]. It has been widely used to inhibit the body motion artifact on EEG signals [35, 36]. Finally, the EEG signal was decomposed using Independent Component Analysis, aided by the ICLabel plug-in, to remove interfering signals originating from various sources, such as blinks, muscle artifacts, electrocardiograms, and linear noise [37].

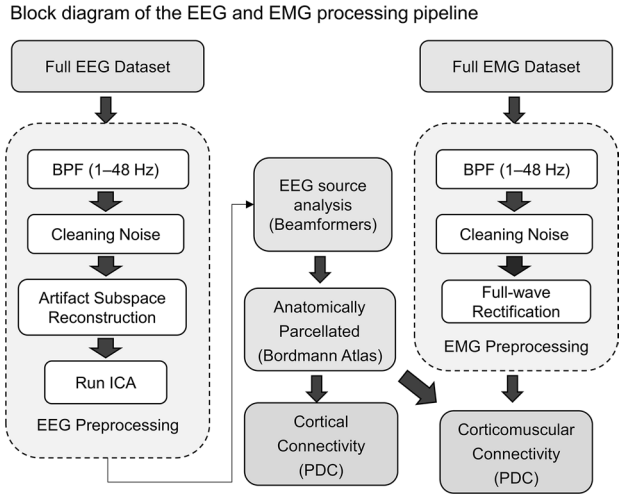

Fig. 2 Schematic of the EEG processing flow. The EEG and EMG data are filtered using a 1–48 Hz band-pass filter, and the 50 Hz line noise is removed using the EEGLAB Cleanline plug-in. For EMG data, full wave rectification is also required. Furthermore, for EEG data, we use Artifact Subspace Reconstruction to remove the data segments polluted by large artifacts, such as body movements. Finally, with the help of the ICLabel plug-in, independent component analysis (ICA) is used to decompose the EEG signal to remove interference signals from different sources.

Construction of the Cortico-muscular Network

According to research by Van de Steen [38], causal connectivity measures derived from sensor time series cannot be interpreted as interactions between brain sources because mixing effects caused by volume conduction can lead to false connectivity. Therefore, in this study, we first reconstructed the source of the time series of the EEG sensor and then analyzed the directional connectivity between the cortex and muscle. Further, considering the low density of the EEG channels in this study, we chose the beamforming algorithm to reconstruct the source of EEG. Low-density (19-channel) EEG source reconstructions with beamformers have been shown to be feasible for functional connectivity analysis [39]. Particularly, the neural correlates of motor behavior can only be captured using source functional connectivity based on beamformers. First, the head model, also known as the forward model, was generated utilizing the boundary element method and the ICBM-152 brain architecture [40]. Cortical time-series data were computed using inverse modeling based on the beamforming algorithm. The sources were confined to the cortex, and the reconstructed time-series data were projected to the region of interest (ROI), as defined by the Brodmann Atlas (BA) [41]. We chose the dorsolateral prefrontal cortex (DL-PFC; BA10, 46, 47), frontal eye fields (FEF; BA8, 9), sensorimotor cortex (SMC; BA1, 2, 3, 4, 6), posterior parietal cortex (PPC; BA5,

7), superior temporal cortex (STC; BA22, 40), and visual cortex (VC; BA17, 18, and 19) as ROIs.

To construct the corticomuscular network, we used PDC to calculate the directed functional connectivity between various cortical regions, as well as between the two hemispheric SMCs and the contralateral muscles. PDC is a mathematical measure used in signal processing and time-series analysis to quantify the directed influence between pairs of signals within a system. It is a type of frequency domain causality measure that is based on the concept of Granger causality [42]. In this study, we used the open-source toolbox HERMES to calculate PDC within the 4–48 Hz frequency range [43]. We selected this range as it encompasses the main frequency bands commonly analyzed in EEG studies and includes the frequency bands traditionally analyzed for cortical-muscle coupling. The duration of the time window was set at 6 s. This choice was based on the fact that in our symmetric VR scene setup, a 6-s window corresponds to a half rotation around the room at the rotation speed of 30°/s, allowing the participants to experience all visual scenes. To improve the robustness and sensitivity of our analysis, we chose a step size of 2 s for the time window. This smaller step size increased the number of overlapping windows for analysis, thereby providing more samples for averaging. Moreover, the model order p was determined using the Akaike information criterion and was set at 9 [44]. Next, we calculated node strength as the sum of the link weights connected to the node, in order to characterize the strength of interaction between the node and the network.

Statistical Analysis

Data from the study were thoroughly analyzed using IBM SPSS Statistics version 26.0 (IBM, Armonk, USA). The level of statistically significant differences was set at $P < 0.05$, with P-values reported to denote statistical significance. All mean differences are reported alongside their corresponding 95% confidence intervals for better representation of the results.

We commenced the analysis with a χ^2 test to evaluate the impact of sensory conflict on self-motor perception. Following this, to assess the influence of sensory conflict on postural stability and brain networks, we used a paired t-test to compare the differences in COP sway area, MSE, and node strengths under congruent *versus* incongruent conditions. The normality of these difference values was confirmed using the Shapiro-Wilk test, satisfying the prerequisite for the application of the paired t-test. Datasets that passed the Shapiro-Wilk test with a P-value >0.05 were considered to follow a normal distribution.

Next, we shifted our focus to the influence of sensory conflict on the cortico-muscular directed network. For this purpose, we applied a two-factor repeated-measures analysis of variance (ANOVA). This allowed us to discern potential interactions and primary effects of two within-subject factors, namely directionality and sensory information consistency. We again resorted to the Shapiro-Wilk test to confirm the normality of the residuals. The degrees of freedom, F-value, and corresponding P-value resulting from the ANOVA are duly reported.

Finally, we conducted a thorough investigation into the specific impacts of sensory congruence on the connectivity between various calf muscles and the cerebral cortex. Paired t-tests were carried out for each muscle-cortex pair. The results were interpreted in light of the broader connectivity trends among various muscles, thereby providing a comprehensive understanding of how sensory congruence or conflict influences cortico-muscular interactions.

Results

Effects of Sensory Conflict on COP and Spatial Orientation

The sway area and MSE of the COP trajectories were calculated and displayed in Fig. 3. First, the Shapiro-Wilk test shows that the differences between the three sets of data all conform to a normal distribution (sway area: $P = 0.074$; MSE_ML: $P = 0.23$; MSE_AP: $P = 0.35$). Therefore, here we used a paired t-test to analyze the effect of consistency of sensory information on the performance of stance balance. The results showed that under incongruent conditions, participants' COP sway area was significantly larger than congruent conditions (mean difference = 312.3 mm^2, 95% CI (confidence interval): 72.0–552.6 mm^2, $P = 0.014$). In addition, the complexity of participants' COP was found to be significantly lower under sensory conflict compared to congruent conditions (ML: mean difference = 0.16, 95% CI = 0.054–0.28, $P = 5.7 \times 10^{-3}$; AP: mean difference = 0.29, 95% CI = 0.16–0.52, $P = 1.51 \times 10^{-4}$).

Further, by analyzing the motion perception reports, we found that sensory conflict significantly influenced participants' spatial orientation [$\chi^2(1) = 5.0$, $P = 0.025$]. Specifically, under consistent conditions, all participants accurately perceived their rotation as clockwise. However, in the presence of sensory conflict, 12 participants perceived themselves as rotating clockwise (consistent with the actual direction of motion) and 6 participants perceived themselves as rotating counterclockwise (misled by visual information).

Effect of Sensory Conflict on the Cortico-muscular Directed Network

Under incongruent conditions, information flow between sensory processing areas such as the SMC, posterior parietal

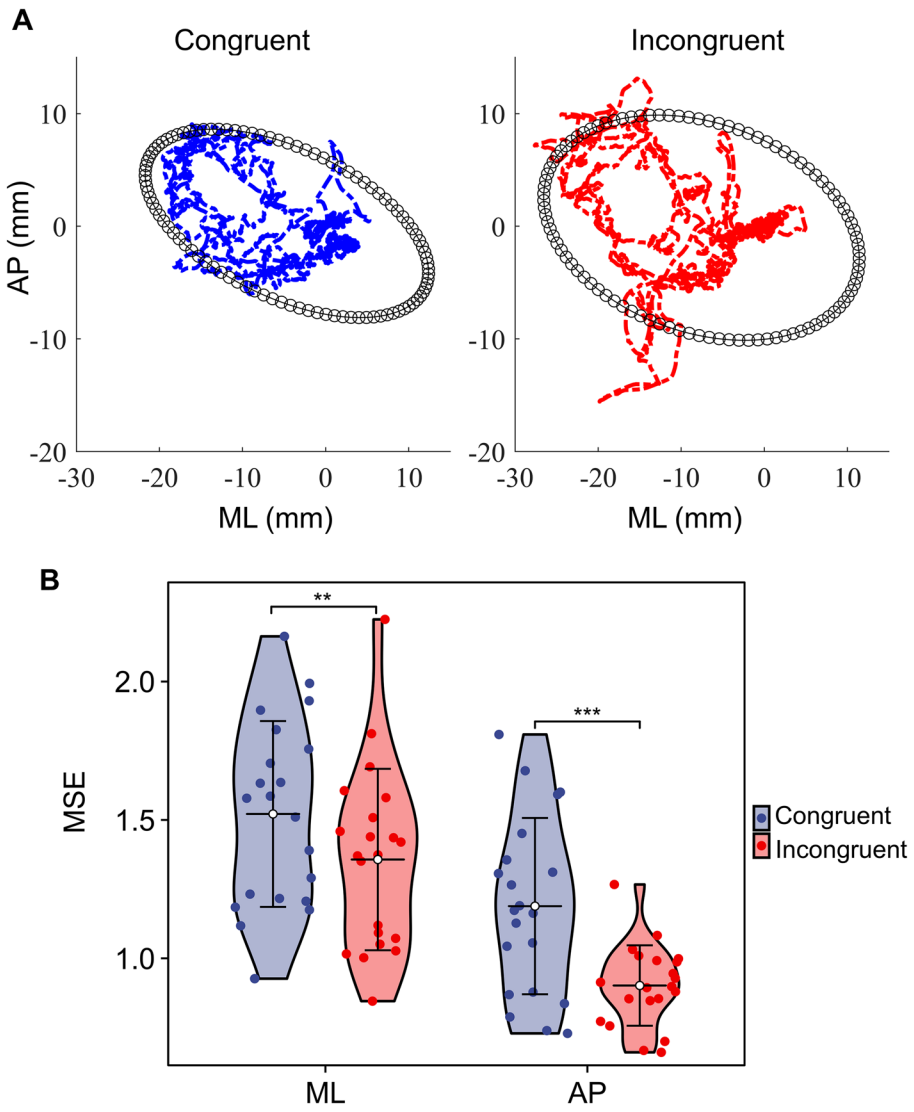

Fig. 3 Effect of sensory conditions on standing stability. **A** The average COP sway area and trajectory for all 21 participants. The mean COP trajectories for the congruent and incongruent conditions are shown, respectively, by the blue and red curves. The black ellipses quantify 85% of the total area covered in the ML (medial-lateral) and AP (anterior-posterior) directions. **B** Multi-scale sample entropy (MSE) of the COP trajectory to determine the effect of sensory conflict on standing stability between congruent and incongruent conditions. $n = 21$; $^{*}P < 0.05$, $^{**}P < 0.01$, $^{***}P < 0.001$, paired t-tests.

cortex (PPC), and visual cortex (VC) was reduced compared to sensory congruent conditions (Fig. 4A). To validate this difference, we calculated the node strength of each cortical region and conducted a paired t-test analysis. Before conducting these t-tests, the normality of the data distribution was assessed using the Shapiro-Wilk test. The test results indicated that the differences in the node strengths of all six cortical regions were normally distributed (DL-PFC: $P = 0.59$, FEF: $P = 0.37$, SMC: $P = 0.91$, PPC: $P = 0.33$, STC: $P = 0.22$, VC: $P = 0.11$). Further paired t-tests showed that, during incongruent conditions, the node strength of the SMC (mean difference = 1.40, 95% CI = 0.89–1.92, $P < 0.001$) and the PPC (mean difference = 1.11, 95% CI = 0.66–1.57, $P < 0.001$) were significantly lower than under congruent conditions (Fig. 4B). However, no statistically significant differences were found between the two conditions in the VC ($P = 0.79$), STC ($P = 0.62$), DL-PFC ($P = 0.19$), and FEF ($P = 0.69$).

Figure 5A depicts the direction information flow between the sensorimotor cortex and calf muscles. We applied the two-factor repeated-measures analysis of variance (ANOVA) to examine the influence of directionality and sensory information consistency on the average strength of cortical-muscular connectivity (Fig. 5B). Before conducting the two-factor ANOVA, we assessed the assumption of normality for our residuals, which is crucial for the validity of ANOVA results. We utilized the Shapiro-Wilk test for each group. The test results confirmed that the residuals from each group conformed to a normal distribution, as all P-values were greater than 0.05. Hence, we concluded that the assumption of normality was met. The interaction between directionality and sensory information consistency had a statistically significant impact on the average connectivity strength, $F_{(1, 18)} = 56.42$, $P < 0.001$. Consequently, we assessed the individual effects of these within-subject factors. Specifically, under both congruent and conflicting conditions, the

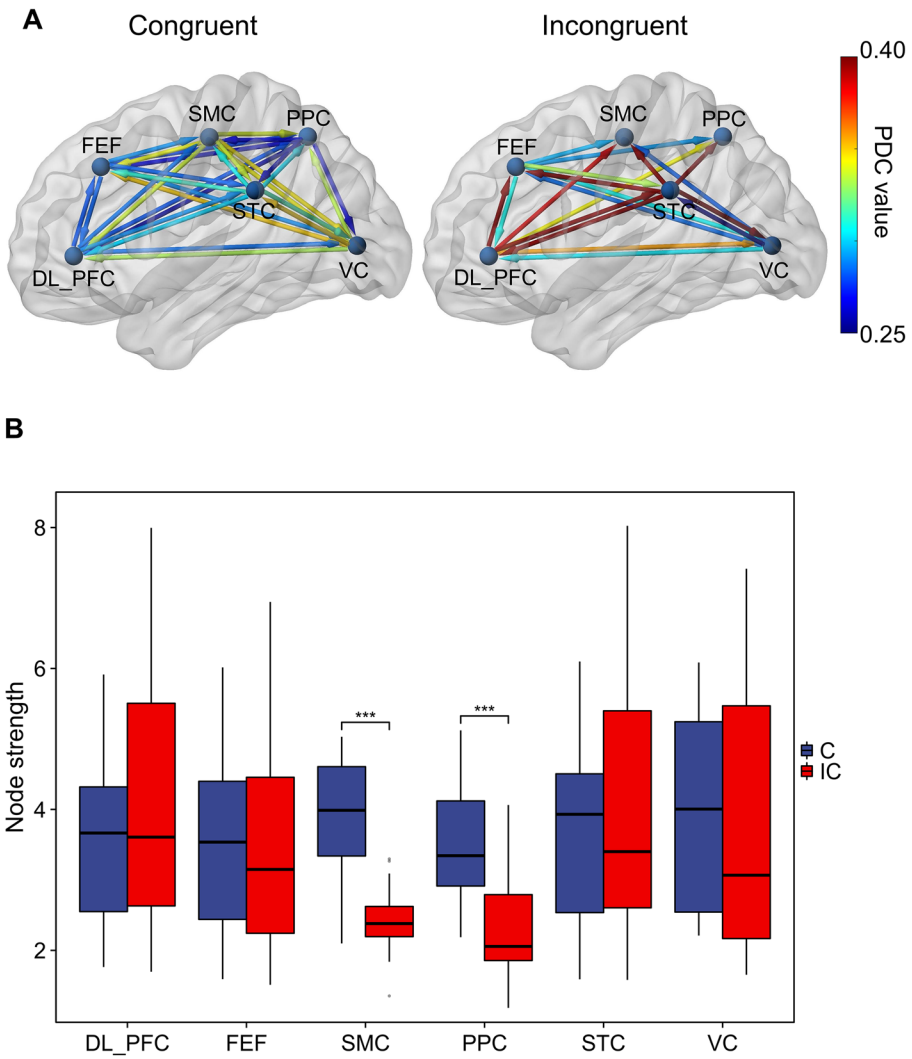

Fig. 4 Effect of sensory conditions on the cortical network. **A** The average directed functional connectivity strength between six cortical regions in each condition (sensory congruence and incongruence). **B** Node strength of each cortical region in the two conditions. The upper and lower error bars of the bins correspond to the data's upper and lower quartiles, respectively. $n = 21$, $^{*}P < 0.05$, $^{**}P < 0.01$, paired *t*-tests. PDC, partial directed coherence; DL_PFC, dorsolateral prefrontal cortex; FEP, frontal eye field cortex; SMC, sensorimotor cortex; PPC, posterior parietal cortex; STC, superior temporal cortex; VC, visual cortex; C, congruent; IC, incongruent.

strength of connectivity from the cortex to muscle was found to be stronger than that from muscle to the cortex ($P < 0.001$), with differences of 0.34 (95% CI: 0.32–0.37) and 0.21 (95% CI: 0.18–0.23), respectively. Importantly, we found that, under conditions of sensory conflict, the strength of connectivity from the cortex to muscle was significantly lower than that under conditions of sensory congruence, with a difference of 0.12 (95% CI: 0.01–0.16), $P < 0.001$. Conversely, from muscle to cortex, the connectivity strength under sensory conflicting conditions was significantly higher than under sensory congruent conditions, with a difference of 0.0040 (95% CI: 0.0025–0.0060), $P < 0.001$.

Further, we assessed the specific effects of sensory consistency on each connection pair, as shown in Table 1. Overall, the connectivity among various muscles exhibited similar trends, with the cortical-muscle connectivity being weaker during sensory conflict than sensory congruence, and the muscle-cortical connectivity was stronger during sensory conflict than sensory congruence. This difference was statistically significant for most connectivity pairs ($P < 0.05$), except for that from the left SOL to the right SMC, and from the left SMC to the right GM ($P > 0.05$).

Discussion

In this study, we aimed to investigate the relationship between multisensory integration, cortical-muscular control, and postural stability by analyzing the directed cortical-muscular interactions and COP trajectory under sensory conflicts. This provides information for a better understanding of the neural mechanisms of standing balance control.

We first analyzed participants' COP data and reports of motion perception. We found that, compared to sensory congruence, sensory conflict led to an increase in the magnitude of postural fluctuations and a reduction in complexity. In addition, 33% of participants were misled by visual information concerning the direction of movement during

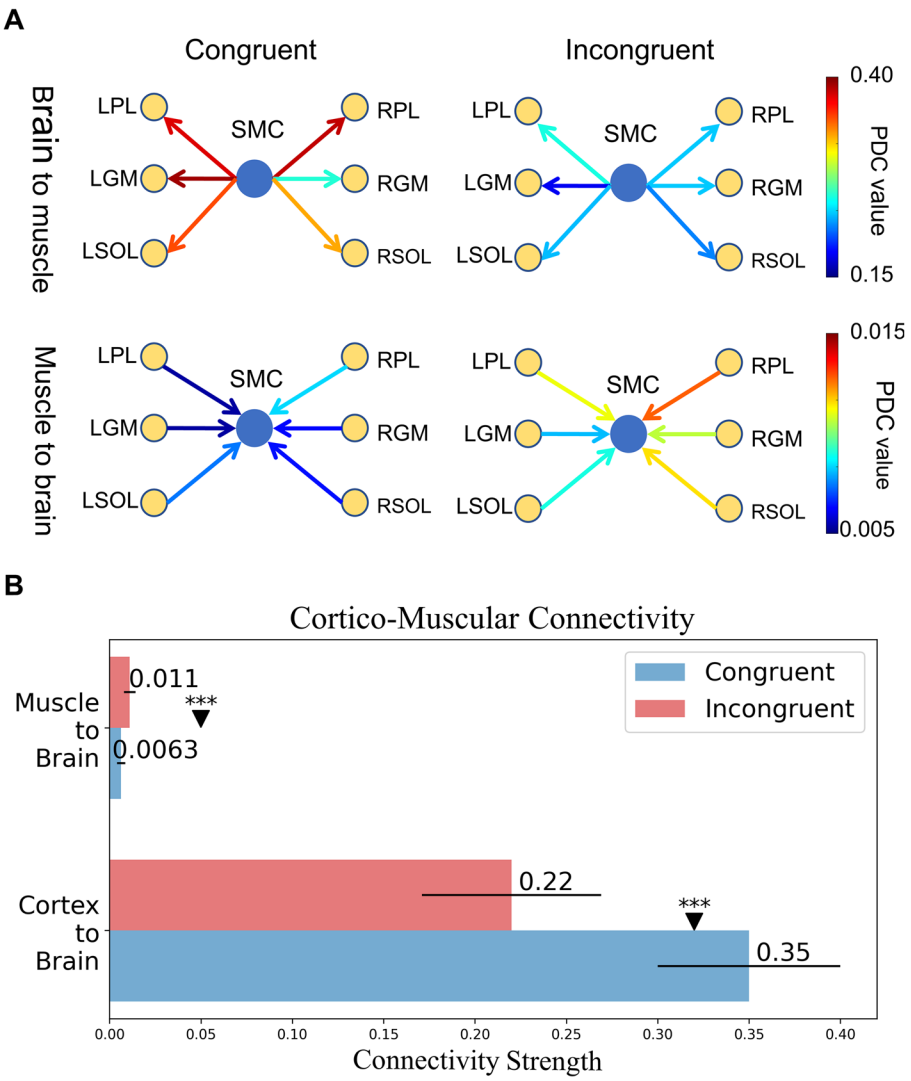

Fig. 5 Effect of sensory condition on the cortico-muscular network. **A** The average strength of the directed functional connectivity between the sensorimotor cortex and each calf muscle. The first pair of images represents the strength of the connectivity from the cortex to the muscle, and the second pair represents the connectivity from the muscle to the cortex. The first column of images represents cortico-muscular connectivity strength under sensory congruence, while the second column represents sensory incongruence. **B** The average intensity of cortical-to-muscle and muscle-to-cortical information flow in the congruent and conflicting conditions. $n = 19$, $^{*}P < 0.05$, $^{**}P < 0.01$, $^{***}P < 0.001$, two-way ANOVA with repeated measures to test the effects of direction and sensory congruency on corticomuscular connectivity. R, right; L, left; SMC, sensorimotor cortex; PL, peroneus longus; GM, gastrocnemius medial; SOL, soleus. ▼, significant differences in cortico-muscular connectivity between congruent and conflicting conditions.

Table 1 Directed interaction between the cortex and muscles. A paired *t*-test was used to examine differences in contralateral cortico-muscular directional connectivity between the two sensory conditions in 19 participants.

Type	Pair	Strength [mean (SD)]		Difference		
		Congruent	Conflicting	Mean difference	95% CI	*P*-value
Brain R ↓ Muscle L	SMC→PL	0.38 (0.11)	0.23 (0.11)	0.15	0.081, 0.21	<0.001
	SMC→GM	0.38 (0.14)	0.17 (0.12)	0.21	0.12, 0.29	<0.001
	SMC→SOL	0.35 (0.14)	0.22 (0.12)	0.12	0.045, 0.20	0.0041
Brain R ↑ Muscle L	PL→SMC	0.0027 (0.0021)	0.0056 (0.0027)	0.0029	0.0017, 0.0041	<0.001
	GM→SMC	0.0025 (0.0011)	0.0042 (0.0023)	0.0018	0.00047, 0.0030	0.01
	SOL→SMC	0.0038 (0.0024)	0.0047 (0.0026)	0.00097	−0.00047, 0.0024	0.18
Brain L ↓ Muscle R	SMC→PL	0.43 (0.14)	0.24 (0.11)	0.19	0.11, 0.27	<0.0015
	SMC→GM	0.25 (0.11)	0.22 (0.098)	0.029	−0.032, 0.088	0.33
	SMC→SOL	0.32 (0.1)	0.22 (0.13)	0.10	0.028, 0.18	0.0097
Brain L ↑ Muscle R	PL→SMC	0.0035 (0.004)	0.0065 (0.003)	0.003	0.00073, 0.0052	0.012
	GM→SMC	0.0029 (0.0024)	0.0049 (0.0022)	0.002	0.001, 0.0030	<0.001
	SOL→SMC	0.0034 (0.0016)	0.0055 (0.003)	0.0022	0.00042, 0.0039	0.017

CI, confidence interval; R, right; L, left; SMC, sensorimotor cortex; PL, peroneus longus; GM, gastrocnemius medial; SOL, soleus.

sensory conflict. Postural control is a complex process that involves interactions between multiple physiological systems and control mechanisms [45]. The high complexity of postural fluctuations indicates a high degree of adaptability. The flexible, dynamic posture process enables the human body to adapt to the complex environment and unpredictable changes [46]. Studies have found that the complexity of postural fluctuations decreases with age and disease [47, 48], giving rise to the "complexity loss hypothesis" proposed by Lipsitz and Goldberger [46, 49]. This hypothesis suggests that a reduction in the ability of physiological systems to construct complex interaction networks precipitates compromised physiological functions. Thus, the decreased complexity of postural control under sensory conflict may reflect a decrease in the adaptive adjustment of the postural control system, culminating in less adaptable and more rigid postural responses.

Furthermore, to investigate the mechanism of standing balance control, we analyzed the directed connectivity of the cortico-muscular network. Our results revealed that, during sensory conflict, information interaction in the multisensory integration network, centered on the PPC and SMC, is generally decreased and the processing of multisensory information shifted from integration to separation, which aligns with previous studies [50]. Most notably, we found that the directed connectivity from the cortex to the muscles was significantly reduced during sensory conflict, while the directed connectivity from the muscles to the cortex was significantly increased. It is well known that cortico-muscular coherence reflects both descending motor output from cortex to muscle and ascending somatosensory information feedback from muscle to motor cortex [51, 52]. Thus, our findings indicate that sensory conflict leads to diminished cortical control over muscles, as well as enhanced somatosensory feedback from muscles to the cortex. This may be related to the reduction of information interaction in multisensory integrated networks. In standing balance control, the brain needs to integrate and coordinate the multisensory information to build unified and stable cognitive information about body posture and motion. On this basis, the nervous system can appropriately activate muscles to adapt to complex environments [53, 54]. Our findings suggest that the reduction of information interaction in cortical multisensory integration may result in impaired motor control, highlighting the importance of sensory processing in movement and motor function. In addition, the enhanced feedback from the muscles to the cortex may serve as a compensatory mechanism when vision does not provide valid motor information (visual and self-motor conflict). Previous research has found that when visual information is not providing valid motor information, the human body relies more heavily on somatosensory information [55]. This could also partly explain why most people are still able to maintain balance even when sensory information is in conflict.

Finally, we found the cortex-to-muscle connectivity was significantly stronger than the muscle-to-cortex connectivity. This matches earlier results of CMC studies related to the lower limbs [26]. This asymmetry may be related to the hierarchical organization phase of the motor system. The cortical-muscle connectivity is generally stronger, mainly due to the role of this connectivity in transmitting motor commands from the brain to the muscles, making voluntary movements possible. In contrast, feedback from muscles to the cortex, although crucial for proprioception and motor learning, is less direct and robust [56].

Despite the novel insights provided by our study, we acknowledge several limitations. First, the novelty of our study design, which involves a unique combination of EEG, EMG, and balance data analysis, means that our findings may not be directly comparable to those of previous studies. Second, our study design, which involved a specific balance task involving sensory conflict, may not fully capture the complexity of real-world multisensory integration and postural control. Third, our sample size was relatively small, and the use of an experimental paradigm that induced artificial instability in the subjects' posture could have introduced variability into our data. Despite employing multiple methods to minimize this, a degree of uncertainty might have persisted, potentially affecting our results. This may be why consistent trends were found across all connections, but some did not reach statistical significance. An increased sample size might allow for more robust statistical outcomes. Fourth, we did not collect comprehensive data on the subjects' subjective experiences, such as feelings of motion sickness, which could potentially influence their postural control and cortical muscle interactions. Future research should aim to address these limitations by incorporating a wider range of tasks and conditions, increasing the sample size, including diverse participant groups, and collecting more detailed data on participants' subjective experiences. Despite these limitations, we believe our study provides valuable preliminary insights into the role of multisensory integration in cortical muscle control and postural stability.

Acknowledgments This work was supported by the National Defense Foundation Strengthening Program Technology Field Fund Project of China (2021-JCJQ-JJ-1029), the Science Technology Plan Project of Zhejiang Province (2023C03159), the Science Foundation of National Health and Family Planning Commission-Medical Health Science and Technology Project of Zhejiang Provincial Health (WKJ-ZJ-2334), and the key projects of major health science and technology plan of Zhejiang Province (WKJ-ZJ-2129).

Conflict of Interest The authors declare that there are no conflicts of interest.

References

1. Macpherson JM, Horak FB. Posture. In: Principles of Neural Science, 5th ed. McGraw Hill, 2014: 935–958.
2. Keshavarz B, Riecke BE, Hettinger LJ, Campos JL. Vection and visually induced motion sickness: How are they related? Front Psychol 2015, 6: 472.
3. Fushiki H, Kobayashi K, Asai M, Watanabe Y. Influence of visually induced self-motion on postural stability. Acta Otolaryngol 2005, 125: 60–64.
4. Cheng Q, Li CT. Top-down modulation of outcome processing in primary sensory cortex for flexible behavior. Neurosci Bull 2021, 37: 889–891.
5. van Atteveldt N, Murray MM, Thut G, Schroeder CE. Multisensory integration: Flexible use of general operations. Neuron 2014, 81: 1240–1253.
6. Dokka K, Park H, Jansen M, DeAngelis GC, Angelaki DE. Causal inference accounts for heading perception in the presence of object motion. Proc Natl Acad Sci U S A 2019, 116: 9060–9065.
7. Shams L, Beierholm UR. Causal inference in perception. Trends Cogn Sci 2010, 14: 425–432.
8. Rohe T, Ehlis AC, Noppeney U. The neural dynamics of hierarchical Bayesian causal inference in multisensory perception. Nat Commun 1907, 2019: 10.
9. Ernst MO, Banks MS. Humans integrate visual and haptic information in a statistically optimal fashion. Nature 2002, 415: 429–433.
10. Fetsch CR, Turner AH, DeAngelis GC, Angelaki DE. Dynamic reweighting of visual and vestibular cues during self-motion perception. J Neurosci 2009, 29: 15601–15612.
11. Wang G, Yang Y, Wang J, Hao Z, Luo X, Liu J. Dynamic changes of brain networks during standing balance control under visual conflict. Front Neurosci 2022, 16: 1003996.
12. Liang T, Zhang Q, Liu X, Lou C, Liu X, Wang H. Time-frequency maximal information coefficient method and its application to functional corticomuscular coupling. IEEE Trans Neural Syst Rehabil Eng 2020, 28: 2515–2524.
13. Houston M, Li X, Zhou P, Li S, Roh J, Zhang Y. Alterations in muscle networks in the upper extremity of chronic stroke survivors. IEEE Trans Neural Syst Rehabil Eng 2021, 29: 1026–1034.
14. Conway BA, Halliday DM, Farmer SF, Shahani U, Maas P, Weir AI. Synchronization between motor cortex and spinal motoneuronal pool during the performance of a maintained motor task in man. J Physiol 1995, 489(Pt 3): 917–924.
15. Mendez-Balbuena I, Huethe F, Schulte-Mönting J, Leonhart R, Manjarrez E, Kristeva R. Corticomuscular coherence reflects interindividual differences in the state of the corticomuscular network during low-level static and dynamic forces. Cereb Cortex 2012, 22: 628–638.
16. Salenius S, Salmelin R, Neuper C, Pfurtscheller G, Hari R. Human cortical 40 Hz rhythm is closely related to EMG rhythmicity. Neurosci Lett 1996, 213: 75–78.
17. Brown P, Salenius S, Rothwell JC, Hari R. Cortical correlate of the *Piper* rhythm in humans. J Neurophysiol 1998, 80: 2911–2917.
18. Murayama N, Lin YY, Salenius S, Hari R. Oscillatory interaction between human motor cortex and trunk muscles during isometric contraction. Neuroimage 2001, 14: 1206–1213.
19. Pohja M, Salenius S. Modulation of cortex-muscle oscillatory interaction by ischaemia-induced deafferentation. Neuroreport 2003, 14: 321–324.
20. Marsden JF, Brown P, Salenius S. Involvement of the sensorimotor cortex in physiological force and action tremor. Neuroreport 2001, 12: 1937–1941.
21. Baker MR, Baker SN. The effect of diazepam on motor cortical oscillations and corticomuscular coherence studied in man. J Physiol 2003, 546: 931–942.
22. Riddle CN, Baker SN. Manipulation of peripheral neural feedback loops alters human corticomuscular coherence. J Physiol 2005, 566: 625–639.
23. Witham CL, Riddle CN, Baker MR, Baker SN. Contributions of descending and ascending pathways to corticomuscular coherence in humans. J Physiol 2011, 589: 3789–3800.
24. Tsujimoto T, Mima T, Shimazu H, Isomura Y. Directional organization of sensorimotor oscillatory activity related to the electromyogram in the monkey. Clin Neurophysiol 2009, 120: 1168–1173.
25. Ozdemir RA, Contreras-Vidal JL, Paloski WH. Cortical control of upright stance in elderly. Mech Ageing Dev 2018, 169: 19–31.
26. Liang T, Hong L, Xiao J, Wei L, Liu X, Wang H, *et al*. Directed network analysis reveals changes in cortical and muscular connectivity caused by different standing balance tasks. J Neural Eng 2022, 19. https://doi.org/10.1088/1741-2552/ac7d0c.
27. Huurnink A, Fransz DP, Kingma I, van Dieën JH. Comparison of a laboratory grade force platform with a Nintendo Wii Balance Board on measurement of postural control in single-leg stance balance tasks. J Biomech 2013, 46: 1392–1395.
28. Leach JM, Mancini M, Peterka RJ, Hayes TL, Horak FB. Validating and calibrating the Nintendo Wii balance board to derive reliable center of pressure measures. Sensors (Basel) 2014, 14: 18244–18267.
29. Paillard T, Noé F. Techniques and methods for testing the postural function in healthy and pathological subjects. Biomed Res Int 2015, 2015: 891390.
30. Costa M, Goldberger AL, Peng CK. Multiscale entropy analysis of biological signals. Phys Rev E 2005, 71: 021906.
31. Gow B, Peng CK, Wayne P, Ahn A. Multiscale entropy analysis of center-of-pressure dynamics in human postural control: Methodological considerations. Entropy 2015, 17: 7926–7947.
32. Delorme A, Makeig S. EEGLAB: An open source toolbox for analysis of single-trial EEG dynamics including independent component analysis. J Neurosci Methods 2004, 134: 9–21.
33. Mullen TR, Kothe CAE, Chi YM, Ojeda A, Kerth T, Makeig S, *et al*. Real-time neuroimaging and cognitive monitoring using wearable dry EEG. IEEE Trans Biomed Eng 2015, 62: 2553–2567.
34. Chang CY, Hsu SH, Pion-Tonachini L, Jung TP. Evaluation of artifact subspace reconstruction for automatic artifact components removal in multi-channel EEG recordings. IEEE Trans Biomed Eng 2020, 67: 1114–1121.
35. Peterson SM, Ferris DP. Group-level cortical and muscular connectivity during perturbations to walking and standing balance. Neuroimage 2019, 198: 93–103.
36. Shenoy Handiru V, Alivar A, Hoxha A, Saleh S, Suviseshamuthu ES, Yue GH, *et al*. Graph-theoretical analysis of EEG functional connectivity during balance perturbation in traumatic brain injury: A pilot study. Hum Brain Mapp 2021, 42: 4427–4447.
37. Pion-Tonachini L, Kreutz-Delgado K, Makeig S. ICLabel: An automated electroencephalographic independent component classifier, dataset, and website. Neuroimage 2019, 198: 181–197.
38. Van de Steen F, Faes L, Karahan E, Songsiri J, Valdes-Sosa PA, Marinazzo D. Critical Comments on EEG Sensor Space Dynamical Connectivity Analysis. Brain Topogr 2019, 32: 643–654.
39. Nguyen-Danse DA, Singaravelu S, Chauvigné LAS, Mottaz A, Allaman L, Guggisberg AG. Feasibility of reconstructing source functional connectivity with low-density EEG. Brain Topogr 2021, 34: 709–719.
40. Fuchs M, Drenckhahn R, Wischmann HA, Wagner M. An improved boundary element method for realistic volume-conductor modeling. IEEE Trans Biomed Eng 1998, 45: 980–997.

41. Zilles K, Zilles K, Amunts K. Centenary of Brodmann's map—conception and fate. Nat Rev Neurosci 2010, 11: 139–145.
42. Baccalá LA, Sameshima K. Partial directed coherence: A new concept in neural structure determination. Biol Cybern 2001, 84: 463–474.
43. Niso G, Bruña R, Pereda E, Gutiérrez R, Bajo R, Maestú F, *et al*. HERMES: Towards an integrated toolbox to characterize functional and effective brain connectivity. Neuroinformatics 2013, 11: 405–434.
44. Akaike H. Citation Classic - a new look at the statistical-model identification. CC/ENG Tech Appl Sci 1981, 51: 22–22.
45. Horak FB, Macpherson JM. Postural orientation and equilibrium. In: Handbook of Physiology: Exercise: Regulation and Integration of Multiple Systems. Oxford University Press, 1996: 255–292.
46. Lipsitz LA. Dynamics of stability: The physiologic basis of functional health and frailty. J Gerontol A Biol Sci Med Sci 2002, 57: B115–B125.
47. Costa M, Priplata AA, Lipsitz LA, Wu Z, Huang NE, Goldberger AL, *et al*. Noise and poise: Enhancement of postural complexity in the elderly with a stochastic-resonance-based therapy. Europhys Lett 2007, 77: 68008.
48. Gruber AH, Busa MA, Gorton GE III, Van Emmerik RE, Masso PD, Hamill J. Time-to-contact and multiscale entropy identify differences in postural control in adolescent idiopathic scoliosis. Gait Posture 2011, 34: 13–18.
49. Lipsitz LA, Goldberger AL. Loss of 'complexity' and aging. Potential applications of fractals and chaos theory to senescence. JAMA 1992, 267: 1806–1809.
50. Rideaux R, Storrs KR, Maiello G, Welchman AE. How multisensory neurons solve causal inference. Proc Natl Acad Sci U S A 2021, 118: e2106235118.
51. Airaksinen K, Lehti T, Nurminen J, Luoma J, Helle L, Taulu S, *et al*. Cortico-muscular coherence parallels coherence of postural tremor and MEG during static muscle contraction. Neurosci Lett 2015, 602: 22–26.
52. Fang Y, Daly JJ, Sun J, Hvorat K, Fredrickson E, Pundik S, *et al*. Functional corticomuscular connection during reaching is weakened following stroke. Clin Neurophysiol 2009, 120: 994–1002.
53. Takakusaki K. Functional neuroanatomy for posture and gait control. J Mov Disord 2017, 10: 1–17.
54. Takakusaki K, Takahashi M, Obara K, Chiba R. Neural substrates involved in the control of posture. Adv Robotics 2017, 31: 2–23.
55. Fetsch CR, Pouget A, DeAngelis GC, Angelaki DE. Neural correlates of reliability-based cue weighting during multisensory integration. Nat Neurosci 2011, 15: 146–154.
56. Yang Y, Dewald JPA, van der Helm FCT, Schouten AC. Unveiling neural coupling within the sensorimotor system: Directionality and nonlinearity. Eur J Neurosci 2018, 48: 2407–2415.

frontiers | Frontiers in Neuroscience

TYPE Original Research
PUBLISHED 05 October 2022
DOI 10.3389/fnins.2022.1003996

OPEN ACCESS

EDITED BY
Mark Schmuckler,
University of Toronto Scarborough, Canada

REVIEWED BY
Hendrik Reimann,
University of Delaware, United States
Ajitkumar Mulavara,
KBRwyle, United States

*CORRESPONDENCE
Jun Liu
liujun@zju.edu.cn

†These authors have contributed equally to this work and share first authorship

SPECIALTY SECTION
This article was submitted to Perception Science, a section of the journal Frontiers in Neuroscience

RECEIVED 26 July 2022
ACCEPTED 20 September 2022
PUBLISHED 05 October 2022

CITATION
Wang G, Yang Y, Wang J, Hao Z, Luo X and Liu J (2022) Dynamic changes of brain networks during standing balance control under visual conflict. *Front. Neurosci.* 16:1003996. doi: 10.3389/fnins.2022.1003996

Dynamic changes of brain networks during standing balance control under visual conflict

Guozheng Wang[1†], Yi Yang[2†], Jian Wang[2], Zengming Hao[3], Xin Luo[2] and Jun Liu[1*]

[1]College of Biomedical Engineering and Instrument Science, Zhejiang University, Hangzhou, China, [2]Department of Sports Science, College of Education, Zhejiang University, Hangzhou, China, [3]Department of Rehabilitation Medicine, The First Affiliated Hospital, Sun Yat-sen University, Guangzhou, China

Stance balance control requires a very accurate tuning and combination of visual, vestibular, and proprioceptive inputs, and conflict among these sensory systems may induce posture instability and even falls. Although there are many human mechanics and psychophysical studies for this phenomenon, the effects of sensory conflict on brain networks and its underlying neural mechanisms are still unclear. Here, we combined a rotating platform and a virtual reality (VR) headset to control the participants' physical and visual motion states, presenting them with incongruous (sensory conflict) or congruous (normal control) physical-visual stimuli. Further, to investigate the effects of sensory conflict on stance stability and brain networks, we recorded and calculated the effective connectivity of source-level electroencephalogram (EEG) and the average velocity of the plantar center of pressure (COP) in healthy subjects (18 subjects: 10 males, 8 females). First, our results showed that sensory conflict did have a detrimental effect on stance posture control [sensor $F(1, 17) = 13.34$, $P = 0.0019$], but this effect decreases over time [window*sensor $F(2, 34) = 6.72$, $P = 0.0035$]. Humans show a marked adaptation to sensory conflict. In addition, we found that human adaptation to the sensory conflict was associated with changes in the cortical network. At the stimulus onset, congruent and incongruent stimuli had similar effects on brain networks. In both cases, there was a significant increase in information interaction centered on the frontal cortices ($p < 0.05$). Then, after a time window, synchronized with the restoration of stance stability under conflict, the connectivity of large brain regions, including posterior parietal, visual, somatosensory, and motor cortices, was generally lower in sensory conflict than in controls ($p < 0.05$). But the influence of the superior temporal lobe on other cortices was significantly increased. Overall, we speculate that a posterior parietal-centered cortical network may play a key role in integrating congruous sensory information. Furthermore, the

dissociation of this network may reflect a flexible multisensory interaction strategy that is critical for human posture balance control in complex and changing environments. In addition, the superior temporal lobe may play a key role in processing conflicting sensory information.

KEYWORDS

electroencephalography, sensory conflict, standing balance control, effective connectivity, virtual reality

Introduction

Stance balance control is a complex process in which the brain must continuously combine multisensory information from the visual, vestibular, and somatosensory systems to activate muscles for proper posture or movement. Vision plays an important role in the control of posture, and when these three sensory systems are isolated and tested for balance, it has been found that vision is the most important contributor to balance (Hansson et al., 2010). However, the source of visual motion is inherently ambiguous, and the movement of objects in the environment and self-movement can cause similar visual stimuli (Fushiki et al., 2005). In some complex environments, the conflict between visual and nonvisual information may lead to unstable posture, vertigo, and even falls (Keshavarz et al., 2015). Theoretically, the brain could mitigate this problem by combining visual signals with other types of information. Human mechanics studies have shown that the integration of sensory information used for postural control appears dynamically regulated to adapt to changing environmental conditions and available sensory information (Peterka and Loughlin, 2004; Mahboobin et al., 2009). And numerous psychophysical studies have shown that during multisensory processing, the brain needs to make judgments about the source of multimodal sensory cues, arbitrating between sensory integration, and segregation (Dokka et al., 2010, 2019; Shams and Beierholm, 2010; Acerbi et al., 2018; Rohe et al., 2019). It performs weighted fusion for sensory signals from common sources and separate processing for sensory information from independent sources (Ernst and Banks, 2002; Fetsch et al., 2009).

The exact neural mechanisms of multisensory interactions are still unclear, but several cortical regions have been identified as a crucial contribution (Bolton, 2015). Neurophysiological studies in macaques have shown that multisensory information is combined in the dorsal division of the medial superior temporal area and the ventral intraparietal area. Both areas contain neurons that show selectivity for optic flow patterns and directional tuning for inertial motion in darkness (Tanaka et al., 1986; Duffy and Wurtz, 1991; Page and Duffy, 2003; Gu et al., 2006), and some of these neuronal populations are sensitive to congruent stimuli and others to incongruent stimuli. Neuroimaging studies in humans have also localized multiple multisensory cortices, including numerous areas in the parietal cortex (e.g., the ventral intraparietal area), temporal cortex (e.g., the caudal superior temporal polysensory region), and frontal cortex. Further, congruency of sensory cues was also found to affect cortical activation, with stronger activation in the posterior insula and temporal lobes during sensory conflict and increased activation in the primary and secondary visual cortex when sensory cues were congruent (Roberts et al., 2017); Hemodynamic studies have shown that medial temporal and medial superior temporal regions have stronger activation in conflict conditions compared to congruent conditions (Nguyen et al., 2020). In addition, the subjective strength of the vertiginous sensation was negatively correlated with the hemodynamic activity of the intraparietal sulcus and supramarginal gyrus.

Although previous studies have identified many cortical regions that are significantly activated during multisensory interactions, the interactions within and between the relevant cortical regions remain to be investigated. It is well known that multisensory processing requires the coordinated activity of different cortical areas, and key mechanisms involved in these processes include local neural oscillations and connections between distant cortical areas (von Stein and Sarnthein, 2000; Keil and Senkowski, 2018). Therefore, it is important to study the flow of information across multiple cortical areas that process and integrate sensory cues. Traditional neuroimaging methods are limited by fixed recordings and low temporal resolution, such as functional magnetic resonance imaging (fMRI) and functional near-infrared spectroscopy (fNIRS). In contrast, electroencephalography (EEG) is a promising method for assessing human cortical interactions during dynamic homeostasis due to its high temporal resolution and portability (Gramann et al., 2011). Although EEG may be limited by low spatial resolution and artifact contamination, cortical activity can be obtained by source analysis techniques while removing artifacts from it by blind source separation techniques such as independent component analysis (ICA), thereby improving spatial resolution and reducing artifact contamination (Gwin et al., 2010).

In the present study, we hypothesized that cross-modal differences in sensory information affect the brain's strategies for multisensory processing in stance balance control and that this can be revealed by quantitative measures of interactions between relevant cortical regions. Here, according to our working hypothesis, we combined a rotating platform and a virtual reality (VR) headset to control participants' body movements and visual information to construct incongruous (sensory conflict) or congruous (normal control) physical-visual rotational stimuli. And the information flow in the cortical network was measured quantitatively by partial directed coherence (PDC, a time-varying, frequency-selective, and directional functional connectivity analysis tool) (Baccala and Sameshima, 2001; Friston, 2011).

Materials and methods

Participants

Twenty-two college students participated in this study. Subjects were volunteers from the local university campus who responded to a network advertisement. All participants had no neurological, skeletal, or muscular problems and normal or corrected vision and signed a written informed consent form. The Ethics Committee of Zhejiang University Psychological Science Research Center permitted our experiment (issued no. 2020-003). Four participants were excluded from data analysis because of strides/stumbles during the experiment. Finally, data from 18 participants [10 males, 8 females, age 24.1 $\pm$ 2.3 years (mean $\pm$ *SD*)] were involved in the statistical analysis.

Experimental design

In this study, we used a rotating platform and a VR headset to control the participants' body movements and visual information. The rotation platform (All Controller, Nanjing, P. R. China) can rotate counterclockwise and clockwise with a maximum rotation speed of 96 deg/s. The VR headset used the VIVE Pro Eye wireless kit produced by HTC, which can present a simulated laboratory environment through the Unity3D program (Outside of the programmed scene movement, normal head movements are also picked up by the IMU in the VR headset and change the perspective of the virtual scene accordingly). We used the written Unity3D program to control both the rotating platform and the visual scene in the VR headset, setting both "congruent" (visual information synchronized with the actual body movement) and "incongruent" (visual information conflicting with the actual body movement) experimental conditions.

In the congruent condition, we did not provide additional control in the VR headset. In this case, the participant moved clockwise with the rotating platform at 30°/s relative to the ground, while that motion was picked up by the IMU in the VR headset, and the visual scene in his eyes moved counterclockwise relative to him at 30°/s (just as in a natural rotation in a stationary environment, the visual scene should be stationary relative to the ground, but moving in the opposite direction relative to ourselves). In the incongruent condition, our goal is to construct a scene that should be seen with counterclockwise motion at the same speed in the case of clockwise motion. This that the visual scene provides a message in the opposite direction of the actual motion, with the same intensity. In this case, we added an additional 60°/s of clockwise motion to the scene of the VR headset. At this point, the participant's body moves clockwise at 30°/s, and the visual scene in his eyes also moves clockwise at 30°/s. In both the congruent and incongruent conditions, the platform and the visual scene began to move after 30 s of standing and stopped after 36 s of uniform rotation at 30 deg/s; The acceleration and deceleration processes were completed within 1 s; Participants were then asked to continue standing quietly for 34 s, and then rest for 5 min waiting for the next test task.

The experimental setup and settings are shown in **Figure 1**. Before the start of the formal test, we informed the participants of the experimental procedure, and all participants familiarized themselves with each condition. In the formal test, each participant was asked to stand on the force plate with arms crossed over the chest in a shoulder-width position. All subjects were instructed to keep their eyes open (normal blinks were allowed) and look straight ahead throughout the experiment, which was ensured by an eye-tracking system built into the VR headset. The force plate was placed in the center of the rotating platform. Next, all participants were asked to maintain standing balance to complete three test tasks (stationary standing baseline, congruent and incongruent physical-visual stimuli). The order in the three tasks was randomized and had 5 min of rest between different test tasks. In the standing baseline condition, the rotating platform and the VR scene remained motionless for 100 s.

Data collection and preprocessing

In this study, we mainly collected plantar center of pressure (COP) data and EEG data from participants during the experimental task. We placed the Wii balance board in the center of the rotating platform and measured the subjects' COP under the three experimental tasks with a sampling rate of 100 Hz. Many studies have verified the validity and reliability of the Wii balance board in COP measures (Clark et al., 2010; Huurnink et al., 2013; Leach et al., 2014). The validity of the COP data in this study is discussed in **Supplementary Figure 1**. The EEG signals were acquired with the ANTNeuro EEG device, containing 32 channels in the 10–20 standard regime, and the impedance of all electrodes was kept below 5 k ohms throughout the experiment, at a sampling rate of 1,000 Hz sampling.

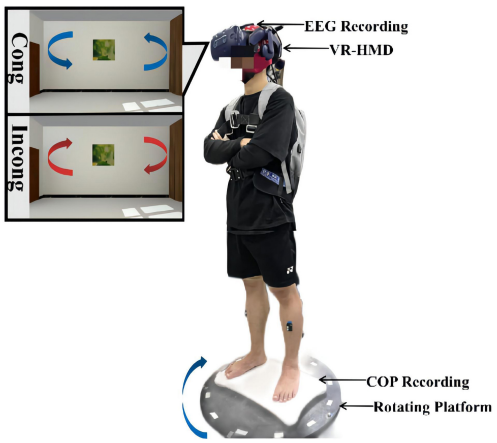

FIGURE 1
Schematic diagram of the experimental setup and installation. The experimental system was composed of an EEG acquisition device, a VR headset, a force measurement platform, and a rotating platform. During the experiment, the participants stood on the force measurement platform and were asked to look straight ahead with their hands on their chests the whole time. Both physical and visual distractions were applied through the rotating platform and the VR headset. The rotation was always clockwise, while the visual scene was rotated counterclockwise at the same speed in the congruent condition and clockwise at the same speed in the incongruent condition.

We preprocessed the COP and EEG data in a custom script in Matlab. First, we discard the signals in the acceleration or deceleration phase of the rotation platform and then divide the COP data and EEG data into six phases: baseline (BS, 12 s before platform start), rotating1 (R1, 0–12 s after platform start), rotating2 (R2, 12–24 s after platform start), rotating3 (R3, 24–36 s after platform start), after1 (A1, 0–12 s after platform stop), and after2 (A2, 12–24 s after platform stop). The COP data were filtered using a 20 Hz low-pass, 2nd order, zero-lag Butterworth filter. Furthermore, the mean of the filtered data was removed.

Sway area quantifies 85% of the total area covered in the ML and AP directions using an ellipse to fit the COP data, which is considered an index of overall postural performance (Palmieri et al., 2002; Paillard and Noe, 2015). Sway mean velocity is calculated by dividing the COP trajectory distance by the duration, which is considered to be the reliable dynamic indicator of the efficiency of posture control (the smaller the speed, the better the posture control) (Paillard and Noe, 2015; Luo et al., 2018). We calculated mean sway velocity of the COP signal as follows:

$$MV = \frac{\sum_{i=1}^{N} \sqrt{(x_{i+1} - x_i)^2 + (y_{i+1} - y_i)^2} * F}{N}$$

where x(i) and y(i) are the COP displacements in the ML and AP directions, respectively, N = number of samples, F = sampling frequency.

We processed the EEG data mainly based on a custom script in the EEGLAB toolbox (Delorme and Makeig, 2004), it was first band-pass filtered from 1 to 48 Hz, and the 50 Hz line noise was removed using the EEGLAB Cleanline plug-in. Further, to remove artifacts from body motion during rotation, the EEG data segments contaminated with large artifacts were removed using Artifact Subspace Reconstruction (ASR) (Mullen et al., 2015), where the threshold was set to 20 standard deviations and ensured that at least 62.5 percent (Every 12 s data is guaranteed to leave 7.5 s) of the data were retained. Finally, the EEG signal was decomposed using ICA with the aid of the ICLabel plug-in to remove interfering signals such as blinks, muscle artifacts, electrocardiogram, and linear noise that are not homologous to the EEG (Pion-Tonachini et al., 2019). The processing flow of EEG data is shown in **Figure 2**.

Electroencephalogram sourcing analysis and connectivity computation

The EEG source analysis allows us to study cortical dynamics from the potential cortical source activity estimated from the sensor space EEG. Here, we used a standardized low-resolution EEG tomography software package for source localization (Pascual-Marqui, 2002). First, a head model (forward model) was created using a Boundary Element Method based on the ICBM152 brain anatomy (Fuchs et al., 1998; Mazziotta et al., 2001). Inverse modeling based on a standardized low-resolution electromagnetic tomography algorithm was used to compute cortical time series data. The sources were restricted to the cortex, and the reconstructed time series were projected to the region of interest (ROI) defined by the Brodmann atlas (Zilles and Amunts, 2010). Specifically, we selected the following seven cortical regions as ROIs: dorsolateral prefrontal cortex (DL-PFC; BA10, 46, 47), frontal eye field cortex (FEF; BA8, 9), motor cortex (MC; BA4, 6), primary somatosensory (S1; BA1, 2, 3), posterior parietal cortex (PPC; BA5, 7), superior temporal cortex (STC; BA22, 40), visual cortex (VC; BA17, 18, 19).

After obtaining the activity of the seven cortical regions of interest, we used PDC to perform an effective connectivity analysis (Baccala and Sameshima, 2001). PDC, a frequency domain extension of Granger causality, can be used to calculate the strength of directed information flow between cortical regions. We used the open-source toolbox HERMES to calculate PDC for theta (4–8 Hz) and alpha (8–12 Hz) bands, where the time window was set to 3 s with 50% overlap (Each segment of 7.5 s of valid data is divided into 4 windows), and the model order p was determined using the Akaike information criterion. Then node strength was computed as the sum of weights of links connected to the node.

Statistical analysis

First, to determine the effect of sensory conflict on stance stability, we used two-way repeated measures ANOVA to assess the effects of the time window and sensory condition on COP sway velocity. Differences in COP sway velocity within rotating phase (R1, R2, R3) or after rotating phase (A1, A2) were assessed with two-way repeated measures ANOVAs with sensory condition (incongruent, congruent) and time window (per 12 s) factor. Differences in COP sway velocity during the movement state transitions were assessed with repeated measures ANOVAs, which compared the baseline to the mean of the rotating and after rotating phases in both sensory conditions. In ANOVAs, predicted effects and/or interactions were explored further with simple effects analyses, and unexpected effects were explored further with Bonferroni *post-hoc* tests.

Further, in order to know the effect of incongruent and congruent rotational stimuli on brain networks, we used paired *t*-tests to analyze the differences in network connection and node strength between two rotational stimuli to baseline. Further, we examined the effect of time windows (R1, R2, and R3) and sensory status on node strength using two-way repeated measures ANOVA and Bonferroni *post-hoc* tests for data from the interference period. In the analysis of cortical connections, $p < 0.05$ was defined as a significant difference, and all *p*-values were corrected for the false discovery rate (FDR) method (Benjamini and Hochberg, 1995). Significant connections corresponding to $p < 0.05$ were plotted onto MRI templates using the BrainNet Viewer toolbox (Xia et al., 2013), where red represents significantly stronger, and blue represents significantly weaker. Studentized residuals were tested for normality by Shapiro-Wilk's test, and non-normal data were analyzed using the Wilcoxon signed-rank test or Friedman two-way analysis of variance.

Results

Effect of sensory conflict on standing balance

To investigate the effect of sensory conflict on standing postural stability, we collected participants' center of plantar pressure (COP) in both sensory conditions and recorded their trajectories (**Figure 3A**). Using a paired *t*-test showed that the range of COP sway was significantly greater in incongruent condition than in congruent condition ($P = 0.0019$). This suggests that sensory conflict has a detrimental effect on stance stability.

Further, to investigate the dynamic effects of sensory conflict on standing posture stability, we used two-way repeated measures ANOVA to assess the effects of the time window and sensory condition on standing posture stability, as shown in **Figure 3B**. First, the sway velocity increased substantially in both sensory conditions after the platform started to rotate (**Figure 3B**). A repeated measures ANOVA contrasting average sway velocity at the two windows of baseline with an average of three windows in rotation period confirmed it [window $F(1, 17) = 108.14$, $P = 8.7e\text{-}11$], and also sway velocity significantly greater in the incongruent condition than in the congruent condition [sensor $F(1, 17) = 12.11$, $P = 0.0029$].

Then, we analyzed the sway velocity during the rotation duration (R1, R2, R3) using repeated measures ANOVA. The results showed that the sway speed of participants decreased significantly over time [window $F(2, 34) = 49.38$, $P = 8.8e\text{-}11$], which reflected the adaptation of the humans to the balance disturbance. And the sway velocity was significantly greater in the incongruent condition than in the congruent condition [sensor $F(1, 17) = 13.34$, $P = 0.0019$], which reflected the detrimental effect of sensory conflict on the standing balance. More importantly, we found a significant interaction effect of the two factors [window*sensor $F(2, 34) = 6.72$, $P = 0.0035$]. This implies that the detrimental effect of sensory conflict on stance stability diminishes over time. Bonferroni pairwise comparisons also demonstrated that the sway velocity in the incongruent condition was significantly greater than that in the congruent condition only during the first time window of platform rotation (R1: $P = 0.063$), with no significant difference between the two subsequent windows (R2: $P = 0.099$; R3: $P = 0.40$).

Finally, we analyzed the sway velocity after the platform was stopped. The results show that the mean sway velocity after platform stop is still significantly larger than the baseline [window $F(1, 17) = 43.71$, $P = 4.0e\text{-}06$], indicating that there are some after effects of the disturbance. Further, analysis of the sway velocity for the two windows after platform stopping showed that the sway velocity decreased over time [window $F(1, 17) = 45.38$, $P = 3.0e\text{-}06$] and was greater for those experiencing sensory conflict [sensor $F(1, 17) = 18.99$, $P = 4.3e\text{-}04$]. In addition, a significant interaction effect was also shown between the two factors [window*Sensor $F(1, 17) = 9.85$, $P = 0.006$]. Bonferroni pairwise comparisons also demonstrated that the sway velocity after the incongruent condition was significantly greater than that in the congruent condition only during the first time window after platform stop (A1: $P = 0.0019$). This also implies that the detrimental effect of sensory conflict on stance stability diminishes over time (A2: $P = 0.11$).

Changes in brain networks under multisensory stimuli

To quantify the status of cortical information flow during equilibrium under multisensory stimuli, we constructed a cortical effective connectivity network using a partial directed coherence function (PDC). **Figures 4A**, **5A** show the significant changes in effective cortical connectivity ($p < 0.05$, false

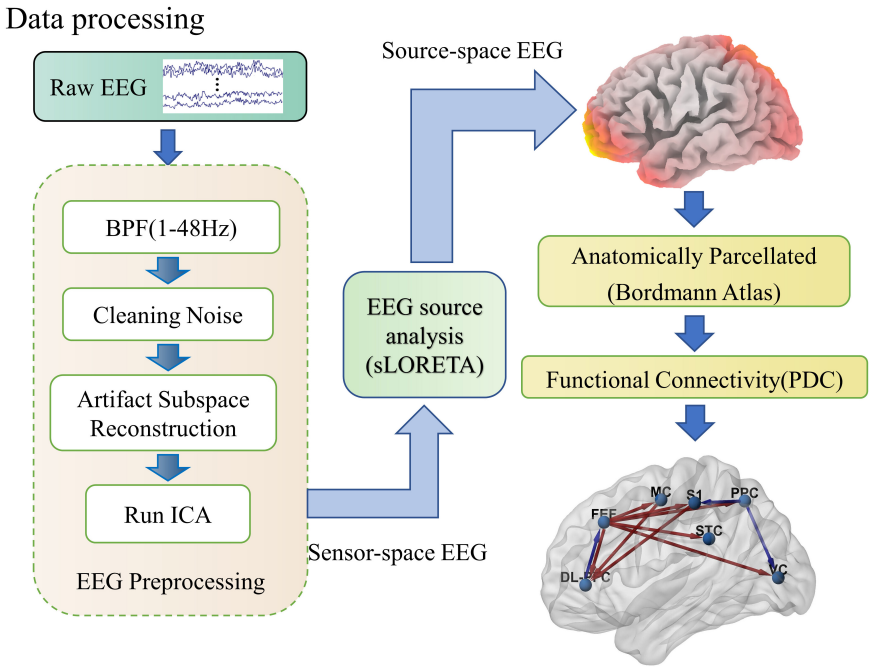

FIGURE 2
Schematic diagram of the EEG processing flow. As shown in the figure, EEG processing includes three parts: preprocessing, soliton source analysis, and network connection calculation. In the preprocessing, raw EEG is cleaned up by band-pass filtering, removal of linear interference, artifact spatial reconstruction, and independent component analysis steps. Then the sensor space EEG is transformed into source activity and clustered into regions of interest by the sLORETA software package. Finally, the effective connections between cortical regions of interest are calculated quantitatively using PDC.

discovery rate correction) in the rotational stimuli compared to the stationary baseline. The red/blue lines represent effective connectivity during rotational stimulation significantly greater/less than during stationary standing (**Supplementary Figures 2**, **3** provide the specific *p*-value for each connection pair).

First, at the onset of the rotating stimulus (R1), the effective connections centered in the frontal lobe were significantly increased compared to the baseline. From the first columns of **Figures 4A**, **5A**, we can find that all frontal (DL-PFC, FEF, SMA) regions have enhanced effective connections with other regions in the congruent condition. While in the incongruent condition, in addition to significant activation of the frontal cortical-centered networks compared to the baseline, there was a significant increase in the outflow of information from the superior temporal lobe.

Second, after a period of sustained rotational stimulation (R2, R3), we found a wide activation of cortical networks in the theta band compared to the baseline (as shown in the third and second columns of **Figure 4A**). In the congruent condition, the effective connections between the visual cortex, motor cortex, somatosensory cortex, posterior parietal lobe, and superior temporal lobe were generally significantly enhanced, forming a network of information interactions centered on parietal-temporal extensions to visual and sensorimotor cortices. In the incongruent condition, we mainly found a significant enhancement of information flow from the temporal lobe to other regions. In addition, the trends were similar in the alpha to theta bands, but the alpha band activated fewer connections during stimulation than the theta band (**Figure 5A**).

Then, we calculated the node strength in the posterior parietal and superior temporal cortices to further explore the effect of multisensory stimuli. Paired *t*-tests were used to determine the difference in node strength between rotating phase (R1, R2, R3) and baseline and were corrected for multiple comparisons using Bonferroni as shown in **Figures 4B**, **5B**. We could see that the posterior parietal lobe node strength was significantly greater in sensory congruent rotational stimulation compared to the baseline (Theta: $P_{R1} = 0.0013$, $P_{R2} = 0.00040$, $P_{R3} = 0.0060$; alpha: $P_{R1} = 0.034$, $P_{R2} = 0.0041$, $P_{R3} = 0.019$), while there was no significant change during the sensory conflict (Theta: $P_{R1} = 0.091$, $P_{R2} = 0.087$, $P_{R3} = 0.22$; Alpha: $P_{R1} = 0.64$, $P_{R2} = 0.14$, $P_{R3} = 0.87$). In addition, node strength in the superior temporal lobe increased significantly in both of congruent (Theta: $P_{R1} = 0.015$, $P_{R2} = 0.0095$, $P_{R3} = 0.0016$; alpha: $P_{R1} = 0.050$, $P_{R2} = 0.035$, $P_{R3} = 0.013$) and incongruent (Theta: $P_{R1} = 0.010$, $P_{R2} = 0.0060$, $P_{R3} = 0.00030$; alpha: $P_{R1} = 0.057$, $P_{R2} = 0.029$, $P_{R3} = 0.00090$) condition.

Finally, we analyze the difference in the effective cortical network between the congruent and incongruent conditions

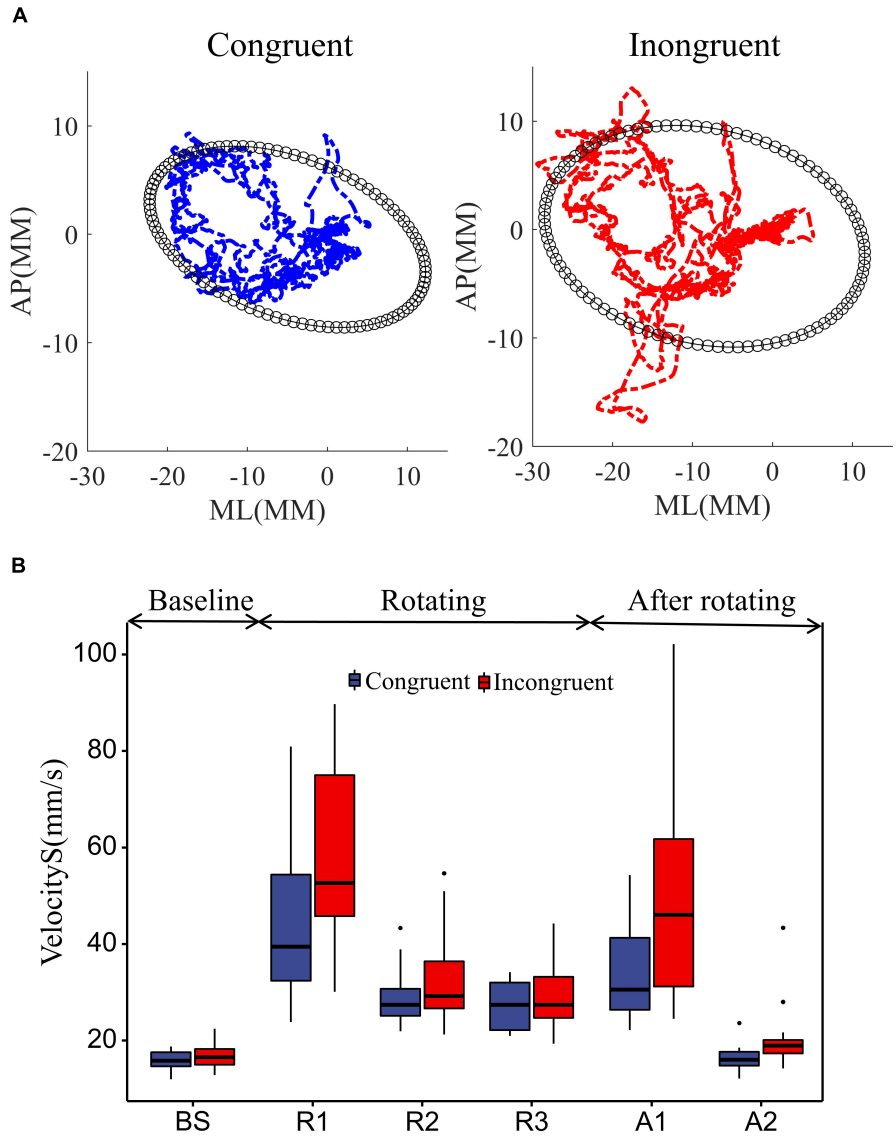

FIGURE 3
Effect of rotational stimuli on stance stability. **(A)** The mean COP sway trajectories and area for all 18 participants. The blue and red curves represent the mean COP trajectories in the congruent and incongruent conditions, respectively. The black ellipse quantifies 85% of the total area covered in the ML and AP directions, using the ellipse to fit the data. **(B)** Comparative analysis of participant sway velocities between congruent and incongruent conditions. According to the starting and ending points of the rotating stimuli, we divided the COP data into BS (12 s before platform initiation), R1 (0–12 s after platform initiation), R2 (12–24 s after platform initiation), R3 (24–36 s after platform initiation), and A1 (0–12 s after platform stop), A2 (12–24 s after platform stop). We used two-way repeated measures ANOVA to assess the effects of the time window and sensory condition on standing posture stability. Differences in COP sway velocity within rotating phase (R1, R2, R3) and after rotating phase (A1, A2) were assessed with two-way repeated measures ANOVAs with sensory condition (incongruent, congruent) and time window. Differences in COP sway velocity during the movement state transitions were assessed with repeated measures ANOVAs, which compared the baseline to the mean of the rotating and after rotating phases in both sensory conditions. In ANOVAs, predicted effects and/or interactions were explored further with simple effects analyses, and unexpected effects were explored further with Bonferroni *post-hoc* tests. The upper and lower error bars of the bins are the upper and lower quartiles of the data, respectively.

($p < 0.05$, false discovery rate correction), as shown in Figure 6A, where the red/blue lines represent the effective connections in the incongruent condition significantly greater/less than the congruent condition (Supplementary Figure 4 provides the specific *p*-value for each connection pair). First, At the beginning of the rotational stimulus (R1), there are no effective connections with significant differences between the congruent and incongruent conditions. Then, after a while (R2, R3), a similar phenomenon was observed for both alpha and theta bands; that is, the network of effective connections centered in the parietal lobe is significantly weaker in the incongruent condition compared to the congruent condition,

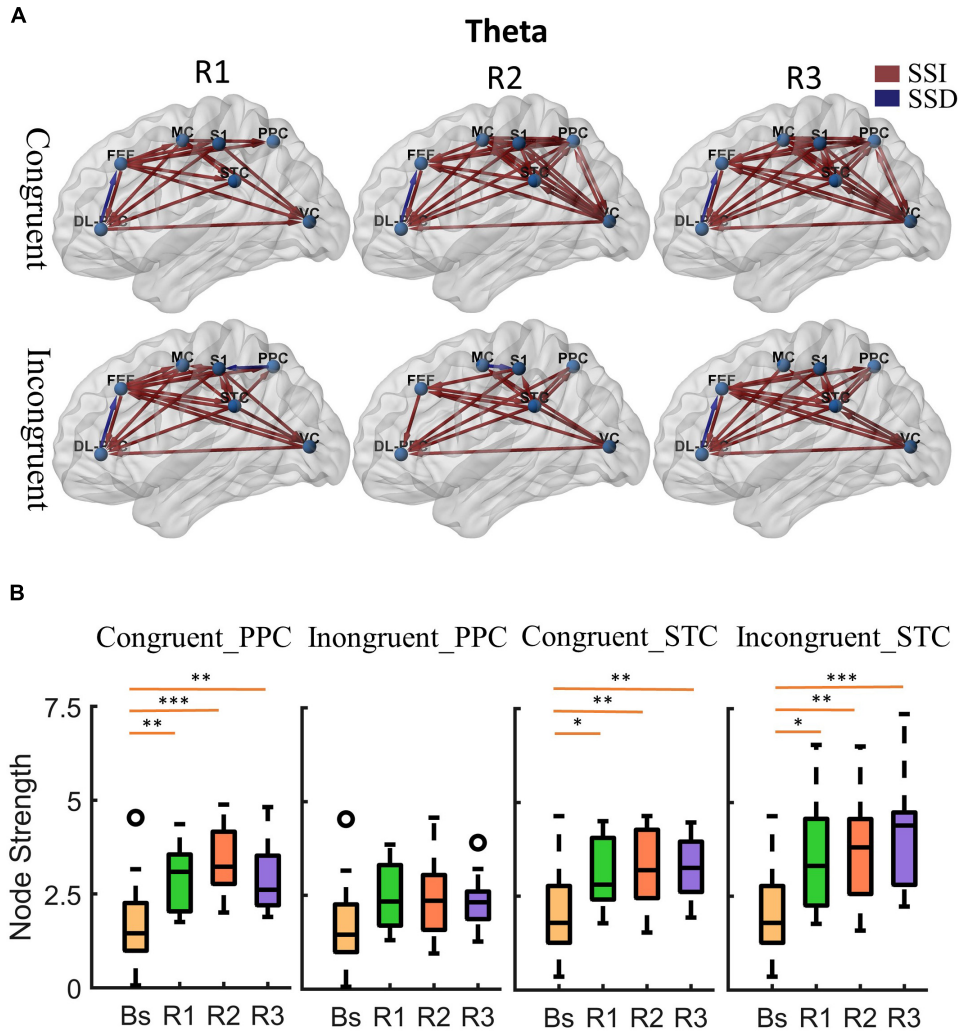

FIGURE 4
Cortical activity in theta band. **(A)** Changes of theta band cortical connectivity compared to standing baseline in congruent and incongruent conditions. Red lines indicate a statistically significant increase (SSI) in connectivity compared to baseline, and blue lines indicate a statistically significant decrease (SSD) in connectivity compared to baseline ($p < 0.05$). Significances were calculated using paired *t*-tests and corrected by the false discovery rate (FDR) method. The cortical areas of interest are as follows: dorsolateral prefrontal cortex (DL-PFC), frontal eye field cortex (FET), motor cortex (MC), primary somatosensory (S1), posterior parietal cortex (PPC), superior temporal cortex (STC), visual cortex (VC). The arrows represent the direction of information flow. **(B)** Theta band node strength in posterior parietal and superior temporal cortices. Paired *t*-tests were used to determine the difference in node strength between rotating phase (R1, R2, R3) and baseline and were corrected for multiple comparisons using Bonferroni. Congruent _PPC: Node strength of posterior parietal cortex in the congruent condition. Inongruent_PPC: Node strength of posterior parietal cortex in the incongruent condition. Congruent _STC: Node strength of superior temporal cortex in the congruent condition. Inongruent_STC: Node strength of superior temporal cortex in the incongruent condition. The upper and lower error bars of the bins are the upper and lower quartiles of the data, respectively. $^{*}p < 0.05$, $^{**}p < 0.01$, $^{***}p < 0.001$.

but the information flow from the superior temporal lobe is significantly stronger.

Further, to analyze the differences in node strengths between the congruent and incongruent conditions. We used two-way repeated measures ANOVA with Bonferroni *post-hoc* tests to assess the effects of the time window and sensory condition on node strengths, as shown in Figure 6B. We can also find that the node strengths of the posterior parietal lobe in the congruent condition are significantly greater than those in the incongruent condition [Theta: sensor $F(1, 17) = 15.25$, $P = 0.0011$, $P_{R2} = 0.0045$, $P_{R3} = 0.021$; alpha: sensor $F(1, 17) = 8.59$, $P = 0.0093$, $P_{R1} = 0.032$, $P_{R2} = 0.0045$, $P_{R3} = 0.019$], while the node strengths of the temporal lobe in the incongruent condition are significantly greater than those in the congruent condition [Theta: sensor $F(1, 17) = 4.79$, $P = 0.043$, $P_{R3} = 0.015$; alpha: sensor $F(1, 17) = 4.56$, $P = 0.048$, $P_{R3} = 0.017$]. In terms of time window factor, there was no statistically significant difference in the node strengths of both posterior parietal

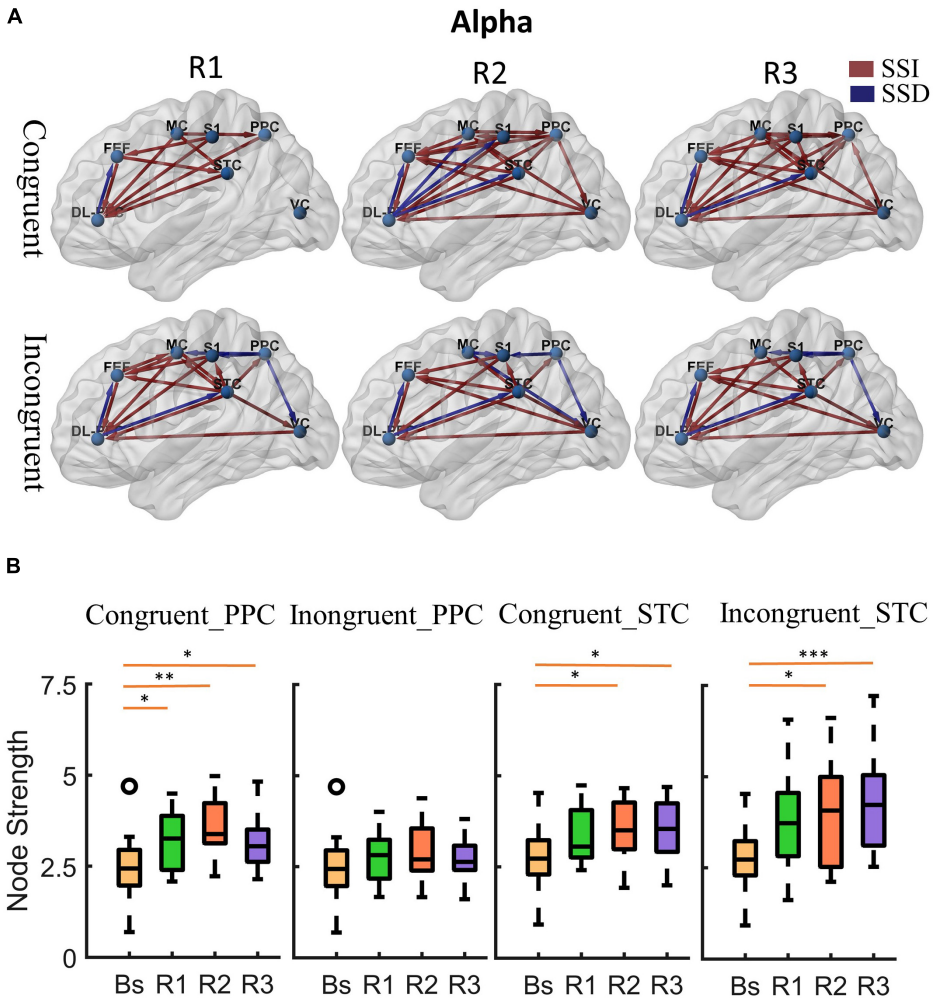

FIGURE 5
Cortical activity in alpha band. **(A)** Changes of alpha band cortical connectivity compared to standing baseline in congruent and incongruent conditions. **(B)** Alpha band node strength in posterior parietal and superior temporal cortices. $^{*}p < 0.05$, $^{**}p < 0.01$, $^{***}p < 0.001$.

[Theta: window $F(2, 34) = 1.22$, $P = 0.31$; alpha: window $F(2, 34) = 2.51$, $P = 0.096$] and superior temporal lobes [window $F(2, 34) = 0.80$, $P = 0.46$; alpha: window $F(2, 34) = 0.87$, $P = 0.43$].

Discussion

In the present study, we combined a rotating platform and a VR headset to control the participants' physical and visual motion states. Then we analyzed the effective connectivity dynamics changes and postural stability of subjects under visual and actual motion congruent or incongruent. We mainly find that: (1) Sensory conflict had a significant detrimental effect on postural stability. However, human can adapt to this detrimental effect over time. (2) The recovery of humans standing balance under sensory conflict was associated with changes in the cortical network. At the onset of the rotational stimulus, sensory congruent and incongruent rotational stimuli had similar effects on brain networks. And after a while, synchronization with the restoration of balance control, congruent and incongruent stimuli had broad and different effects on cortical networks.

The role of frontal cortex

In the present study, we found that although sensory conflict significantly negatively affected participants' balance control at the beginning, this effect diminished and disappeared over time. This suggests that the humans has an adaptive capacity to balance challenges in sensory conflict. Furthermore, we found that effective connectivity networks centered in the frontal cortex were significantly activated during the beginning of balance challenges and persisted throughout the task, regardless of the sensory condition.

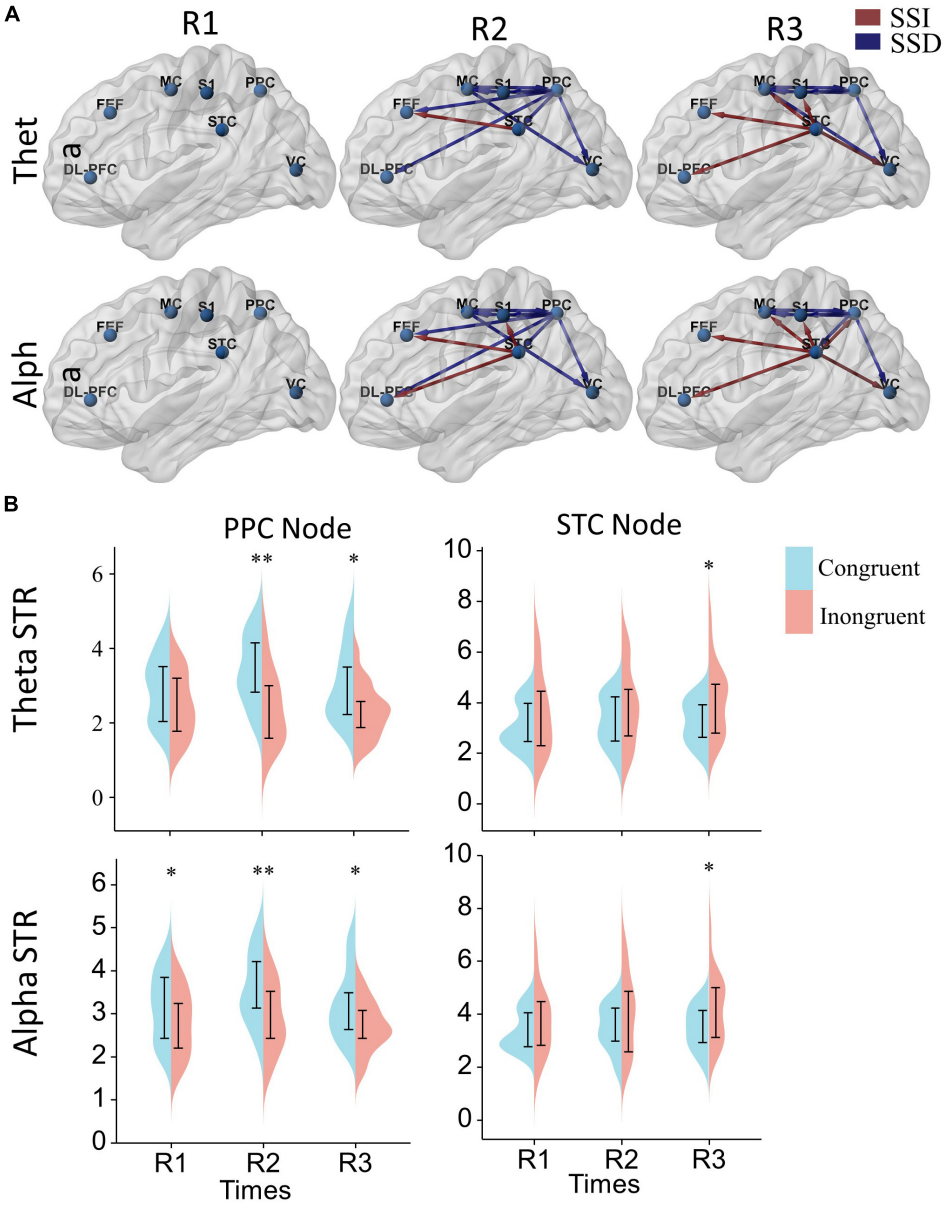

FIGURE 6
The effect of sensory conflict on cortical effective connectivity networks. **(A)** Significant changes in effective cortical connectivity in the incongruent condition compared to the congruent condition. Red connections indicate significantly stronger connectivity in the conflict condition, and blue connections indicate significantly weaker connectivity in the conflict condition ($p < 0.05$). Significance levels were calculated by paired *t*-test and corrected by the false discovery rate (FDR) method. The arrows represent the direction of information flow. **(B)** Differences in node strength (STR) in the posterior parietal and superior temporal lobes. A two-way repeated measures ANOVA with Bonferroni *post-hoc* tests to assess the effects of the time window and sensory condition on node strengths. $^{*}p < 0.05$, $^{**}p < 0.01$.

Actually, the frontal cortex has long been widely known to play an important role in reasoning, decision-making, and adaptive behavior (Mihara et al., 2008). Also, the frontal lobes are thought to have an important role in balance control; several studies have shown increased activation of the frontal lobes during balance perturbations (Clark et al., 2014; Fujita et al., 2016). And the intensity of frontal activation is positively correlated with task difficulty and inversely correlated with balance performance (Lu et al., 2015; Osofundiya et al., 2016). In addition, in multisensory processing, several studies suggest that the frontal lobes may play a role in multisensory causal inference, participating in the arbitration of integration and dissociation, and may be critical to the brain's flexibility in multisensory information processing (Rohe and Noppeney, 2015; Cao et al., 2019). Here, We also found that rotational stimulation

first activated the frontal cortex. Then synchronized with the restoration of balance control, in congruent and incongruent conditions, the sensory systems of the brain connectivity network showed integrated and dissociated connectivity, respectively. This may be a crucial mechanism for humans stance balance control during complex and variable environments.

Multisensory integration network

During balance control under congruent conditions, we found a general increase in information interaction between the posterior parietal, superior temporal, motor, somatosensory, and visual cortices in the theta and alpha band. It forms a network of information interactions centered on parietal-temporal extensions to visual and sensorimotor cortices, which may be a vital neural process for multisensory integration in the stand balance control.

Actually, many studies have highlighted the important role of the posterior parietal and superior temporal lobes in sensory integration and suggest that multisensory information may be combined in it (Calvert, 2001; Beauchamp et al., 2004; Macaluso and Driver, 2005). By using neuroimaging, multiple cortical regions in the human brain's parietal and temporal lobes can respond to stimuli of more than one modality (Bremmer et al., 2001; Macaluso and Driver, 2001), which agrees with single-cell recordings of cortical heteromodal neurons in these regions in other primates (Graziano et al., 2002). Further, neurophysiological studies in primates have shown that the activity of some multisensory neurons in the superior temporal and posterior parietal lobes is regulated by changes in the reliability of cues on trial, similar to the dynamic adjustment of psychophysical weights, which are a hallmark of sensory weighting integration (Schaafsma and Duysens, 1996; Bremmer et al., 2002; Gu et al., 2008; Morgan et al., 2008; Fetsch et al., 2011). In addition, oscillations and synchronization in the alpha spectrum and below are increasingly understood as a component of neuronal communication and integration. Theta oscillations are also suggested to coordinate different brain functions (e.g., updating motor planning after somatosensory input-the sensory-motor integration hypothesis) (Bland and Oddie, 2001). Jensen and colleagues describe theta oscillations can be used as a carrier wave for information transfer between brain regions (Jensen and Colgin, 2007). Further findings from performing a pathfinding task in a VR environment suggest that the mechanism of sensorimotor integration is guided by theta oscillations (Caplan et al., 2003).

Taken together, during balance control under congruent physical-visual stimuli, it is not surprising that we found network activation centered on the parietal-temporal lobe in the theta and alpha band, which may reflect the cortical information interaction process of multisensory integration.

Flexible multisensory processing under sensory conflict

The effective connectivity of cortical networks under sensory conflict significantly differed from control. First, during the conflicting sensory condition, we found a general paucity of information flow across cortical areas involved in the sensory integration network centered in the parietal-temporal lobe. This may reflect a flexible multisensory interaction strategy, and separate processing of sensory cues may be a general response to sensory information mismatch. In addition, during sensory cue conflict, we also found a significant increase in the influence of the superior temporal lobe on other cortical regions, and the posterior parietal centered cortical network was significantly diminished. This may reflect functional specialization of the superior temporal and posterior parietal lobes.

Although no previous studies have proposed specific functional differences between the superior temporal lobe and the posterior parietal lobe, it has been shown as early as in primate neurophysiological studies that the posterior parietal and superior temporal lobes differ in their response properties to sensory stimuli (Chen et al., 2013; Cao et al., 2019). It has been found that there are roughly equal populations of neurons in the superior temporal lobe that are sensitive to congruent or incongruent stimuli, whereas more populations of neurons in the posterior parietal lobe are sensitive to congruent stimuli (Yang et al., 2011; Chen et al., 2013). It is well known that congruent neurons may be the neural basis of sensory integration, but the role of opposite neurons has puzzled neuroscience for a long time (Morgan et al., 2008; Fetsch et al., 2011). In recent years, some researchers have suggested that combining opposite and congruent neurons may help people make multisensory causal inferences for the flexible processing of multisensory information. Signals were attributed to the same event driving sensory integration when congruent cells are more active. In contrast, when opposite cells are more active, they are attributed to different events for independent multisensory processing (Zhang et al., 2019; Badde et al., 2021; Rideaux et al., 2021).

These studies' conclusions are mutually supportive of our study's results. The posterior parietal lobe is the center of sensory integration, and its information interaction with other cortical is enhanced mainly when sensory cues are congruent. In contrast, the superior temporal lobe also plays a role in the arbitration of sensory integration and segregation, and it should be activated in both incongruent and congruent stimuli but may play a greater role in the sensory conflict.

Conclusion

The present study analyzed the effective connectivity dynamics changes during standing balance control under

visual-actual motion congruent and incongruent. We found that the recovery of humans standing balance was associated with changes in the cortical network and synchronized with the recovery of the balance control congruent and incongruent stimuli had broad and different effects on cortical networks. During sensory congruent, information interactions among sensory systems are significantly enhanced and integrated. While during the sensory conflict, information pathways between visual and sensorimotor systems are almost disconnected, and only the influence of the superior temporal lobe on other cortical regions significantly increases. These results may reflect a flexible multisensory interaction strategy critical for human posture balance control in complex and changing environments.

Data availability statement

The raw data supporting the conclusions of this article will be made available by the authors, without undue reservation.

Ethics statement

The studies involving human participants were reviewed and approved by the Ethics Committee of Zhejiang University Psychological Science Research Center permitted our experiment (issued no. 2020-003). The patients/participants provided their written informed consent to participate in this study. Written informed consent was obtained from the individual(s) for the publication of any potentially identifiable images or data included in this article.

Author contributions

GW and YY were involved in study design, article writing and revision, and data collection. ZH was involved in study design and article revision. XL was involved in experimental data collection and study design. JW and JL were involved in study design, article revision, organization, and equipment provision. All authors agreed to be accountable for the content of the work.

Funding

This work was supported by the Public Welfare Project of Zhejiang Province (No. LGF19H090023), the Key Research and Development Program of Shanxi (No. 2020ZDLSF04-03), the China National Key R&D Program Project (No. 2018YFF0300502), and the National Key Research and Development Program of China (No. 2019YFC1711800) and the National Defense Foundation Strengthening Program Technology Field Fund Project of China (2021-JCJQ-JJ-1029).

Acknowledgments

We thank Anke Hua and Kangli Dong for their assistance with study design and statistical interpretation.

Conflict of interest

The authors declare that the research was conducted in the absence of any commercial or financial relationships that could be construed as a potential conflict of interest.

Publisher's note

All claims expressed in this article are solely those of the authors and do not necessarily represent those of their affiliated organizations, or those of the publisher, the editors and the reviewers. Any product that may be evaluated in this article, or claim that may be made by its manufacturer, is not guaranteed or endorsed by the publisher.

Supplementary material

The Supplementary Material for this article can be found online at: https://www.frontiersin.org/articles/10.3389/fnins.2022.1003996/full#supplementary-material

References

Acerbi, L., Dokka, K., Angelaki, D. E., and Ma, W. J. (2018). Bayesian comparison of explicit and implicit causal inference strategies in multisensory heading perception. *PLoS Comput. Biol.* 14:e1006110.

Baccala, L. A., and Sameshima, K. (2001). Partial directed coherence: A new concept in neural structure determination. *Biol. Cybern.* 84, 463–474. doi: 10.1007/PL00007990

Badde, S., Hong, F., and Landy, M. S. (2021). Causal inference and the evolution of opposite neurons. *Proc. Natl. Acad. Sci. U.S.A.* 118:e2106235118. doi: 10.1073/pnas.2112686118

Beauchamp, M. S., Lee, K. E., Argall, B. D., and Martin, A. (2004). Integration of auditory and visual information about objects in superior temporal sulcus. *Neuron* 41, 809–823. doi: 10.1016/S0896-6273(04)00070-4

Benjamini, Y., and Hochberg, Y. (1995). Controlling the false discovery rate: A practical and powerful approach to multiple testing. *J. R. Stat. Soc. Series B (Methodological)* 57, 289–300.

Bland, B. H., and Oddie, S. D. (2001). Theta band oscillation and synchrony in the hippocampal formation and associated structures: The case for its role in sensorimotor integration. *Behav. Brain Res.* 127, 119–136. doi: 10.1016/s0166-4328(01)00358-8

Bolton, D. A. (2015). The role of the cerebral cortex in postural responses to externally induced perturbations. *Neurosci. Biobehav. Rev.* 57, 142–155. doi: 10.1016/j.neubiorev.2015.08.014

Bremmer, F., Klam, F., Duhamel, J. R., Ben Hamed, S., and Graf, W. (2002). Visual-vestibular interactive responses in the macaque ventral intraparietal area (VIP). *Eur. J. Neurosci.* 16, 1569–1586. doi: 10.1046/j.1460-9568.2002.02206.x

Bremmer, F., Schlack, A., Schlack, A., Zafiris, O., Kubischik, M., Hoffmann, K., et al. (2001). Polymodal motion processing in posterior parietal and premotor cortex: A human fMRI study strongly implies equivalencies between humans and monkeys. *Neuron* 29, 287–296. doi: 10.1016/s0896-6273(01)00198-2

Calvert, G. A. (2001). Crossmodal processing in the human brain: Insights from functional neuroimaging studies. *Cereb. Cortex* 11, 1110–1123. doi: 10.1093/cercor/11.12.1110

Cao, Y., Summerfield, C., Park, H., Giordano, B. L., and Kayser, C. (2019). Causal inference in the multisensory brain. *Neuron* 102, 1076–1087e1078. doi: 10.1016/j.neuron.2019.03.043

Caplan, J. B., Madsen, J. R., Schulze-Bonhage, A., Aschenbrenner-Scheibe, R., Newman, E. L., and Kahana, M. J. (2003). Human theta oscillations related to sensorimotor integration and spatial learning. *J. Neurosci.* 23, 4726–4736. doi: 10.1523/JNEUROSCI.23-11-04726.2003

Chen, A., Deangelis, G. C., and Angelaki, D. E. (2013). Functional specializations of the ventral intraparietal area for multisensory heading discrimination. *J. Neurosci.* 33, 3567–3581. doi: 10.1523/JNEUROSCI.4522-12.2013

Clark, D. J., Christou, E. A., Ring, S. A., Williamson, J. B., and Doty, L. (2014). Enhanced somatosensory feedback reduces prefrontal cortical activity during walking in older adults. *J. Gerontol. A Biol. Sci. Med. Sci.* 69, 1422–1428. doi: 10.1093/gerona/glu125

Clark, R. A., Bryant, A. L., Pua, Y., McCrory, P., Bennell, K., and Bennell, K. (2010). Validity and reliability of the Nintendo Wii Balance Board for assessment of standing balance. *Gait Posture* 31, 307–310.

Delorme, A., and Makeig, S. (2004). EEGLAB: An open source toolbox for analysis of single-trial EEG dynamics including independent component analysis. *J Neurosci. Methods* 134, 9–21. doi: 10.1016/j.jneumeth.2003.10.009

Dokka, K., Kenyon, R. V., Keshner, E. A., and Kording, K. P. (2010). Self versus environment motion in postural control. *PLoS Comput. Biol.* 6:e1000680. doi: 10.1371/journal.pcbi.1000680

Dokka, K., Park, H., Jansen, M., DeAngelis, G. C., and Angelaki, D. E. (2019). Causal inference accounts for heading perception in the presence of object motion. *Proc. Natl. Acad. Sci. U.S.A.* 116, 9060–9065. doi: 10.1073/pnas.1820373116

Duffy, C. J., and Wurtz, R. H. (1991). Sensitivity of MST neurons to optic flow stimuli. I. A continuum of response selectivity to large-field stimuli. *J. Neurophysiol.* 65, 1329–1345. doi: 10.1152/jn.1991.65.6.1329

Ernst, M. O., and Banks, M. S. (2002). Humans integrate visual and haptic information in a statistically optimal fashion. *Nature* 415, 429–433. doi: 10.1038/415429a

Fetsch, C. R., Pouget, A., DeAngelis, G. C., and Angelaki, D. E. (2011). Neural correlates of reliability-based cue weighting during multisensory integration. *Nat. Neurosci.* 15, 146–154. doi: 10.1038/nn.2983

Fetsch, C. R., Turner, A. H., DeAngelis, G. C., and Angelaki, D. E. (2009). Dynamic reweighting of visual and vestibular cues during self-motion perception. *J. Neurosci.* 29, 15601–15612. doi: 10.1523/JNEUROSCI.2574-09.2009

Friston, K. J. (2011). Functional and effective connectivity: A review. *Brain Connect* 1, 13–36. doi: 10.1089/brain.2011.0008

Fuchs, M., Drenckhahn, R., Wischmann, H. A., and Wagner, M. (1998). An improved boundary element method for realistic volume-conductor modeling. *IEEE Trans. Biomed. Eng.* 45, 980–997. doi: 10.1109/10.704867

Fujita, H., Kasubuchi, K., Wakata, S., Hiyamizu, M., and Morioka, S. (2016). Role of the frontal cortex in standing postural sway tasks while dual-tasking: A functional near-infrared spectroscopy study examining working memory capacity. *Biomed Res. Int.* 2016:7053867. doi: 10.1155/2016/7053867

Fushiki, H., Kobayashi, K., Asai, M., and Watanabe, Y. (2005). Influence of visually induced self-motion on postural stability. *Acta Otolaryngol.* 125, 60–64. doi: 10.1080/00016480410015794

Gramann, K., Gwin, J. T., Ferris, D. P., Oie, K., Jung, T. P., Lin, C. T., et al. (2011). Cognition in action: Imaging brain/body dynamics in mobile humans. *Rev. Neurosci.* 22, 593–608. doi: 10.1515/RNS.2011.047

Graziano, M. S., Taylor, C. S., Moore, T., and Cooke, D. F. (2002). The cortical control of movement revisited. *Neuron* 36, 349–362. doi: 10.1016/s0896-6273(02)01003-6

Gu, Y., Angelaki, D. E., and Deangelis, G. C. (2008). Neural correlates of multisensory cue integration in macaque MSTd. *Nat. Neurosci.* 11, 1201–1210. doi: 10.1038/nn.2191

Gu, Y., Watkins, P. V., Angelaki, D. E., and DeAngelis, G. C. (2006). Visual and nonvisual contributions to three-dimensional heading selectivity in the medial superior temporal area. *J. Neurosci.* 26, 73–85. doi: 10.1523/JNEUROSCI.2356-05.2006

Gwin, J. T., Gramann, K., Makeig, S., and Ferris, D. P. (2010). Removal of movement artifact from high-density EEG recorded during walking and running. *J. Neurophysiol.* 103, 3526–3534. doi: 10.1152/jn.00105.2010

Hansson, E. E., Beckman, A., and Hakansson, A. (2010). Effect of vision, proprioception, and the position of the vestibular organ on postural sway. *Acta Otolaryngol.* 130, 1358–1363. doi: 10.3109/00016489.2010.498024

Huurnink, A., Fransz, D. P., Kingma, I., and van Dieën, J. H. (2013). Comparison of a laboratory grade force platform with a Nintendo Wii Balance Board on measurement of postural control in single-leg stance balance tasks. *J. Biomech.* 46, 1392–1395.

Jensen, O., and Colgin, L. L. (2007). Cross-frequency coupling between neuronal oscillations. *Trends Cogn. Sci.* 11, 267–269. doi: 10.1016/j.tics.2007.05.003

Keil, J., and Senkowski, D. (2018). Neural Oscillations orchestrate multisensory processing. *Neuroscientist* 24, 609–626. doi: 10.1177/1073858418755352

Keshavarz, B., Riecke, B. E., Hettinger, L. J., and Campos, J. L. (2015). Vection and visually induced motion sickness: How are they related? *Front. Psychol.* 6:472. doi: 10.3389/fpsyg.2015.00472

Leach, J. M., Mancini, M., Peterka, R. J., Hayes, T. L., and Horak, F. B. (2014). Validating and calibrating the Nintendo Wii balance board to derive reliable center of pressure measures. *Sensors Basel* 14, 18244–18267. doi: 10.3390/s141018244

Lu, C. F., Liu, Y. C., Yang, Y. R., Wu, Y. T., and Wang, R. Y. (2015). Maintaining gait performance by cortical activation during dual-task interference: A functional near-infrared spectroscopy study. *PLoS One* 10:e0129390. doi: 10.1371/journal.pone.0129390

Luo, H. Z., Wang, X., Fan, M., Deng, L., Jian, C., Wei, M., et al. (2018). The effect of Visual stimuli on stability and complexity of Postural control. *Front. Neurol.* 9:48. doi: 10.3389/fneur.2018.00048

Macaluso, E., and Driver, J. (2001). Spatial attention and crossmodal interactions between vision and touch. *Neuropsychologia* 39, 1304–1316. doi: 10.1016/S0028-3932(01)00119-1

Macaluso, E., and Driver, J. (2005). Multisensory spatial interactions: A window onto functional integration in the human brain. *Trends Neurosci.* 28, 264–271. doi: 10.1016/j.tins.2005.03.008

Mahboobin, A., Loughlin, P., Atkeson, C., and Redfern, M. (2009). A. mechanism for sensory re-weighting in postural control. *Med. Biol. Eng. Comput.* 47, 921–929. doi: 10.1007/s11517-009-0477-5

Mazziotta, J., Toga, A., Evans, A., Fox, P., Lancaster, J., Lancaster, J., et al. (2001). A four-dimensional probabilistic atlas of the human brain. *J, Am. Med. Inform. Assoc.* 8, 401–430. doi: 10.1136/jamia.2001.0080401

Mihara, M., Miyai, I., Hatakenaka, M., Kubota, K., and Sakoda, S. (2008). Role of the prefrontal cortex in human balance control. *Neuroimage* 43, 329–336. doi: 10.1016/j.neuroimage.2008.07.029

Morgan, M. L., Deangelis, G. C., and Angelaki, D. E. (2008). Multisensory integration in macaque visual cortex depends on cue reliability. *Neuron* 59, 662–673. doi: 10.1016/j.neuron.2008.06.024

Mullen, T. R., Kothe, C. A., Chi, Y. M., Chi, Y. M., Kerth, T., Makeig, S., et al. (2015). Real-time neuroimaging and cognitive monitoring using wearable dry EEG. *IEEE T. Biomed. Eng.* 62, 2553–2567. doi: 10.1109/Tbme.2015.2481482

Nguyen, N. T., Takakura, H., Nishijo, H., Ueda, N., Ito, S., Fujisaka, M., et al. (2020). Cerebral Hemodynamic responses to the sensory conflict between visual and rotary vestibular stimuli: An Analysis with a multichannel Near-Infrared Spectroscopy (NIRS) system. *Front. Hum. Neurosci.* 14:125. doi: 10.3389/fnhum.2020.00125

Osofundiya, O., Benden, M. E., Dowdy, D., and Mehta, R. K. (2016). Obesity-specific neural cost of maintaining gait performance under complex conditions in community-dwelling older adults. *Clin. Biomech. (Bristol, Avon)* 35, 42–48. doi: 10.1016/j.clinbiomech.2016.03.011

Page, W. K., and Duffy, C. J. (2003). Heading representation in MST: Sensory interactions and population encoding. *J. Neurophysiol.* 89, 1994–2013. doi: 10.1152/jn.00493.2002

Paillard, T., and Noe, F. (2015). Techniques and methods for testing the postural function in healthy and pathological subjects. *Biomed Res. Int.* 2015:891390. doi: 10.1155/2015/891390

Palmieri, R. M., Ingersoll, C. D., Stone, M. B., and Krause, B. A. (2002). Center-of-pressure parameters used in the assessment of postural control. *J. Sport Rehabil.* 11, 51–66. doi: 10.1123/jsr.11.1.51

Pascual-Marqui, R. D. (2002). Standardized low-resolution brain electromagnetic tomography (sLORETA): Technical details. *Methods Find. Exp. Clin. Pharmacol.* 24 Suppl D, 5–12.

Peterka, R. J., and Loughlin, P. J. (2004). Dynamic regulation of sensorimotor integration in human postural control. *J. Neurophysiol.* 91, 410–423. doi: 10.1152/jn.00516.2003

Pion-Tonachini, L., Kreutz-Delgado, K., and Makeig, S. (2019). ICLabel: An automated electroencephalographic independent component classifier, dataset, and website. *Neuroimage* 198, 181–197. doi: 10.1016/j.neuroimage.2019.05.026

Rideaux, R., Storrs, K. R., Maiello, G., and Welchman, A. E. (2021). How multisensory neurons solve causal inference. *Proc. Natl. Acad. Sci. U.S.A.* 118:e2106235118. doi: 10.1073/pnas.2106235118

Roberts, R. E., Ahmad, H., Arshad, Q., Patel, M., Dima, D., Leech, R., et al. (2017). Functional neuroimaging of visuo-vestibular interaction. *Brain Struct. Funct.* 222, 2329–2343. doi: 10.1007/s00429-016-1344-4

Rohe, T., and Noppeney, U. (2015). Cortical hierarchies perform Bayesian causal inference in multisensory perception. *PLoS Biol.* 13:e1002073. doi: 10.1371/journal.pbio.1002073

Rohe, T., Ehlis, A. C., and Noppeney, U. (2019). The neural dynamics of hierarchical Bayesian causal inference in multisensory perception. *Nat. Commun.* 10:1907. doi: 10.1038/s41467-019-09664-2

Schaafsma, S. J., and Duysens, J. (1996). Neurons in the ventral intraparietal area of awake macaque monkey closely resemble neurons in the dorsal part of the medial superior temporal area in their responses to optic flow patterns. *J. Neurophysiol.* 76, 4056–4068. doi: 10.1152/jn.1996.76.6.4056

Shams, L., and Beierholm, U. R. (2010). Causal inference in perception. *Trends Cogn. Sci.* 14, 425–432. doi: 10.1016/j.tics.2010.07.001

Tanaka, K., Hikosaka, K., Saito, H., Yukie, M., Yukie, M., and Iwai, E. (1986). Analysis of local and wide-field movements in the superior temporal visual areas of the macaque monkey. *J. Neurosci.* 6, 134–144.

von Stein, A., and Sarnthein, J. (2000). Different frequencies for different scales of cortical integration: From local gamma to long range alpha/theta synchronization. *Int. J. Psychophysiol.* 38, 301–313.

Xia, M. R., Wang, J. H., and He, Y. (2013). BrainNet viewer: A network visualization tool for human brain connectomics. *PLoS One* 8:e68910. doi: 10.1371/journal.pone.0068910

Yang, Y., Liu, S., Chowdhury, S. A., DeAngelis, G. C., and Angelaki, D. E. (2011). Binocular disparity tuning and visual-vestibular congruency of multisensory neurons in macaque parietal cortex. *J. Neurosci.* 31, 17905–17916. doi: 10.1523/Jneurosci.4032-11.2011

Zhang, W. H., Wang, H., Chen, A., Gu, Y., Lee, T. S., Wong, K. M., et al. (2019). Complementary congruent and opposite neurons achieve concurrent multisensory integration and segregation. *Elife* 8:e43753. doi: 10.7554/eLife.43753

Zilles, K., and Amunts, K. (2010). Centenary of Brodmann's map—conception and fate. *Nat. Rev. Neurosci.* 11, 139–145. doi: 10.1038/nrn2776

frontiers in Physiology

ORIGINAL RESEARCH
published: 22 February 2021
doi: 10.3389/fphys.2021.625553

Age-Related Changes in Standing Balance in Preschoolers Using Traditional and Nonlinear Methods

*Zengming Hao[1], Yi Yang[1], Anke Hua[1], Ying Gao[1] and Jian Wang[1,2]**

[1]Department of Sports Science, College of Education, Zhejiang University, Hangzhou, China, [2]Center for Psychological Sciences, Zhejiang University, Hangzhou, China

Considerable disagreement exists on the linearity of the development of standing balance in children. This study aimed to use different traditional and nonlinear methods to investigate age-related changes in standing balance in preschoolers. A sample of 118 preschoolers took part in this study. A force platform was used to record the center of pressure during standing balance over 15 s in three conditions: eyes open, eyes closed, and/or head extended backward. Detrended fluctuation analysis (DFA), recurrence quantification analysis (RQA), and traditional measures were used to evaluate standing balance. The main results are as follows: (1) Higher range and SD in the anterior-posterior (AP) direction were observed for 5-year-old than for 4-year-old children, while higher DFA coefficient (at shorter time scales) and higher determinism and laminarity in the AP direction were found for 5-year-old children compared to 3- and 4-year-old children; and (2) as sensory conditions became more challenging, all traditional measures increased and DFA coefficients (at shorter and longer time scales) decreased in the AP and mediolateral directions, while determinism and laminarity significantly declined in the AP direction. In conclusion, although increased postural sway, 5-year-old preschool children's balance performance improved, and their control strategy changed significantly compared with the younger preschoolers. Sensory perturbation (eye closure and/or head extension) changed preschoolers' balance performance and control strategy. Moreover, both traditional and nonlinear methods provided complementary information on the control of standing balance in preschoolers.

Keywords: standing balance, preschool children, nonlinear analysis, recurrence quantification analysis, detrended fluctuation analysis

OPEN ACCESS

Edited by:
Luca Faes,
University of Palermo, Italy

Reviewed by:
Pedro Carpena,
University of Malaga, Spain
Paolo Castiglioni,
Fondazione Don Carlo Gnocchi Onlus (IRCCS), Italy

****Correspondence:***
Jian Wang
pclabeeg@zju.edu.cn

Specialty section:
This article was submitted to Fractal and Network Physiology, a section of the journal Frontiers in Physiology

Received: *03 November 2020*
Accepted: *28 January 2021*
Published: *22 February 2021*

Citation:
Hao Z, Yang Y, Hua A, Gao Y and Wang J (2021) Age-Related Changes in Standing Balance in Preschoolers Using Traditional and Nonlinear Methods. Front. Physiol. 12:625553. doi: 10.3389/fphys.2021.625553

INTRODUCTION

Maintaining standing balance is a complex sensorimotor process. It involves multiple sensory systems and actions of muscles distributed over the whole body. A deficit in any sensory systems or integration of multisensory information can affect standing balance (Balasubramaniam and Wing, 2002; Molloy et al., 2003). The control of standing balance is affected by perceptual information, attention, and cognitive processes (Balasubramaniam and Wing, 2002). It should be noted that age is an essential factor affecting standing balance (Hsu et al., 2009). Several studies have found that the ability to control standing balance develops during childhood until

early adult life and deteriorates from 40 to 59 years (Sheldon, 1963; Goble and Baweja, 2018). However, these studies did not cover preschool years, and the development of sensory systems and central nervous systems integration for preschool children is incomplete (Steindl et al., 2006; Hsu et al., 2009; Sá et al., 2018). Nonetheless, intra-modal reweighting was exhibited in children as young as 4 years of age, while inter-modal reweighting was only observed in older children (Bair et al., 2007; Rinaldi et al., 2009). Preschoolers may not effectively suppress the influence of unreliable proprioception and visual information on standing balance (Forssberg and Nashner, 1982; Foudriat et al., 1993). Especially for 3-year-old children, many of them fail to maintain standing balance under some challenging conditions (e.g., eyes closed and/or on a foam surface; Slobounov and Newell, 1994; Verbecque et al., 2016a). Several studies found that younger children sway more with the eyes open than with the eyes closed (Riach and Hayes, 1987; Slobounov and Newell, 1994; Newell et al., 1997a,b). Moreover, an increase in sway amplitude was found for 5-year-old children compared with 3- and 4-year-old children in another study (Verbecque et al., 2016a). These phenomena conflict with the traditional view of the influence of vision and age on standing balance. For typically developing children, postural sway decreases with increasing age under different sensory conditions (Sá et al., 2018; Villarrasa-Sapiña et al., 2019). Nonetheless, considerable disagreement exists on whether this developmental trend occurs linearly or whether turning points can be identified (Kirshenbaum et al., 2001; Rival et al., 2005; Verbecque et al., 2016b).

The most common method for assessing standing balance is the postural sway's characterization by measuring the center of pressure (COP) displacements (Verbecque et al., 2016a). COP signals can be used as an effective method to determine whether a child has sufficient postural control under different sensory conditions. Several studies have shown that COP signals are non-random and nonstationary, containing structural information of the postural control system (Collins and De Luca, 1993; van den Hoorn et al., 2018). However, traditional methods (e.g., range, SD, root mean square, sway velocity, sway path length, and sway area) have been usually used to evaluate the COP signals by assuming that postural sway is stationary (Verbecque et al., 2016a,b). In fact, traditional methods have some limitations for assessing standing balance. For example, one study found that the sway area did not distinguish standing balance between 5-year-old children and 3-year-old children (Slobounov and Newell, 1994). Another study's results showed that sway velocity and Romberg quotient of most traditional measures remained unaltered among different age groups of preschool children (Verbecque et al., 2016a). These results indicate that conventional methods may ignore some critical information about standing balance. In contrast, many nonlinear methods are based on concepts of chaos, fractals, and complexity (Ma et al., 2018; Henriques et al., 2020), which have been used to evaluate the COP signals to understand the dynamics of standing balance in different groups (Doyle et al., 2005; Seigle et al., 2009; Ramdani et al., 2013; Rigoldi et al., 2014; Zhou et al., 2017; Lobo Da Costa et al., 2019). Postural sway variability can be quantified using multiscale entropy (MSE) and fractal dimension (FD). Older adults with lower postural sway complexity experienced more falls in the future, while traditional measures were not associated with future falls (Zhou et al., 2017). FD measures are more reliable than traditional COP measures in assessing standing balance (Doyle et al., 2005). Detrended fluctuation analysis (DFA) can assess the persistent and anti-persistent behaviors of COP signals in different time scales (Peng et al., 1995; Teresa Blázquez et al., 2009, 2010). Besides, recurrence quantification analysis (RQA) was used to investigate the dynamical properties of COP signals, even for a short duration and for nonstationary data (Sylos Labini et al., 2012). Some studies have shown that RQA measures in the anterior-posterior direction are sufficient to distinguish the young and elderly group and even distinguish non-fallers and fallers (Seigle et al., 2009; van den Hoorn et al., 2018). Thus, using nonlinear methods may provide crucial information about COP signals, contributing to more accurate insights into standing balance.

In previous studies, most authors investigated the age-related changes in standing balance in preschoolers under challenging conditions by perturbating the sensory inputs of vision and/or proprioception (Verbecque et al., 2016a,b). Especially for the condition of standing on a foam surface with eyes closed, the vestibular input dominated because both visual and somatosensory inputs had been removed or reduced (Young, 2015). In contrast, preschoolers' development of the vestibular system did not reach functional maturity (Steindl et al., 2006; Hsu et al., 2009; Sá et al., 2018). During the preschool period, proprioception may be the only relatively reliable sensory input for standing balance (Steindl et al., 2006; Hsu et al., 2009). The head extension is also an effective method for evaluating standing balance (Kogler et al., 2000; Buckley et al., 2005; Vuillerme and Rougier, 2005; Paloski et al., 2006; Vuillerme et al., 2008). The head-extended posture is recognized to induce a modification of the vestibular inputs and abnormal sensory inputs from neck proprioceptors, representing a challenge for the postural control system (Vuillerme et al., 2008). Most previous studies reported a standing duration of 30 s and above (Verbecque et al., 2016b). Choosing a longer time for data recording has the advantage of being a more realistic estimation of the standing balance of preschool children. However, it is difficult for children below 5 years to maintain balance with eyes closed for longer durations (Forssberg and Nashner, 1982; Verbecque et al., 2016a). Moreover, preschoolers are easily distracted (Lobo Da Costa et al., 2019). Postural sway data of 15 or 20 s can effectively distinguish the standing balance among different age groups (Newell et al., 1997a; Goble and Baweja, 2018; van den Hoorn et al., 2018). Therefore, a shorter duration (e.g., 15 s) may be suitable for evaluating preschool children's standing balance. In general, the longer the time for data recording, the better the reliability of COP signals' measures. Nonetheless, some nonlinear measures applied to short data also had better reliability (Doyle et al., 2005; Teresa Blázquez et al., 2009; Sylos Labini et al., 2012; van den Hoorn et al., 2018). Fractal measures and RQA measures are more reliable than traditional measures of COP signals in assessing standing balance for a duration of 10 or 15 s (Doyle et al., 2005; van den Hoorn et al., 2018).

Thus, the purpose of the current study was to investigate how age and sensory perturbation affect the control of standing balance for preschool children on a firm surface using traditional and nonlinear methods. The hypotheses were as follows: (1) The balance performance and control strategy of 5-year-old preschool children's standing balance would change significantly compared with the younger preschoolers; (2) sensory perturbations (eye closure and/or head extension) would change the control of preschoolers' standing balance accordingly; and (3) both traditional and nonlinear methods may discriminate the age-related changes in standing balance in preschoolers, and nonlinear methods may provide different information about the effect of age on standing balance.

MATERIALS AND METHODS

Participants

A cross-sectional study was performed in a sample of 118 preschool children. They were grouped according to chronological age: 3-year-old children (n = 40), 4-year-old children (n = 39), and 5-year-old children (n = 39). The parents or guardians of children provided written consent before any measurements. A questionnaire was also completed by the parents or guardians to identify any presence among participants of developmental problems or interest in cooperation, which were all considered exclusion criteria. Participants were recruited from one of the regular preschools in Hangzhou, China. This study was approved by the local ethical committee of Zhejiang University (issued no. 2020-003) and conformed to the Declaration of Helsinki.

Among the 3-year-old children, 90% completed all conditions (four children were excluded because of test failure). Among the 4-year-old children, 97.44% completed all conditions (only one child was excluded because of test failure). Among the 5-year-old children, 100% were able to complete all conditions. In total, the final sample of 113 children are presented, which include 3-year-old children (n = 36), 4-year-old children (n = 38), and 5-year-old children (n = 39). **Table 1** presents the descriptive characteristics of the participants. Body height and body mass increase significantly with age ($p < 0.01$ for height and body mass).

Data Collection

In an upright bipedal stance, participants were asked to stand barefoot on a force plate (0.4 × 0.5 m, 1,000 Hz, model OR 6-5-2000, AMTI Inc., United States) with feet together (Verbecque et al., 2016b) for 15 s. They were asked to stand on a firm surface and keep their arms beside their bodies and stand as still as possible. Standing balance was measured in three non-randomized test conditions: (1) EO: eyes open; (2) EC: eyes closed; and (3) ECHB: eyes closed and head extended backward (Smith et al., 2012). Participants were asked to keep their head in a straight-ahead direction under the condition of EO and EC, and they were asked to tilt their head backward for at least 45° under the condition of ECHB. Each condition was designed to remove or reduce sensory inputs. For the condition of EO, all sensory inputs are available; for the condition of EC, only the visual information is unavailable; and for the condition of ECHB, sensory inputs arising from vision, vestibular system, and neck proprioceptors are removed or reduced (Vuillerme et al., 2008; Smith et al., 2012). All participants familiarize themselves with each condition before the formal test and have 30 s of rest between different conditions. According to previous studies, a visual target used in the condition of EO can enhance children's attention and motivation (Schärli et al., 2013; Verbecque et al., 2016b), and gazing at objects at a near distance (small eye–object distance) can reduce body sway (Verbecque et al., 2016b; Aoki et al., 2018). Thus, in the EO condition, the children were instructed to look at a stationary marker positioned 1 m away and individually adjusted for the eye height. One investigator stayed close to the participant throughout the entire test to prevent them from falling. Once the participant moved their feet or fell, the trial was stopped, and the results were excluded for further analysis.

Data Analysis

Demographic data (gender, height, and body mass) were reported. All signals from the force platform were processed offline using MATLAB software (MathWorks, Natick, MA, United States). The COP positions were calculated from the ground reaction forces and moments of force and then filtered using a 20 Hz low-pass, 2nd order, zero-lag Butterworth filter. Furthermore, the mean of the filtered data was removed. The COP displacements were subsequently analyzed using traditional and nonlinear methods in the anterior-posterior (AP) and mediolateral (ML) directions. Traditional methods included the range, SD, sway mean velocity, sway path length, and sway area, which quantified the postural sway (Verbecque et al., 2016a,b). Nonlinear methods included the DFA and RQA.

The range is the distance between the maximum and minimum COP displacement in the AP and ML directions, representing the entire trial's postural sway. In general, the greater the range, the worse the postural stability (Palmieri et al., 2002; Paillard and Noé, 2015). Because the COP signal of zero mean, SD,

TABLE 1 | Descriptive characteristics of the participants.

Age group	P	N	Gender (M/F)	Height (cm)	Body mass (kg)
3 years	90%	36	19/17	103.44 ± 4.96	17.35 ± 3.16
4 years	97.44%	38	17/21	111.53 ± 4.03	19.19 ± 3.30
5 years	100%	39	21/18	119.71 ± 6.61	23.38 ± 5.47

P, percentage of children that completed all three conditions; N, number of children of whom the results were analyzed; M, male; F, female.

and root mean square (RMS) provide the same result, which is defined as the square root of the mean of the squares of COP displacement in the AP and ML directions. SD is a variability index of COP displacements (Palmieri et al., 2002; Paillard and Noé, 2015; Luo et al., 2018). Path length quantifies the magnitude of the two-dimensional displacement based on the total distance traveled and is considered a valid index (the smaller the path length, the better the postural stability; Paillard and Noé, 2015). Sway mean velocity is calculated by dividing the COP excursion by the duration time, which is considered an index with the greatest reliability, reflecting the efficiency of postural control (the smaller the velocity, the better the postural control; Paillard and Noé, 2015; Luo et al., 2018; van den Hoorn et al., 2018). We calculated Sway mean velocity and Path length of the COP signal as follows:

$$\mathrm{MV\_ml} = \sum_{i=1}^{N} \left| x(i+1) - x(i) \right| * F / N$$

$$\mathrm{MV\_ap} = \sum_{i=1}^{N} \left| y(i+1) - y(i) \right| * F / N$$

$$\mathrm{Path} = \sum_{i=1}^{N} \sqrt{\left(x(i+1) - x(i)\right)^2 + \left(y(i+1) - y(i)\right)^2}$$

where x(i) and y(i) are the COP displacements in the ML and AP directions, respectively, N = number of samples, F = sampling frequency.

Sway area quantifies 85% of the total area covered in the ML and AP directions using an ellipse to fit the COP data, which is considered an index of overall postural performance (Paillard and Noé, 2015; Verbecque et al., 2016a). **Figure 1** shows some details of the sway area calculation of COP trajectory from a 4-year-old child under the condition of ECHB. It can be seen that all traditional measures of COP signals reflect the balance performance with the small the value, the better the balance performance.

Detrended fluctuation analysis is a technique for quantifying the long-range correlation behavior in a time series (Peng et al., 1995), and frequently used to study the behavior of the COP trajectory (Teresa Blázquez et al., 2009, 2010; van den Hoorn et al., 2018; Lobo Da Costa et al., 2019). DFA can measure the relation between COP fluctuations at different time scales by the slope of a linear region on the log-log plot of COP fluctuations vs. time scales (**Figure 2**). Based on the shorter duration of tests in this study, the time window ranged from 0.10 to 4.42 s (van den Hoorn et al., 2018). The COP signal was integrated over time and divided into smaller time windows with 50% overlap. Each time window's linear trend was subtracted, and the root-mean-square fluctuations of the integrated COP around the linear fits were determined. For the log-log plot of COP fluctuations vs. time scales, two linear regions were fitted by minimizing the squared errors between the two fitted lines

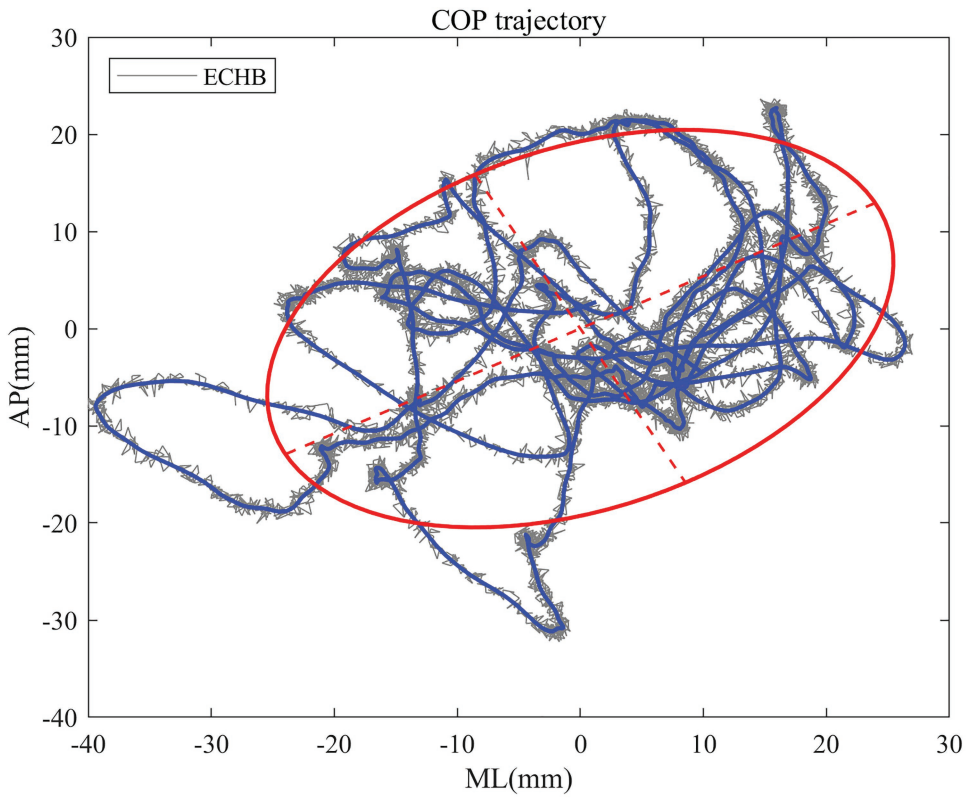

FIGURE 1 | The raw (gray trace) and filtered (blue trace) center of pressure (COP) signals for a 4-year-old child under the condition of eyes closed and head extended backward (ECHB) during 15 s. Estimated sway area (red trace) is superimposed onto the plots of COP trajectory.

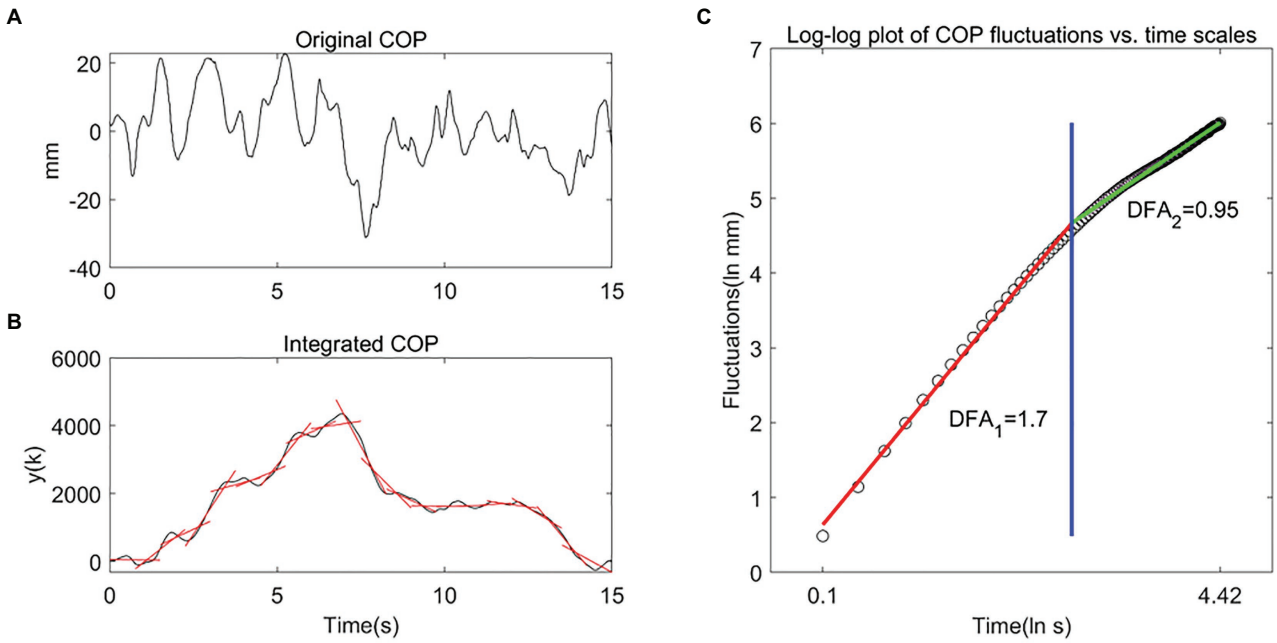

FIGURE 2 | Detrended fluctuation analysis (DFA) method and DFA coefficients. **(A)** Original COP signal in the anterior-posterior (AP) direction from a 4-year-old child under the condition of ECHB during 15 s. **(B)** Integrated COP signal y(k), the red solid line represent the linear trend in each box with 50% overlap. **(C)** Log-log plot of COP fluctuations vs. time scales, DFA_1 (red line) and DFA_2 (green line) reflect the COP fluctuations at shorter (to the left of the blue line) and longer (to the right of the blue line) time scales, respectively.

and actual data (**Figure 2**), and two slopes of different time scales were determined. The first slope (DFA_1) in general greater than 1.5, indicating that a persistent pattern of COP sway. The second slope (DFA_2) in general smaller than 1.5, indicating that an anti-persistent pattern of COP sway. Higher DFA values indicate smoother and more persistent behavior at short (DFA_1) and long (DFA_2) time scales, while lower DFA values indicate less smooth and more anti-persistent behavior at short (DFA_1) and long (DFA_2) time scales (van den Hoorn et al., 2018).

We calculated DFA_1 and DFA_2 of the COP signal as follows:

The original COP signal is integrated as: $y(k)=\sum_{t=1}^{k}[x(t)-\bar{x}]$

where x(t) is the original COP signal at time t, $\bar{x}$ is the average of the entire time series, and $y(k)$ is the integrated COP signal.

The fluctuation of the integrated COP signal is calculated as: $F(n)=\sqrt{\frac{1}{N}\sum_{k=1}^{N}[y(k)-y_n(k)]^2}$

where $y_n(k)$ is the local linear trend, $F(n)$ will increase with the box size n. The slopes of the fitted lines of the log-log plot at short and long time scales are the DFA coefficients (DFA_1 and DFA_2).

Recurrence quantification analysis is a tool for studying the dynamics of a signal. It is based on the construction of a recurrence plot (RP) from which quantitative measures are extracted. The time delay was calculated using the mutual information method, and the embedded dimension was determined using false nearest neighbor analysis. **Figure 3** shows a recurrence plot of a COP signal in the AP direction from a 4-year-old child under the condition of ECHB. RP's features can be quantified by the diagonal lines and vertical lines using Marwan's RQA toolbox (Marwan et al., 2007). Determinism (%DET) refers to the percentage of all recurrences in phase space that form diagonal line lengths longer than a pre-set threshold distance. Higher %DET values indicate a more predictable, less random COP data motion, which is consistent with better balance performance (van den Hoorn et al., 2018). Laminarity (%LAM) refers to the percentage of all recurrences in phase space that forms vertical line lengths longer than a pre-set threshold distance. Higher %LAM values indicate a more intermittent COP motion with more periods of minimal COP fluctuations (van den Hoorn et al., 2018). To avoid the ceiling effect of the %DET and %LAM, minimal length of both diagonal and vertical line features were set as 0.1 s; the recurrence threshold was chosen as 5% of the recurrence rate (Seigle et al., 2009; Ramdani et al., 2013; van den Hoorn et al., 2018).

We calculated Determinism (%DET) and Laminarity (%LAM) of the COP signal as follows:

Recurrence plot is briefly defined as $\mathbf{R}_{i,j}^{m,\varepsilon_i}=\Theta\left(\varepsilon_i-\left\|\vec{x}_i-\vec{x}_j\right\|\right)$

where ε is a predefined threshold and $\vec{x}_i\vec{x}_j$ are phase space trajectories in an m-dimension phase space;

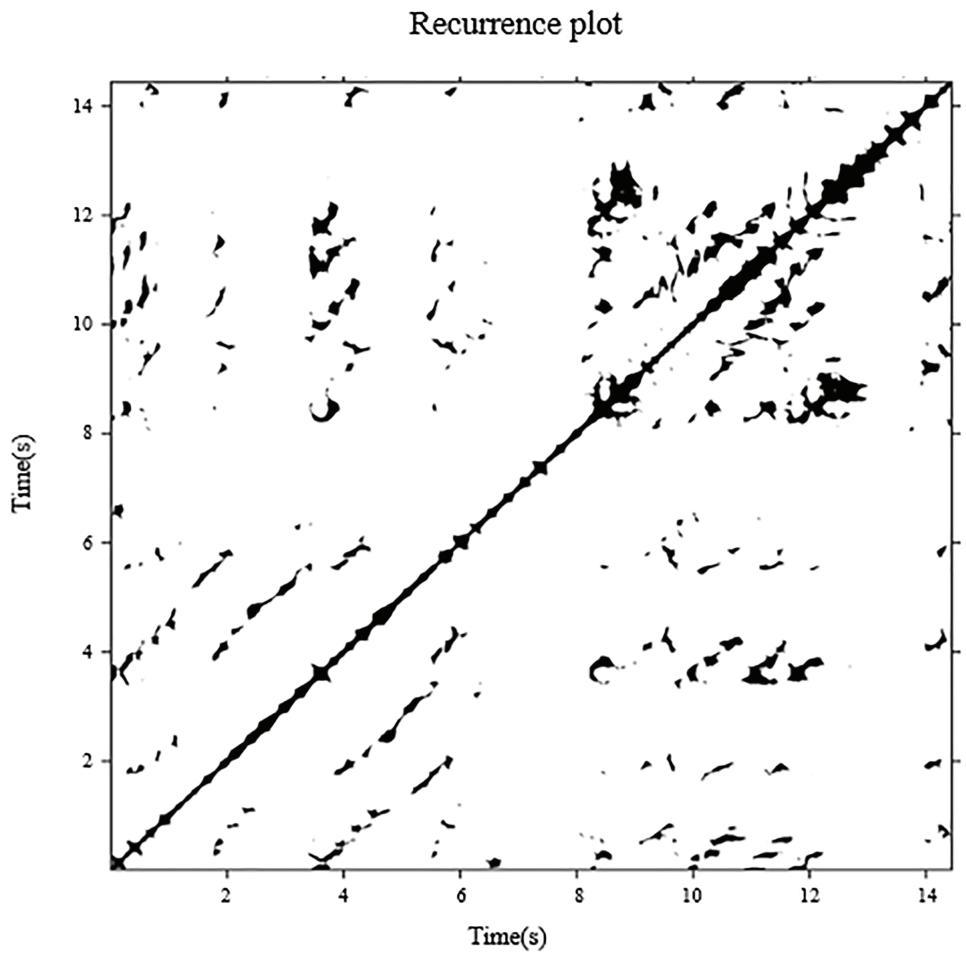

FIGURE 3 | Recurrence plot of a COP signal in the AP direction from a 4-year-old child under the condition of ECHB duration 15 s (time delay = 28 samples, embedded dimension = 3, and recurrence rate = 5%).

$$\%\mathrm{DET} = \frac{\sum_{l=l_{\min}}^{N} lP^{\varepsilon}(l)}{\sum_{i,j}^{N} \mathbf{R}_{i,j}^{m,\varepsilon}} \times 100$$

where $P^{\varepsilon}(l) = \{l_i; i = 1 \ldots N_l\}$ is the frequency distribution of the lengths l of diagonal structures, and N_l is the absolute number of diagonal lines;

$$\%\mathrm{LAM} = \frac{\sum_{v=\mathrm{v}_{\min}}^{N} vP^{\varepsilon}(v)}{\sum_{v=1}^{N} vP^{\varepsilon}(v)} \times 100$$

where $P^{\varepsilon}(v) = \{v_i; i = 1 \ldots N_v\}$ denotes the frequency distribution of the lengths l of vertical structures.

The following measures were selected for analysis. Traditional measures included amplitude (Range), SD, and sway mean velocity (MV) in the AP and ML directions; sway path length (Path) and sway area (Area) were also included. Nonlinear measures included DFA coefficients (DFA_1 and DFA_2), determinism (%DET), and laminarity (%LAM) in the AP and ML directions.

Statistics

Each measure's distribution of normality was tested (Shapiro–Wilk test, $p > 0.05$). A mixed repeated-measures ANOVA with between-subject factors (age) and within-subject factors (condition) was conducted to assess the effects of age and condition on all the measures. Significant interactions were explored further using simple effects analyses and performed with Bonferroni *post hoc* tests. Greenhouse-Geisser corrections were applied for circumstances in which sphericity could not be assumed (Mauchly's test, $p < 0.05$). The significance level was set as $p < 0.05$ with two-tailed. Effect size values (η_p^2) were reported for ANOVA. All statistical testing was conducted using SPSS (IBM SPSS Statistics, Version 25, SPSS Inc., Chicago, IL, United States).

RESULTS

Traditional Measures

Table 2 provides an overview of mean values and SDs for traditional measures of standing balance in each condition

TABLE 2 | Overview of mean values and SDs for traditional measures of standing balance.

	Age group	EO	EC	ECHB
Range_ml (mm)	3 years	33.07 ± 8.85	43.38 ± 12.08	51.26 ± 15.85
	4 years	30.76 ± 8.50	41.53 ± 11.40	52.89 ± 17.31
	5 years	29.69 ± 11.31	44.41 ± 18.57	51.21 ± 17.43
Range_ap (mm)	3 years	32.79 ± 9.35	37.24 ± 11.63	51.95 ± 16.49
	4 years	27.09 ± 7.57	37.27 ± 8.84	47.12 ± 13.43
	5 years	33.92 ± 13.49	42.52 ± 14.94	52.06 ± 19.52
SD_ml (mm)	3 years	6.71 ± 1.64	8.28 ± 2.32	9.98 ± 3.07
	4 years	5.96 ± 1.43	8.12 ± 2.07	9.74 ± 2.85
	5 years	5.77 ± 1.88	8.53 ± 3.25	9.67 ± 2.81
SD_ap (mm)	3 years	6.57 ± 1.85	7.38 ± 2.44	9.78 ± 2.98
	4 years	5.73 ± 1.82	7.26 ± 1.61	9.06 ± 2.33
	5 years	7.17 ± 2.81	8.81 ± 2.97	9.36 ± 2.59
MV_ml (mm/s)	3 years	19.16 ± 6.08	25.39 ± 7.13	31.78 ± 11.36
	4 years	17.53 ± 5.51	26.80 ± 9.19	32.09 ± 11.71
	5 years	17.12 ± 6.27	25.61 ± 11.42	30.88 ± 13.91
MV_ap (mm/s)	3 years	21.85 ± 6.17	26.86 ± 6.95	38.24 ± 10.58
	4 years	17.98 ± 4.24	25.31 ± 7.14	35.22 ± 9.04
	5 years	18.97 ± 8.20	25.71 ± 9.24	35.73 ± 14.87
Path (mm)	3 years	484.76 ± 137.50	617.29 ± 156.29	829.63 ± 243.83
	4 years	420.13 ± 108.33	616.99 ± 182.48	794.92 ± 233.59
	5 years	428.54 ± 169.32	606.14 ± 232.30	788.23 ± 327.28
Area (mm^2)	3 years	517.25 ± 233.98	755.14 ± 450.46	1213.20 ± 759.88
	4 years	410.59 ± 179.09	718.19 ± 297.22	1082.66 ± 554.14
	5 years	515.29 ± 326.91	936.00 ± 654.67	1111.97 ± 657.01

EO, eyes open; EC, eyes closed; ECHB, eyes closed and head extended backward.

classified according to the age group of preschool children. Significant main effects of age were found for Range_ap and SD_ap. *Post hoc* tests revealed that Range_ap ($p = 0.03$) and SD_ap ($p = 0.03$) were significantly higher for the 5-year-old children than for the 4-year-old children. Effect sizes were small to medium, ranging from 0.058 to 0.060 (**Table 3**). No age-related differences were found for Range_ml, SD_ml, MV_ml, MV_ap, Path, and Area. Significant main effects of condition were observed for all traditional measures. Range_ml, Range_ap, SD_ml, SD_ap, MV_ml, MV_ap, Path, and Area significantly increased as conditions became more challenging ($p < 0.01$, all traditional measures). Effect sizes were large, ranging from 0.354 to 0.600 (**Table 4**). No significant age by condition interaction effects for Range_ml, Range_ap, SD_ml, SD_ap, MV_ml, MV_ap, Path, and Area.

TABLE 3 | Main effects of age on traditional measures of standing balance.

	3 years mean	4 years mean	5 years mean	F	*p*	Effect size (η_p^2)
Range_ml (mm)	42.57	41.73	41.77	0.079	0.924	0.001
Range_ap (mm)	40.66	37.16[B]	42.83[B]	3.405	**0.037**	0.058
SD_ml (mm)	8.32	7.94	7.99	0.433	0.650	0.008
SD_ap (mm)	7.91	7.35[B]	8.44[B]	3.512	**0.033**	0.060
MV_ml (mm/s)	25.44	25.48	24.54	0.214	0.808	0.004
MV_ap (mm/s)	28.99	26.17	26.81	1.664	0.194	0.029
Path (mm)	643.89	610.68	607.64	0.588	0.557	0.011
Area (mm^2)	828.53	737.15	854.42	0.965	0.384	0.017

[B]*4-year-old children ≠ 5-year-old children for $p < 0.05$.*
Significant differences are shown in bold font.

Nonlinear Measures

Table 5 provides an overview of mean values and SDs for nonlinear measures of standing balance in each condition classified according to the age group of preschool children. Significant main effects of age were found for DFA_1_ap, %DET_ap, and %LAM_ap. *Post hoc* tests revealed that DFA_1_ap, %DET_ap, and %LAM_ap were not statistically different for the 3- and 4-year-old children ($p > 0.05$ for these measures), DFA_1_ap was significantly higher for the 5-year-old children than 3- ($p < 0.01$) and 4-year-old children ($p = 0.04$), %DET_ap was significantly higher for the 5-year-old children than 3- ($p < 0.01$) and 4-year-old children ($p = 0.02$), and %LAM_ap was significantly higher for the 5-year-old children than 3- ($p < 0.01$) and 4-year-old children ($p < 0.01$). Medium to large effect sizes were found for DFA_1_ap, %DET_ap, and %LAM_ap, ranging from 0.093 to 0.153 (**Table 6**). No age-related differences were found for nonlinear measures (DFA_1_ml, DFA_2_ml, DFA_2_ap, %DET_ml, and %LAM_ml).

Significant main effects of condition were found for DFA_1_ml, DFA_1_ap, DFA_2_ml, DFA_2_ap, %DET_ap, and %LAM_ap. *Post hoc* tests revealed that %DET_ap and %LAM_ap ($p > 0.05$) were not statistically different for the EO and EC. %DET_ap was significantly lower for the ECHB than EO ($p < 0.01$) and

TABLE 4 | Main effects of condition on traditional measures of standing balance.

	EO mean	EC mean	ECHB mean	F	*p*	Effect size (η_p^2)
Range_ml (mm)	31.17^{+*}	43.11$^{+\#}$	51.79$^{*\#}$	88.703	**<0.001**	0.446
Range_ap (mm)	31.27^{+*}	39.01$^{+\#}$	50.38$^{*\#}$	80.884	**<0.001**	0.424
SD_ml (mm)	6.15^{+*}	8.31$^{+\#}$	9.80$^{*\#}$	108.292	**<0.001**	0.496
SD_ap (mm)	6.49^{+*}	7.82$^{+\#}$	9.40$^{*\#}$	60.311	**<0.001**	0.354
MV_ml (mm/s)	17.94^{+*}	25.93$^{+\#}$	31.58$^{*\#}$	83.950	**<0.001**	0.433
MV_ap (mm/s)	19.60^{+*}	25.96$^{+\#}$	36.40$^{*\#}$	165.037	**<0.001**	0.600
Path (mm)	444.48^{+*}	613.47$^{+\#}$	804.27$^{*\#}$	131.230	**<0.001**	0.544
Area (mm^2)	481.04^{+*}	803.11$^{+\#}$	1135.95$^{*\#}$	82.315	**<0.001**	0.428

EO, eyes open; EC, eyes closed; ECHB, eyes closed and head extended backwards.
$^{+}$EO ≠ EC for $p < 0.05$.
*EO ≠ ECHB for $p < 0.05$.
$^{\#}$EC ≠ ECHB for $p < 0.05$.
Significant differences are shown in bold font.

TABLE 5 | Overview of mean values and SDs for nonlinear measures of standing balance.

	Age group	EO	EC	ECHB
DFA_1_ml	3	1.77 ± 0.04	1.73 ± 0.05	1.70 ± 0.08
	4	1.73 ± 0.06	1.72 ± 0.05	1.70 ± 0.07
	5	1.75 ± 0.05	1.73 ± 0.06	1.71 ± 0.08
DFA_1_ap	3	1.72 ± 0.07	1.65 ± 0.08	1.65 ± 0.09
	4	1.71 ± 0.06	1.67 ± 0.07	1.66 ± 0.08
	5	1.73 ± 0.04	1.71 ± 0.06	1.68 ± 0.08
DFA_2_ml	3	1.22 ± 0.15	0.97 ± 0.25	1.04 ± 0.23
	4	1.08 ± 0.21	0.92 ± 0.23	1.01 ± 0.27
	5	1.07 ± 0.22	1.02 ± 0.23	1.05 ± 0.26
DFA_2_ap	3	1.13 ± 0.20	0.99 ± 0.26	1.00 ± 0.16
	4	1.14 ± 0.20	1.06 ± 0.17	1.04 ± 0.23
	5	1.25 ± 0.20	1.09 ± 0.18	0.98 ± 0.22
%DET_ml	3	80.66 ± 6.46	81.47 ± 4.85	79.20 ± 6.70
	4	80.10 ± 5.78	78.95 ± 6.53	77.98 ± 6.01
	5	79.50 ± 6.55	79.94 ± 5.44	80.21 ± 6.21
%DET_ap	3	72.88 ± 8.51	70.60 ± 7.81	69.31 ± 9.93
	4	75.06 ± 7.03	73.82 ± 7.19	70.17 ± 8.15
	5	79.07 ± 6.62	77.38 ± 7.04	72.89 ± 7.76
%LAM_ml	3	83.36 ± 5.03	82.78 ± 3.87	81.62 ± 5.07
	4	82.89 ± 5.30	80.64 ± 5.94	80.58 ± 4.54
	5	81.73 ± 4.94	82.26 ± 4.39	82.81 ± 5.17
%LAM_ap	3	77.46 ± 6.66	75.76 ± 6.30	74.70 ± 7.75
	4	78.94 ± 5.60	77.93 ± 5.60	74.98 ± 6.81
	5	82.95 ± 5.27	81.19 ± 5.25	76.89 ± 6.31

EO, eyes open; EC, eyes closed; ECHB, eyes closed and head extended backward.

EC ($p < 0.01$), and %LAM_ap was significantly lower for the ECHB than EO ($p < 0.01$) and EC ($p < 0.01$). DFA_1_ap was significantly lower for the ECHB than EO ($p < 0.01$) and EC ($p < 0.01$), DFA_2_ml was significantly lower for the ECHB than EO ($p < 0.01$) and EC ($p < 0.01$), DFA_2_ap was significantly lower for the ECHB than EO ($p < 0.01$) and EC ($p < 0.01$), while DFA_1_ml ($p < 0.01$) significantly decreased as conditions became more challenging. Medium to large effect sizes were found for DFA_1_ml, DFA_1_ap, DFA_2_ml, DFA_2_ap, %DET_ap, and %LAM_ap, ranging from 0.120 to 0.172 (**Table 7**). No significant age by condition interaction effects for DFA_1_ml, DFA_1_ap, DFA_2_ml, DFA_2_ap, %DET_ap, and %LAM_ap was founded.

DISCUSSION

The main findings are as follows: (1) 5-year-old children showed more postural sway in the AP direction than 4-year-old children; (2) 5-year-old children showed decreased variability and more intermittent in the AP direction than 3- and 4-year-old children; (3) standing balance in the ML direction was the same for 3- to 5-year-old children; (4) as the sensory conditions became more challenging, the amount and variability of postural sway increased, while intermittency decreased; and (5) traditional and nonlinear methods provide complementary information for evaluating standing balance in preschoolers. These results are discussed below.

Five-Year-Old Children Showed Increased Postural Sway in the AP Direction

According to traditional methods, the age-related difference of standing balance in preschoolers was only found between the 4- and 5-year-old children. This difference was shown with higher Range_ap and SD_ap in the AP direction for the 5-year-old children, consistent with the previous study (Verbecque et al., 2016a). MV_ap, MV_ml, and Path were the same for 3-, 4-, and 5-year-old children, consistent with the previous study (Verbecque et al., 2016a). The mean velocity is the most common measure used to evaluate standing balance (Wachholz et al., 2020; Xiao et al., 2020); however, it ignored some critical information about the control of standing balance (Zhou et al., 2017), especially for preschoolers. Nonetheless, based on the result of the increased postural sway of the 5-year-old children, we cannot conclude that the balance performance of the 5-year-old children has declined, given that 100% of the 5-year-old children in our study completed all three sensory conditions. In comparison, 2.56–10% of younger preschoolers failed to complete the whole test. The number of children able to cope with sensory perturbations (EC or ECHB) increased with age, consistent with previous studies (Slobounov and Newell, 1994; Verbecque et al., 2016a). Therefore, compared with younger preschool children, the balance performance of the 5-year-old children improved rather than declined, which may be associated with a person's ability to safely explore the limits of his or her base of support with an altered control strategy

TABLE 6 | Main effects of age on nonlinear methods of standing balance.

	3 years mean	4 years mean	5 years mean	F	*p*	Effect size (η_p^2)
DFA_1_ml	1.732	1.716	1.732	1.711	0.186	0.031
DFA_1_ap	1.672[A]	1.679[B]	1.706[A,B]	5.082	**0.008**	0.093
DFA_2_ml	1.075	1.005	1.043	1.858	0.161	0.034
DFA_2_ap	1.042	1.079	1.104	1.968	0.145	0.035
%DET_ml	80.44	79.01	79.88	0.968	0.383	0.017
%DET_ap	70.93[A]	73.01[B]	76.45[A,B]	9.604	**<0.001**	0.149
%LAM_ml	82.59	81.37	82.26	1.143	0.323	0.020
%LAM_ap	75.97[A]	77.28[B]	80.34[A,B]	9.906	**<0.001**	0.153

[A]3-year-old children ≠ 5-year-old children for $p < 0.05$.
[B]4-year-old children ≠ 5-year-old children for $p < 0.05$.
Significant differences are shown in bold font.

TABLE 7 | Main effects of condition on nonlinear methods of standing balance.

	EO mean	EC mean	ECHB mean	F	*p*	Effect size (η_p^2)
DFA_1_ml	1.750[+*]	1.726[+#]	1.703[*#]	22.015	**<0.001**	0.172
DFA_1_ap	1.717[+*]	1.678[+]	1.662[*]	17.666	**<0.001**	0.151
DFA_2_ml	1.123[+*]	0.970[+]	1.029[*]	14.776	**<0.001**	0.121
DFA_2_ap	1.171[+*]	1.047[+]	1.008[*]	22.012	**<0.001**	0.171
%DET_ml	80.09	80.12	79.13	1.407	0.247	0.013
%DET_ap	75.67[*]	73.93[#]	70.79[*#]	15.038	**<0.001**	0.120
%LAM_ml	82.66	81.89	81.67	1.761	0.174	0.016
%LAM_ap	79.78[*]	78.29[#]	75.53[*#]	18.211	**<0.001**	0.142

EO, eyes open; EC, eyes closed; ECHB, eyes closed and head extended backwards.
[+]EO ≠ EC for $p < 0.05$.
[*]EO ≠ ECHB for $p < 0.05$.
[#]EC ≠ ECHB for $p < 0.05$.
Significant differences are shown in bold font.

(Dusing, 2016; Verbecque et al., 2016a; Lobo Da Costa et al., 2019). Increased postural sway of 5-year-old children may also be viewed as a positive adaptation to physiological development to ensure that the input to the peripheral sensory receptors exceeds the threshold for detection and enhances the sensory information available to the CNS (Carpenter et al., 2010). Besides, body height and body weight may also affect children's balance performance, as age, body height, and body weight are positively correlated (Hsu et al., 2009). However, the control of standing balance develops during childhood reaching an optimum in early adult life (Sheldon, 1963; Goble and Baweja, 2018); age-related changes in standing balance were found with higher postural sway for 8-year-old children compared with older children (Mickle et al., 2011). These results indicate that the nonlinear developmental trend of standing balance in children (Kirshenbaum et al., 2001; Verbecque et al., 2016b), and traditional measures cannot effectively reflect the age-related changes of balance performance for preschool children.

Five-Year-Old Children Showed Decreased Variability and More Intermittent in the AP Direction

The variability of COP sway decreased for the 5-year-old children compared with 3- and 4-year-old children, as shown with higher DFA_1_ap, consistent with the previous study (Lobo Da Costa et al., 2019). Three- and four-year-old children present a more complicated COP sway than 5-year-old children (Lobo Da Costa et al., 2019; Phinyomark et al., 2020). The higher DFA values are linked to a better standing balance performance (van den Hoorn et al., 2018). Hence, it is clearly shown that DFA can evaluate postural stability and its variations due to age-related changes (Duarte and Sternad, 2008). COP sway's regularity increased for the 5-year-old children compared with 3- and 4-year-old children, as shown by the higher %DET_ap, consistent with the previous study (Lobo Da Costa et al., 2019). Because sample entropy (SEn) was negatively related to the regularity of COP signals (Donker et al., 2007), lower SEn values and higher %DET values indicate a more regular and predictable COP sway. In the current study, 5-year-old children presented a more predictable, less random COP motion, representing better balance performance (van den Hoorn et al., 2018). However, another study found that the regularity of COP sway reflected by SEn did not show a developmental trend in 6- to 12-year-old children (Schärli et al., 2013). These results also indicate the nonlinear developmental trend of standing balance in children (Kirshenbaum et al., 2001; Verbecque et al., 2016b).

Center of pressure sway's intermittency increased for the 5-year-old children compared with the 3- and 4-year-old children, as shown by higher %LAM_ap. The intermittent behavior of COP motion reflects an intermittent control mechanism of standing balance (Nomura et al., 2013; Dutt-Mazumder et al., 2018; Stins and Roerdink, 2018), which is manifested as the COP motion exhibiting changes in COP dynamics from fluctuating to relatively stationary (van den Hoorn et al., 2018). In fact, a decrease in the %LAM was observed with aging for the elderly compared with the young adults, and a reduction in the %LAM was also found for older fallers compared with older non-fallers (van den Hoorn et al., 2018). These results indicate that the intermittency of COP motion increases with age for preschoolers and decreases with age for older people, which may be associated with physiological changes of development or aging (van den Hoorn et al., 2018). Therefore, 5-year-old children showed decreased variability and more intermittent in the AP direction.

Standing Balance Was the Same for 3- to 5-Year-Old Children in the ML Direction

In contrast with the age-related changes of preschoolers' standing balance in the AP direction, no age-related changes of standing balance for traditional and nonlinear measures were found in the ML direction, which may be associated with the control mechanism of standing balance in preschoolers or the sensory conditions adopted in the present study. For example, feet together mainly increase the difficulty of standing balance in the ML direction (Kirby et al., 1987; Izquierdo-Herrera et al., 2018), while the condition of ECHB mainly perturbs the standing balance in the AP direction (Johnson and Van Emmerik, 2012). However, age-related changes in standing balance were found in the ML direction from 4-year-old children to adults (Lemos et al., 2016), and the changes in standing balance were also found in the ML direction between autism spectrum

disorder (ASD) children and typically developing (TD) children (Wang et al., 2016). Moreover, standing balance is different between the AP and ML directions (Błaszczyk and Klonowski, 2001). Therefore, the control of standing balance in preschoolers changes significantly in the AP direction while remaining unaltered in the ML direction.

Sensory Perturbation Changed the Control of Standing Balance

As the sensory conditions became more challenging, the balance performance significantly declined, as shown by higher values of all traditional measures in the AP and ML directions. These results indicated that all traditional measures could effectively reflect the condition-related changes in preschool children's balance performance. Moreover, the control strategy of standing balance changed significantly, as shown by lower values of fractal measures (DFA_1 and DFA_2) in the AP and ML directions. These results indicated that less persistent COP sway at shorter time scales and more anti-persistent pattern of COP sway at longer time scales as conditions became more challenging. Also, there was no difference between EC and EO for %DET in the AP direction, consistent with the previous study (Seigle et al., 2009). Based on these results, it can be seen that eyes closure during quiet standing on a firm surface might not influence the complexity and regularity of the standing balance in preschoolers (Seigle et al., 2009). However, head extension resulted in decreased %DET in the AP direction, which indicated that ECHB, a challenging postural task for preschoolers, caused significant changes in the regularity of the standing balance in preschoolers. These results show that the %DET is not sensitive to visual deprivation for preschoolers. Moreover, no difference was observed between EC and EO for %LAM in the AP direction, consistent with the previous study. It is clearly shown that eye closure during quiet standing on a force platform might not necessarily influence the intermittent control of the standing balance in preschoolers and young adults (van den Hoorn et al., 2018). However, the head extended backward position resulted in the decrease of the %LAM in the AP direction, which indicated that ECHB, as a challenging postural task for preschoolers, caused significant changes in the intermittent control of standing balance. These results show that the %LAM is not sensitive to the visual deprivation for preschoolers. Therefore, traditional and nonlinear methods have distinct sensitivities to different sensory perturbations. The three sensory conditions applied in the present study can effectively change the standing balance and distinguish the age-related changes of standing balance in preschoolers. This testing paradigm has the same effectiveness as the extensively used four sensory conditions on firm and foam surfaces with eyes open and closed. Moreover, under this testing paradigm, the vast majority of preschoolers can complete all the sensory conditions, which is convenient for comparison with older children, young adults, and the elderly and allows for a better understanding of the age-related changes of standing balance during the whole life span (Verbecque et al., 2016a; Goble and Baweja, 2018).

The general view is that the greater the complexity, the better the balance performance, which is contrary to this study's results. This conflicting phenomenon may be associated with the sensory conditions adopted in this study, in which the plantar somatosensory input was not perturbated. Also, the nonstationarity of the COP signals may be another impact factor. Several studies removed the fluctuations at a lower frequency using different methods (Gow et al., 2015; Zhou et al., 2017). However, the COP signals are nonstationary data (Collins and De Luca, 1993), and the control of standing balance is intermittent (van den Hoorn et al., 2018). In fact, many studies' results are consistent with this study's results, which is that the lower the complexity (the higher the regularity), the better the balance performance. For example, lower complexity (MSE) of raw COP signals was found for young adults compared with the elderly (Duarte and Sternad, 2008); lower complexity (SEn) was found under the condition of eyes open compared with eyes closed (Rigoldi et al., 2014); lower complexity (SEn) was also found for 5-year-old children compared with 4-year-old children (Lobo Da Costa et al., 2019). Nonetheless, to investigate the relationship between complexity and balance performance of postural sway in children, standing balance during childhood deserves further investigation.

Both Traditional and Nonlinear Methods Provided Complementary Information

As the sensory condition challenge increased, all traditional measures and fractal measures changed significantly in the AP and ML directions. Nonetheless, no condition-related changes in standing balance for RQA measures were found in the ML direction. It is shown that these RQA measures are not sensitive to the specific sensory condition (Seigle et al., 2009). These results indicate that all traditional measures can evaluate postural stability under different sensory conditions. However, the interpretation of these traditional measures should be considered carefully. For example, the traditional measures indicate that 5-year-old children's standing balance showed more postural sway than 4-year-old children. In contrast, nonlinear measures suggest that 5-year-old children's standing balance showed decreased variability, better balance performance, and more intermittency compared with 4-year-old children. These seemingly conflicting results can be explained by the free energy principle (Friston, 2010; Hur et al., 2019). The free energy principle is called a minimum entropy principle; a low entropy means that the body posture is relatively predictable (Hur et al., 2019). In fact, standing still is impossible for humans since it requires excessive efforts; little control efforts are made with flexible postural sway within a specific range. In addition, more sensory inputs are removed or reduced as the sensory conditions become more challenging (EC or ECHE), while different traditional and nonlinear methods have distinct sensitivities to the different sensory perturbations. The previous study has shown that different measures of COP signal can reflect different information of standing balance control (Luo et al., 2018). Therefore, both traditional and nonlinear methods provide complementary information for evaluating age-related and condition-related changes of standing balance in preschoolers, and the interpretation of these measures should be considered together. Based on the advantages of nonlinear methods applied to even short and nonstationary data, nonlinear methods can be used as a quantitative

tool to assess gait stability in patients with different balance disorders (Sylos Labini et al., 2012) and effectively discern the gait stability between toddlers, young adults, and elderly (Bisi et al., 2014). Thus, these advanced methods can also investigate the gait in preschool and primary school-aged children.

Limitations

In this study, the lack of randomization of the three test conditions could have induced fatigue, influencing the balance performance in preschoolers. However, we did not expect the preschoolers to fatigue because all preschoolers were allowed to rest between different conditions. Each child performed only one trial in each condition for 15 s. Future research for preschool and primary school-aged children is needed to evaluate the developmental trend of standing balance in children.

CONCLUSION

Although increased postural sway, 5-year-old preschool children's balance performance improved, and their control strategy changed significantly compared with the younger preschoolers. Sensory perturbation (eye closure and/or head extension) changed preschoolers' balance performance and control strategy. Moreover, both traditional and nonlinear methods provided complementary information on the control of standing balance in preschoolers.

DATA AVAILABILITY STATEMENT

The data presented in this study are available on request from the corresponding author.

ETHICS STATEMENT

The studies involving human participants were reviewed and approved by Research Ethics Board of Center for Psychological Sciences at Zhejiang University. Written informed consent to participate in this study was provided by the participants' legal guardian/next of kin.

AUTHOR CONTRIBUTIONS

ZH contributed to writing the original draft, revising and editing the manuscript, data collection, data analysis, statistics, and data interpretation. YY and AH contributed to the data collection and data analysis. YG contributed to revising and editing the manuscript. JW contributed to conceptualization of the study, data interpretation, and revising and editing the manuscript. All authors approved the submitted version of the manuscript.

FUNDING

This research was funded by the National Key Research and Development Project of China (2018YFF0300502). We acknowledge the support from National Natural Science Foundation of China (31911530767).

ACKNOWLEDGMENTS

We are very grateful to the preschool and parents for their collaboration.

REFERENCES

Aoki, O., Otani, Y., and Morishita, S. (2018). Effect of eye-object distance on body sway during galvanic vestibular stimulation. *Brain Sci.* 8:191. doi: 10.3390/brainsci8110191

Bair, W., Kiemel, T., Jeka, J. J., and Clark, J. E. (2007). Development of multisensory reweighting for posture control in children. *Exp. Brain Res.* 183, 435–446. doi: 10.1007/s00221-007-1057-2

Balasubramaniam, R., and Wing, A. M. (2002). The dynamics of standing balance. *Trends Cogn. Sci.* 6, 531–536. doi: 10.1016/S1364-6613(02)02021-1

Bisi, M. C., Riva, F., and Stagni, R. (2014). Measures of gait stability: performance on adults and toddlers at the beginning of independent walking. *J. Neuroeng. Rehabil.* 11:131. doi: 10.1186/1743-0003-11-131

Błaszczyk, J. W., and Klonowski, W. (2001). Postural stability and fractal dynamics. *Acta Neurobiol. Exp.* 61, 105–112.

Buckley, J. G., Anand, V., Scally, A., and Elliott, D. B. (2005). Does head extension and flexion increase postural instability in elderly subjects when visual information is kept constant? *Gait Posture* 21, 59–64. doi: 10.1016/j.gaitpost.2003.11.005

Carpenter, M. G., Murnaghan, C. D., and Inglis, J. T. (2010). Shifting the balance: evidence of an exploratory role for postural sway. *Neuroscience* 171, 196–204. doi: 10.1016/j.neuroscience.2010.08.030

Collins, J. J., and De Luca, C. J. (1993). Open-loop and closed-loop control of posture: a random-walk analysis of center-of-pressure trajectories. *Exp. Brain Res.* 95, 308–318. doi: 10.1007/BF00229788

Donker, S. F., Roerdink, M., Greven, A. J., and Beek, P. J. (2007). Regularity of center-of-pressure trajectories depends on the amount of attention invested in postural control. *Exp. Brain Res.* 181, 1–11. doi: 10.1007/s00221-007-0905-4

Doyle, T. L., Newton, R. U., and Burnett, A. F. (2005). Reliability of traditional and fractal dimension measures of quiet stance center of pressure in young, healthy people. *Arch. Phys. Med. Rehabil.* 86, 2034–2040. doi: 10.1016/j.apmr.2005.05.014

Duarte, M., and Sternad, D. (2008). Complexity of human postural control in young and older adults during prolonged standing. *Exp. Brain Res.* 191, 265–276. doi: 10.1007/s00221-008-1521-7

Dusing, S. C. (2016). Postural variability and sensorimotor development in infancy. *Dev. Med. Child Neurol.* 58, 17–21. doi: 10.1111/dmcn.13045

Dutt-Mazumder, A., Rand, T. J., Mukherjee, M., and Newell, K. M. (2018). Scaling oscillatory platform frequency reveals recurrence of intermittent postural attractor states. *Sci. Rep.* 8:11580. doi: 10.1038/s41598-018-29844-2

Forssberg, H., and Nashner, L. M. (1982). Ontogenetic development of postural control in man: adaptation to altered support and visual conditions during stance. *J. Neurosci.* 2, 545–552. doi: 10.1523/JNEUROSCI.02-05-00545.1982

Foudriat, B. A., Di Fabio, R. P., and Anderson, J. H. (1993). Sensory organization of balance responses in children 3–6 years of age: a normative study with diagnostic implications. *Int. J. Pediatr. Otorhinolaryngol.* 27, 255–271. doi: 10.1016/0165-5876(93)90231-Q

Friston, K. (2010). The free-energy principle: a unified brain theory? *Nat. Rev. Neurosci.* 11, 127–138. doi: 10.1038/nrn2787

Goble, D. J., and Baweja, H. S. (2018). Normative data for the BTrackS balance test of postural sway: results from 16,357 community-dwelling individuals who were 5 to 100 years old. *Phys. Ther.* 98, 779–785. doi: 10.1093/ptj/pzy062

Gow, B., Peng, C., Wayne, P., and Ahn, A. (2015). Multiscale entropy analysis of center-of-pressure dynamics in human postural control: methodological considerations. *Entropy* 17, 7926–7947. doi: 10.3390/e17127849

Henriques, T., Ribeiro, M., Teixeira, A., Castro, L., Antunes, L., and Costa-Santos, C. (2020). Nonlinear methods most applied to heart-rate time series: a review. *Entropy* 22:309. doi: 10.3390/e22030309

Hsu, Y., Kuan, C., and Young, Y. (2009). Assessing the development of balance function in children using stabilometry. *Int. J. Pediatr. Otorhinolaryngol.* 73, 737–740. doi: 10.1016/j.ijporl.2009.01.016

Hur, P., Pan, Y., and DeBuys, C. (2019). Free energy principle in human postural control system: skin stretch feedback reduces the entropy. *Sci. Rep.* 9:16870. doi: 10.1038/s41598-019-53028-1

Izquierdo-Herrera, R., García-Massó, X., González, L., Wade, M. G., and Stoffregen, T. A. (2018). Visual tasks and stance width influence the spatial magnitude and temporal dynamics of standing body sway in 6- to 12-year old children. *Hum. Mov. Sci.* 59, 56–65. doi: 10.1016/j.humov.2018.03.017

Johnson, M. B., and Van Emmerik, R. E. A. (2012). Effect of head orientation on postural control during upright stance and forward lean. *Mot. Control.* 16, 81–93. doi: 10.1123/mcj.16.1.81

Kirby, R. L., Price, N. A., and MacLeod, D. A. (1987). The influence of foot position on standing balance. *J. Biomech.* 20, 423–427. doi: 10.1016/0021-9290(87)90049-2

Kirshenbaum, N., Riach, C., and Starkes, J. (2001). Non-linear development of postural control and strategy use in young children: a longitudinal study. *Exp. Brain Res.* 140, 420–431. doi: 10.1007/s002210100835

Kogler, A., Lindfors, J., Odkvist, L. M., and Ledin, T. (2000). Postural stability using different neck positions in normal subjects and patients with neck trauma. *Acta Otolaryngol.* 120, 151–155. doi: 10.1080/000164800750000801

Lemos, L. F. C., David, A. C. D., and Mota, C. B. (2016). Development of postural balance in Brazilian children aged 4-10 years compared to young adults. *Braz. J. Kinanthrop. Hum. Perform.* 18, 419–428. doi: 10.5007/1980-0037.2016v18n4p419

Lobo Da Costa, P. H., Verbecque, E., Hallemans, A., and Vieira, M. F. (2019). Standing balance in preschoolers using nonlinear dynamics and sway density curve analysis. *J. Biomech.* 82, 96–102. doi: 10.1016/j.jbiomech.2018.10.012

Luo, H., Wang, X., Fan, M., Deng, L., Jian, C., Wei, M., et al. (2018). The effect of visual stimuli on stability and complexity of postural control. *Front. Neurol.* 9:48. doi: 10.3389/fneur.2018.00048

Ma, Y., Shi, W., Peng, C., and Yang, A. C. (2018). Nonlinear dynamical analysis of sleep electroencephalography using fractal and entropy approaches. *Sleep Med. Rev.* 37, 85–93. doi: 10.1016/j.smrv.2017.01.003

Marwan, N., Romano, M. C., Thiel, M., and Kurths, J. (2007). Recurrence plots for the analysis of complex systems. *Phys. Rep.* 438, 237–329. doi: 10.1016/j.physrep.2006.11.001

Mickle, K. J., Munro, B. J., and Steele, J. R. (2011). Gender and age affect balance performance in primary school-aged children. *J. Sci. Med. Sport* 14, 243–248. doi: 10.1016/j.jsams.2010.11.002

Molloy, C. A., Dietrich, K. N., and Bhattacharya, A. (2003). Postural stability in children with autism spectrum disorder. *J. Autism Dev. Disord.* 33, 643–652. doi: 10.1023/B:JADD.0000006001.00667.4c

Newell, K. M., Slobounov, S. M., Slobounova, B. S., and Molenaar, P. C. M. (1997a). Short-term non-stationarity and the development of postural control. *Gait Posture* 6, 56–62. doi: 10.1016/S0966-6362(96)01103-4

Newell, K. M., Slobounov, S. M., Slobounova, E. S., and Molenaar, P. C. M. (1997b). Stochastic processes in postural center-of-pressure profiles. *Exp. Brain Res.* 113, 158–164. doi: 10.1007/BF02454152

Nomura, T., Oshikawa, S., Suzuki, Y., Kiyono, K., and Morasso, P. (2013). Modeling human postural sway using an intermittent control and hemodynamic perturbations. *Math. Biosci.* 245, 86–95. doi: 10.1016/j.mbs.2013.02.002

Paillard, T., and Noé, F. (2015). Techniques and methods for testing the postural function in healthy and pathological subjects. *Biomed. Res. Int.* 2015, 1–15. doi: 10.1155/2015/891390

Palmieri, R. M., Ingersoll, C. D., Stone, M. B., and Krause, B. A. (2002). Center-of-pressure parameters used in the assessment of postural control. *J. Sport Rehabil.* 11, 51–66. doi: 10.1123/jsr.11.1.51

Paloski, W. H., Wood, S. J., Feiveson, A. H., Black, F. O., Hwang, E. Y., and Reschke, M. F. (2006). Destabilization of human balance control by static and dynamic head tilts. *Gait Posture* 23, 315–323. doi: 10.1016/j.gaitpost.2005.04.009

Peng, C. K., Havlin, S., Stanley, H. E., and Goldberger, A. L. (1995). Quantification of scaling exponents and crossover phenomena in nonstationary heartbeat time series. *Chaos* 5, 82–87. doi: 10.1063/1.166141

Phinyomark, A., Larracy, R., and Scheme, E. (2020). Fractal analysis of human gait variability via stride interval time series. *Front. Physiol.* 11:333. doi: 10.3389/fphys.2020.00333

Ramdani, S., Tallon, G., Bernard, P. L., and Blain, H. (2013). Recurrence quantification analysis of human postural fluctuations in older fallers and non-fallers. *Ann. Biomed. Eng.* 41, 1713–1725. doi: 10.1007/s10439-013-0790-x

Riach, C. L., and Hayes, K. C. (1987). Maturation of postural sway in young children. *Dev. Med. Child Neurol.* 29, 650–658. doi: 10.1111/j.1469-8749.1987.tb08507.x

Rigoldi, C., Galli, M., Mainardi, L., and Albertini, G. (2014). Evaluation of posture signal using entropy analysis and fractal dimension in adults with down syndrome. *Comput. Methods Biomech. Biomed. Engin.* 17, 474–479. doi: 10.1080/10255842.2012.692781

Rinaldi, N. M., Polastri, P. F., and Barela, J. A. (2009). Age-related changes in postural control sensory reweighting. *Neurosci. Lett.* 467, 225–229. doi: 10.1016/j.neulet.2009.10.042

Rival, C., Ceyte, H., and Olivier, I. (2005). Developmental changes of static standing balance in children. *Neurosci. Lett.* 376, 133–136. doi: 10.1016/j.neulet.2004.11.042

Sá, C. D. S. C., Boffino, C. C., Ramos, R. T., and Tanaka, C. (2018). Development of postural control and maturation of sensory systems in children of different ages a cross-sectional study. *Braz. J. Phys. Ther.* 22, 70–76. doi: 10.1016/j.bjpt.2017.10.006

Schärli, A. M., van de Langenberg, R., Murer, K., and Müller, R. M. (2013). Postural control and head stability during natural gaze behaviour in 6- to 12-year-old children. *Exp. Brain Res.* 227, 523–534. doi: 10.1007/s00221-013-3528-y

Seigle, B., Ramdani, S., and Bernard, P. L. (2009). Dynamical structure of center of pressure fluctuations in elderly people. *Gait Posture* 30, 223–226. doi: 10.1016/j.gaitpost.2009.05.005

Sheldon, J. H. (1963). The effect of age on the control of sway. *Gerontol. Clin.* 5, 129–138. doi: 10.1159/000244784

Slobounov, S. M., and Newell, K. M. (1994). Dynamics of posture in 3- and 5-year-old children as a function of task constraints. *Hum. Mov. Sci.* 13, 861–875. doi: 10.1016/0167-9457(94)90022-1

Smith, A., Ulmer, F., and Wong, D. (2012). Gender differences in postural stability among children. *J. Hum. Kinet.* 33, 25–32. doi: 10.2478/v10078-012-0041-5

Steindl, R., Kunz, K., Schrott-Fischer, A., and Scholtz, A. W. (2006). Effect of age and sex on maturation of sensory systems and balance control. *Dev. Med. Child Neurol.* 48, 477–482. doi: 10.1017/S0012162206001022

Stins, J. F., and Roerdink, M. (2018). Unveiling intermittency in the control of quiet upright standing: beyond automatic behavior. *Front. Neurol.* 9:850. doi: 10.3389/fneur.2018.00850

Sylos Labini, F., Meli, A., Ivanenko, Y. P., and Tufarelli, D. (2012). Recurrence quantification analysis of gait in normal and hypovestibular subjects. *Gait Posture* 35, 48–55. doi: 10.1016/j.gaitpost.2011.08.004

Teresa Blázquez, M., Anguiano, M., de Saavedra, F. A., Lallena, A. M., and Carpena, P. (2009). Study of the human postural control system during quiet standing using detrended fluctuation analysis. *Physica A* 388, 1857–1866. doi: 10.1016/j.physa.2009.01.001

Teresa Blázquez, M., Anguiano, M., de Saavedra, F. A., Lallena, A. M., and Carpena, P. (2010). Characterizing the human postural control system using detrended fluctuation analysis. *J. Comput. Appl. Math.* 233, 1478–1482. doi: 10.1016/j.cam.2008.04.038

van den Hoorn, W., Kerr, G. K., van Dieën, J. H., and Hodges, P. W. (2018). Center of pressure motion after calf vibration is more random in fallers than non-fallers: prospective study of older individuals. *Front. Physiol.* 9:273. doi: 10.3389/fphys.2018.00273

Verbecque, E., Costa, P. H. L. D., Meyns, P., Desloovere, K., Vereeck, L., and Hallemans, A. (2016a). Age-related changes in postural sway in preschoolers. *Gait Posture* 44, 116–122. doi: 10.1016/j.gaitpost.2015.11.016

Verbecque, E., Vereeck, L., and Hallemans, A. (2016b). Postural sway in children: a literature review. *Gait Posture* 49, 402–410. doi: 10.1016/j.gaitpost.2016.08.003

Villarrasa-Sapiña, I., Estevan, I., Gonzalez, L., Marco-Ahulló, A., and García-Massó, X. (2019). Dual task cost in balance control and stability in children from 4–7 years old. *Early Child Dev. Care* 190, 1–10. doi: 10.1080/03004430.2019.1590349

Vuillerme, N., Chenu, O., Pinsault, N., Fleury, A., Demongeot, J., and Payan, Y. (2008). Can a plantar pressure-based tongue-placed electrotactile biofeedback improve postural control under altered vestibular and neck proprioceptive conditions? *Neuroscience* 155, 291–296. doi: 10.1016/j.neuroscience.2008.05.018

Vuillerme, N., and Rougier, P. (2005). Effects of head extension on undisturbed upright stance control in humans. *Gait Posture* 21, 318–325. doi: 10.1016/j.gaitpost.2004.04.007

Wachholz, F., Tiribello, F., Promsri, A., and Federolf, P. (2020). Should the minimal intervention principle be considered when investigating dual-tasking effects on postural control? *Brain Sci.* 10:1. doi: 10.3390/brainsci10010001

Wang, Z., Hallac, R. R., Conroy, K. C., White, S. P., Kane, A. A., Collinsworth, A. L., et al. (2016). Postural orientation and equilibrium processes associated with increased postural sway in autism spectrum disorder (ASD). *J. Neurodev. Disord.* 8:43. doi: 10.1186/s11689-016-9178-1

Xiao, S., Wang, B., Zhang, X., Zhou, J., and Fu, W. (2020). Acute effects of high-definition transcranial direct current stimulation on foot muscle strength, passive ankle kinesthesia, and static balance: a pilot study. *Brain Sci.* 10:246. doi: 10.3390/brainsci10040246

Young, Y. (2015). Assessment of functional development of the otolithic system in growing children: a review. *Int. J. Pediatr. Otorhinolaryngol.* 79, 435–442. doi: 10.1016/j.ijporl.2015.01.015

Zhou, J., Habtemariam, D., Iloputaife, I., Lipsitz, L. A., and Manor, B. (2017). The complexity of standing postural sway associates with future falls in community-dwelling older adults: the mobilize Boston study. *Sci. Rep.* 7:2924. doi: 10.1038/s41598-017-03422-4

Conflict of Interest: The authors declare that the research was conducted in the absence of any commercial or financial relationships that could be construed as a potential conflict of interest.